KfK 2566
EUR 5751e
Januar 1978

Convective Heat Transfer from Rough Surfaces with Two-dimensional Ribs: Transitional and Laminar Flow

M. Dalle Donne, L. Meyer
Institut für Neutronenphysik und Reaktortechnik
Projekt Schneller Brüter

Kernforschungszentrum Karlsruhe

KERNFORSCHUNGSZENTRUM KARLSRUHE

Institut für Neutronenphysik und Reaktortechnik
Projekt Schneller Brüter

KfK 2566
EUR 5751e

Convective Heat Transfer from Rough Surfaces with Two-dimensional Ribs: Transitional and Laminar Flow

M. Dalle Donne* and L. Meyer

*Euratom, delegated to the Fast Reactor Project, Karlsruhe

Kernforschungszentrum Karlsruhe GmbH, Karlsruhe

Abstract

Measurements of friction factor and heat transfer coefficients for two rods of 18.9 mm O.D. with two-dimensional roughness, each in two different outer smooth tubes have been performed in turbulent and laminar flow. The turbulent flow results indicate that the flow was not thermally fully established, the isothermal data however agree reasonably well with our previously obtained general correlation. Laminar flow results can be correlated best when the Reynolds and Graetz numbers are evaluated at the temperature $T_{\bar{W}}$ average between the temperature of the inner rod surface and of the outer smooth surface of the annulus, the average being weighted over the two surfaces.

Konvektiver Wärmeübergang von Oberflächen mit zwei-dimensionalen Rauhigkeitsziffern: Laminare Strömung und Wärmeübergangsbereich

Zusammenfassung

Messungen des Reibungs- und Wärmeübertragungskoeffizienten in turbulenter und laminarer Strömung wurden an zwei mit künstlicher zweidimensionaler Rauhigkeit versehenen Stäben mit einem Durchmesser von 18.9 mm jeweils in zwei verschiedenen Außenrohren durchgeführt. Die Ergebnisse bei turbulenter Strömung lassen darauf schließen, daß die Strömung thermisch nicht voll ausgebildet war, die isothermen Ergebnisse stimmen jedoch gut mit unserer an anderen Stäben gefundenen allgemeinen Korrelation überein.

Die Ergebnisse bei laminarer Strömung werden am besten mit der Reynolds- und der Graetz-Zahl korreliert, die sich ergeben, wenn die mittlere Temperatur $T_{\bar{W}}$ zwischen der Staboberflächentemperatur und der Wandtemperatur des äußeren Rohres, gewichtet mit deren Oberflächen, zur Bestimmung der Stoffwerte benutzt wird.

1. Introduction

The experiments to measure the heat transfer and friction coefficients from rough surfaces are generally performed with a single heated rough rod contained in a concentric smooth tube (annulus), although reactor fuel elements are made up of a number of parallel fuel pins placed in regular arrays and cooled by gas flowing parallel to the pins. The experimental data obtained in these single rod experiments are then "transformed" in such a way that they can be applied to large regular arrays of rough rods.

The results of the heat transfer and friction coefficient measurements in annuli with an inner rough rod performed in the past at the Heat Transfer Laboratory of the Institute of Neutron Physics and Reactor Engineering of the Karlsruhe Nuclear Center have been published /1,2,3,4/. The transformation of these experimental data was performed with the Dalle Donne - Meerwald method /1/. More recent measurements with rods roughened by two-dimensional rectangular ribs and three dimensional ribs have been transformed with a new and improved method /5,6,7/. This new method holds for the turbulent flow and it is based on the assumption that the velocity and temperature profiles normal to the rough surface can be described by the universal laws of the wall:

$$u^+ = 2.5 \ln \frac{y}{h} + R(h_W^+) \qquad (1)$$

$$t^+ = 2.5 \ln \frac{y}{h} + G(h_W^+) \qquad (2)$$

where u^+ and t^+ are the dimensionless velocity and temperature at the distance y from the rough wall, h is the height of the ribs of the roughness, and $R(h_W^+)$ and $G(h_W^+)$ are the dimensionless velocity and temperature at the point y=h, i.e. at the tip of the ribs.

In this assumption it is implicit that the parameters, which have influence on the velocity and temperature profiles, i.e. on the friction and heat transfer coefficients, do so through the quantities $R(h_W^+)$ and $G(h_W^+)$ only.

Zum Druck am: 5.1.1978

For the transformation of the friction factors the cross section of the annulus is divided into two regions, the inner one pertaining to the rough inner rod, the outer one to the outer smooth tube. The separation line is given by the line of no shear. As in the Maubach method /8/, it is assumed that this separation line is determined by the intersection of the two velocity profiles starting from the inner rough rod and from the outer smooth surface respectively. In the new method, however, the slope of the velocity profile relative to the smooth wall is assumed to be a function of the friction factor of the inner rough rod, to take into account a larger amount of experimental information on the position of the zero shear stress line.

For the transformation of the heat-transfer coefficients it is assumed that the above mentioned universal temperature profile holds over the whole cross section of the annulus from the inner rough surface over the line of zero shear up to the outer smooth surface, which is taken to coincide with the surface of zero heat flux. $G(h_W^+)$ is determind by the measurement of the temperatures of the two walls of the annulus. In this way we obtain a temperature profile with well defined boundary conditions (q_1 = heat flux at the rough wall, q_2 = heat flux at the smooth wall = 0), which correspond to those of the central coolant subchannels of rough clusters of rods.

The present transformation method has been applied to a geometrical configuration typical of a fuel element of a gas cooled fast reactor. In this it was assumed that the velocity and temperature profiles in cross sections of the coolant subchannels of the bundle are given by the logarithmic expressions shown above. The parameters $R(h_W^+)$ and $G(h_W^+)$ and the effect of the determing parameters mentioned above are considered as invariant in the transformation from annulus to bundle geometry. By integration of the velocity and temperature profiles in the coolant subchannels the average values $\bar{u}^+$ and $\bar{t}^+$ of these profiles are obtained. These average values are directly connected with the friction factors and Stanton numbers through the expressions:

$$\bar{u}^+ = (2/f_R)^{\frac{1}{2}} \qquad (3)$$

$$\bar{t}^+ = (f_R/2)^{\frac{1}{2}}/St_R \qquad (4)$$

In this way the values of the friction factor coefficient f_R and of the Stanton number St_R of the various coolant subchannels of bundles of rough rods can be calculated and the pressure drop and wall temperatures of the rods can be determinded. This method was used for the evaluation of experiments with two rod bundles of twelve /9/ and nineteen rough rods respectively /10/. Experiments, which have been carried out in the helium high pressure loop of the Institute of Neutron Physics and Reactor Engineering at Karlsruhe. The agreement between theoretical prediction and measurements was excellent /9,11,12/. The 19 rod bundle mentioned above had rods of 18.9 mm O.D.; the dimensions of the rectangular roughness ribs are given in Table I, while the $R(h_W^+)$ and $G(h_W^+)$ values used in the evaluation (cfr. equation (8) and (9) of page 91 of reference /11/) were obtained by means of annuli experiments with air and rough rods of 34 mm O.D. /5,6/. The manufacturers of these rods were not the same , which manufactured the 18.9 mm rods. To check if the differences in the manufacturing process and/or the different coolant (atmospheric air in the annulus, high pressure helium in the bundle) were having some effect, we decided to test directly two rods of the 19-rod bundle, previously tested in the helium loop /10/, in the annulus air rig. Furthermore the use of rods of smaller diameter would allow us more accurate experiments at low flows, that is in the transition region between fully rough flow (where the parameter $R(h^+)$ is quasi-constant) and hydraulically smooth flow (the velocity profile is the same as for a smooth surface), and in laminar flow. These flow regimes are important for the low power operation and accidental situations of a gas-cooled fast reactor core. Up to now only scarce information is available for these flow regimes /5,6/.

The experimental apparatus used in the present experiment is the same as that used for the experiments to test 34 mm O.D. rough rods in annuli reported in /5/ and /6/. A detailed description of the apparatus and of the procedure used to obtain the experimental data is given in those references.

Table I shows the geometrical characteristics of the two rough rods tested during the present investigation. The roughness ribs are nominally the same, however, while the ribs of rod "19" have sharp edges, the ribs on rod "18" have been rounded on the edges. This was done to investigate the effects of edge-rounding on friction and heat transfer coefficients. Rod "18" had a roughened steel portion 735 mm long, as in the 19 rod bundle, while in rod 19" the roughened steel length was 436 mm only. The rest of the rods was made up of thicker copper tubes of the same outside diameter, to reduce the electrical heat production outside the rough portion of the rods. Each rod was tested in two outer smooth tubes. Table I shows the ratio l/D (l = length of rough surface, D = hydraulic diameter of the annulus) obtained for each of these four test sections.

2. Experimental Results

2.1 Friction Factors. Isothermal runs ($T_W/T_B=1$). Turbulent flow

Table II shows the results of the isothermal runs for flow in turbulent regime. The friction factors and all the other data were obtained by averaging the local data for $22.7 \leqslant \frac{l}{D} \leqslant 27.2$ and for $15.8 \leqslant \frac{l}{D} \leqslant 19.0$ for rod "18" and for $10.5 \leqslant \frac{l}{D} \leqslant 15.0$ and for $7.3 \leqslant \frac{l}{D} \leqslant 10.5$ for rod "19" in the tubes 40.4 and 50.0 mm I.D. respectively. Although these $\frac{l}{D}$ values are relatively low, the local friction data appeared to be constant, apart from scattering due to the measurement of relatively small pressure differences. This was probably due to some sort of stabilizing inlet effect of the smooth copper rod, which helped to reach fully established flow conditions.

Figures 1 to 4 show the untransformed friction factors versus Reynolds number for the rods 18 and 19 in the outer smooth tubes of 40.4 mm and 50.0 mm I.D. respectively. Figures 5 to 8 show the transformed friction factors of the inner rough rods. (Figures 1 to 8 show both isothermal friction factors and friction factors with heat transfer. In this section we will deal with isothermal friction factors only.) For sufficiently high Reynolds numbers these are more or less constant (region of fully rough flow). In the figures 1 to 8 a line representing the friction factor for turbulent flow in smooth tubes is given for comparison.

Figures 9 and 10 show the isothermal $R(h^+)$ values obtained, as the f_1 values as well, with the new transformation method shortly described in the introduction. The region of fully rough flow ($R(h^+)$ = constant) is quite evident for $h^+ \geq 40 \div 50$. For rod 19, data were obtained also in the transition region between fully rough flow and hydraulically smooth flow, where the rough surface "behaves" like a smooth one ($R(h^+) = 2.5 \ln h^+ + 5.5$). The transition region data can be correlated by the equations:

$$R(h^+) = 3.42 \left(1 + \frac{9.35}{(h^+)^{1.4}}\right) \quad \text{for test section } 19/40.4 \tag{5}$$

$$R(h^+) = 3.1 \left(1 + \frac{9.35}{(h^+)^{1.4}}\right) \quad \text{for test section } 19/50 \tag{6}$$

The $R(\infty)$ values in the fully rough flow region are given in Table I for the four test sections investigated. Fig. 11 shows the four $R(\infty)$ values versus $h/\hat{y}$. Plotted is also the prediction from the general correlation obtained by the systematic experiments with the 34 mm O.D. rods /5,6/. The agreement with the data for rod 19 is good. Rod 19 had ribs with sharp edges as the 34 mm O.D. rods. As axpected the data for rod 18 are higher (about 11%). This corresponds to a decrease of the transformed friction factors of about 5%. Variations of this sort for rounding of the rib tips have been already observed in the past /13/.

2.2 Friction factors. Runs with heat transfer ($T_W/T_B>1$). Turbulent flow (Re_W > 3000)

Table III shows the results of the runs with heat transfer for flow in turbulent regime. All the data are averaged as in Table II.

Figures 1 to 4 show the friction factors versus the Reynolds number evaluated at the inner rod wall temperature for the rods 18 and 19 in the outer smooth tubes of 40.4 mm and 50 mm I.D. at various temperature levels:

$T_W/T_B = 1$ (T_{WM}=room temperature, isothermal runs)

$T_W/T_B \approx 1.3 \div 1.4$ ($T_{WM} \approx 150^oC$)

$T_W/T_B \approx 1.8 \div 1.9$ ($T_{WM} \approx 360^oC$)

$T_W/T_B \approx 2.2 \div 2.45$ ($T_{WM} \approx 550^oC$)

Figures 5 to 8 show the transformed friction factors of the inner rough rods for the same runs. The increase of temperature produces a considerable decrease of the friction factors. Figures 12 to 15 show the $R(h_W^+)$ values for thermal runs versus h_W^+. The $R(h_W^+)$ values increase with T_W/T_B. This effect has been already observed previously by us /5,6/, however it is here quantitatively more pronounced. The reason for this could be:

- The inner rough rods, when heated, are bowing. It is known that friction factors of an annulus are the highest when the inner rod is perfectly centered. A certain excentricity makes the friction factors smaller, therefore increases the $R(h_W^+)$ values.

- The temperature profiles in the cross section of the gas flow are not yet fully established. The copper smooth rods brazed at the end of the inner rough rods have a large thermal conductivity in axial direction and the rods themselves

are not very long in terms of l/D (see Table I), therefore the region where the variation of wall temperature of the inner rough rods is linear in axial direction is short, especially at the highest temperature.

Various correction factors have been tried to take account of the temperature effect on the present $R(h_W^+)$ values. The most successful has been to correlate the data in terms of the parameter

$$R(h_W^+)1 = R(h_W^+) - \frac{0.055}{h/\hat{y}} \left(\frac{T_W}{T_1}\right)^{1.5} \qquad (7)$$

which differ from that used in references /5,6/, mainly because the correction factor is a function of $h/\hat{y}$ rather then of h_W^+. Figures 16 to 19 show this parameter vs h_W^+ for the four test sections investigated. With the exception of test section "19" in the outer smooth tube of 50 mm I.D the temperature effect is practically eliminated. For test section "19" in the tube 50 mm however an appreciable temperature effect is still present (see Fig.19). This test section is indeed the shortest in terms of l/D of those tested (see Table I) and this is again an indication that the excessive temperature effect may be given by the fact that the temperature profile in the cross section of the gas flow is not fully established.

2.3 Heat transfer results. Turbulent flow (Re_W >3000)

Figures 20 to 23 show the heat transfer results in the plot $G(h_W^+)$ versus h_W^+ for the four test sections investigated. Also here the T_W/T_B effect increases the $G(h_W^+)$ values, which is equivalent to a decrease of the heat transfer coefficient. As for the $R(h_W^+)$ values, the T_W/T_B effect is higher than for the data of references /5,6/. The present data can be correlated by the parameter $GPR1 = \frac{G(h_W^+)}{Pr^{0.44}} \left(\frac{T_W}{T_B}\right)^{0.68}$ (see Figures 24 to 27) while for the data of references /5,6/ the exponent of T_W/T_B was 0.5. The reasons for this discrepance are probably

the same which we think are producing a higher temperature effect on $R(h_W^+)$ (see the previous section 2.2). Figures 28 and 29 show the parameter

$$GPRO1 = \frac{G(h_W^+)}{Pr^{0.44}} \left(\frac{T_W}{T_B}\right)^{-0.68} \left(\frac{h}{0.01(r_2-r_1)}\right)^{-0.053} \quad (8)$$

versus h_W^+ for the two rods 18 and 19 respectively. The exponent of $\frac{h}{r_2-r_1}$ equal to -0.053 is suggested by the correlations published in references /5,6/. However Figures 28 and 29 show that here the required exponent of $\frac{h}{r_2-r_1}$ to bring the points together should be considerably higher especially for the rough tube "19". This is a further indication that the temperature profiles are not fully established. Indeed the $G(h_W^+)$ values are lower for the test sections which have a smaller l/D (l = heated length). The $G(h_W^+)$ values for fully established flow are of course higher (this means lower heat transfer coefficients) than those for not fully established flow. The GPRO1 values obtained here for the rods "18" and "19" are lower than those predicted by the general correlation of reference /5,6/ and this again indicates not fully established temperature profiles.

2.4 Friction factors. Laminar and transition flow ($Re_W \leq 3000$)

Table IV shows the isothermal and Table V the results with heat transfer for $Re_W \leq 3000$, which can be considered in laminar ($Re_W \leq 1800$) or in transition flow between laminar and turbulent ($1800 < Re_W \leq 3000$) (see Ref. /5,6/). Fig. 30 shows the friction factors for the rod "18" in the outer smooth tube of 40.4 mm I.D. versus the Reynolds number. The tests were performed with flow upwards and downwards, the test section being vertical. One can see from the Figure that the friction factors for the upward flow are much smaller than those for downward flow, especially at low Reynolds numbers. These large differences are given by the fact that during the evaluation of the friction factors the buoyancy effect was neglected. This has a negligible

effect for the turbulent flow in presence of large pressure differences, at low flows however the effect is considerable. The density difference of the flowing medium air, in the test section and in the pressure tubing outside the test section has been taken into account by the factor:

$$\pm\, g\Delta l\ (\rho_{Bm} - \rho_{PT}) \qquad (9)$$

in the friction equation (see Appendix I).
Figures 31 and 32 show the friction factors for the test section 18/40.4 corrected for the buoyancy effect for upward and downward flow respectively. The discrepancy has been eliminated.

Figure 33 gives the friction factor for the test section 19/40.4 (⊙) and for the test section 19/50 (⧖, ◇, ⊡). Also here the T_W/T_B effect, which increases the friction factors in the laminar flow region, is evident. In Figures 30 to 33 the lines given represent the theoretical friction factors for isothermal flow, namely for the turbulent flow the Prandtl-Nikuradse equation for flow in smooth tubes:

$$\frac{1}{\sqrt{8}} = 4\ \lg_{10}(Re\sqrt{f})\ -0.4 \qquad (10)$$

and for the laminar flow, the theoretical equation for flow in smooth annuli:

$$f = \frac{16}{Re}\ \frac{(1-\alpha)^2}{1+\alpha^2 - \frac{1-\alpha^2}{\ln\frac{1}{\alpha}}} \qquad (11)$$

with $\alpha = \frac{r_1}{r_2}$.

With laminar flow the friction factors with heat transfer are considerably higher than the theoretical isothermal values predicted by equation (11), while for rod "18" the experimental isothermal values are about 10% lower than the theoretical values. Rough surfaces behave in laminar flow like smooth surfaces, however since the friction factors are strongly affected by the definition of the hydraulic diameter, it is not said a

priori that the friction factors should be the same for rough and smooth surfaces. The definition of the hydraulic diameter used in the present work, using the volumetric diameter of the rough surface, appears appropriate for the considered roughness (h/b = 1, P/h = 9), thus this 10% discrepancy could be due to other causes as well, such as errors in the measurement of mass flow or pressure drop along the test section at very low flow, or excentricity of the inner rod, which produces a decrease of the friction factors /14/.

The temperature effect observed in the present experiment for the laminar flow is considerably higher than that obtained from calculations for smooth tubes /15,16/ and for annuli /17/, which were performed with variable fluid properties. However this is also the case of experimental data for flow in smooth tubes /18,19/. Dalle Donne and Bowditch found for laminar flow of air and helium in horizontal smooth tubes in presence of large temperature differences between wall and gas that the data could be correlated by the equation:

$$f_B = \frac{16}{Re_W} \qquad (12)$$

This equation was subsequently confirmed by an exhaustive literature survey of Taylor for many different gases and experimental data /19/. Dalle Donne and Bowditch gave also an intuitive explanation of their experimental findings:

"Very important from a theoretical point of view is the fact that friction coefficients have to be evaluated at the gas bulk temperature and Reynolds numbers at the wall temperature. This is probably due to the fact that friction coefficients depend upon a balance of forces parallel to the axis of the tube, i.e. pressure drops, which are related to the total cross section area and therefore must be evaluated at the gas bulk temperature, and shear stresses which must be evaluated at the wall temperature, where they are originated." /18/

Based on this explanation we tried to correlate our present friction factor data in laminar flow. Figures 34 to 36 show all the laminar friction factors of the present investigation in the plot f_B versus Re_W, whereby the friction factor f_B has been evaluated at the gas bulk temperature, while the Reynolds number has been evaluated at a temperature $T_{\bar{W}}$ average between the temperature of the inner rod surface and of the outer smooth surface, the average being weighted over the two surfaces:

$$T_{\bar{W}} = \frac{T_{W1}S_1 + T_{W2}S_2}{S_1 + S_2} \qquad (13)$$

As one can see from the graphs the temperature effect is practically eliminated, both for upward and downward flow. Thus any buoyancy effect on the shape of the velocity profile cannot account for the measured friction factor dependance on temperature.

The correlation found by experiment has, to the knowledge of the authors, not yet been verified by analysis, but it is rather important for the temperature and pressure drop calculation for the fuel elements of a Gas Cooled Fast Reactor, especially during accidental situations in presence of laminar flow and it was incorporated in the computer code SAGAPO, which is being developed for those calculations /20,21/.

At this point it should be noticed that the temperature effect on laminar friction factor found in the present work is considerably smaller than that obtained in references /5,6/. This is very likely due to the fact that experiments of references /5,6/ were performed with a vertical annulus with downward flow and no correction for buoyancy effects was introduced in the evaluation of the experimental data. A comparison of Figures 30 and 32 shows that in this case the temperature effect on laminar friction factors is largely overestimated.

2.5 Heat transfer results. Laminar and transition flow ($Re_W \leqslant 3000$)

Table V shows the heat transfer results for $Re_W \leqslant 3000$, which can be considered in laminar or in turbulent flow between laminar and turbulent ($Re_W \leqslant 3000$, see Ref. /5,6/).
Figure 37 shows the heat transfer results in terms of Nusselt number Nu_B versus the Graetz number Gz_B*. In the figure curves show the results obtained by the calculations of Coney and El-Shaarawi /22/ and Heaton, Reynolds and Kays /23/ for flow of gases (Pr=0.7) in annuli with $r_1/r_2=0.5$. An empirical line is shown as well, due to McAdams for laminar flow in tubes /24/ which closely approximates for $Gz_B < 0.08$ the theoretical relationship obtained by Graetz for laminar flow of fluids for parabolic distribution of velocity and uniform wall temperature. The scatter of the experimental points in figure 37 is considerable; a T_W/T_B effect is evident, the Nusselt number values being systematically lower for higher T_W/T_B ratios. Figure 38 shows the data in the plot $Nu_B(T_W/T_B)^{0.5}$ versus Gz_B. The systematic T_W/T_B effect has been eliminated, but the scatter remains high especially at the highest and lowest values of Gz_B. Figure 39 shows the same data in the plot Nu_B versus $Gz_{\bar{W}}$ where the definition of $Gz_{\bar{W}}$ is:

$$Gz_{\bar{W}} = \frac{1}{D\ Re_{\bar{W}} Pr} \qquad (14)$$

This definition of Graetz number has been suggested by the successful correlation of the friction factors in terms of f_B and $Re_{\bar{W}}$. In figure 39 the scatter is further reduced especially at the low values of $Gz_{\bar{W}}$. This is plausible, because the tests with the low values of $Gz_{\bar{W}}$ are for the higher flows of air in the test section, where the measurements of pressure drop, mass flow, gas temperature and power are more precise.

---

* The definition of Graetz number used in the present work is: $Gz = \frac{1}{D\ Re\ Pr}$, sometimes in the literature the other definition of Graetz number is used: $Gz = \frac{D\ Re\ Pr}{1}$.

Furthermore natural convection effects are more important at low flows. Indeed the points of Fig.39 for $Gz_{\overline{W}} > 0.02$ show that the Nusselt numbers for upward flow tend to be slightly higher than for downward flow, a fact which could be very well explained by the superposition of a certain amount of natural convection to the studied forced convection. Considering this natural convection effect and the relatively large experimental errors possible at very low flows, agreement of the experimental data with the McAdams line is surprisingly good for $Gz_{\overline{W}} > 0.02$. For $Gz_{\overline{W}} < 0.02$ the experimental Nusselt numbers are higher than those predicted by McAdams, but this is obviously due to the fact that for those tests the flow was not laminar (for $Gz_{\overline{W}} < 0.02$, $Re_{\overline{W}} > \approx 1800$). The other two correlations of Coney and El-Shaarawi /22/ and especially that of Heaton, Reynolds and Kays /23/ predict higher Nusselt numbers at low $Gz_{\overline{W}}$ values than the experimental data obtained in the present work.

3. Conclusions

Measurements of friction factor and heat transfer coefficients for two rods of 18.9 mm O.D. with two-dimensional roughness, each in two different outer smooth tubes have been performed in turbulent and laminar flow. In turbulent flow the isothermal friction factors of the rod 19 (with sharp edge ribs) agree well with the values predicted by our previously obtained general correlation /5,6/. The friction factors for the rod 18 with rounded edges are about 5% lower than those predicted by the general correlation. A correlation has been found for the isothermal $R(h^+)$ for rod 19 in the transition region between fully rough and hydraulically smooth flow.

The temperature effect both on the friction ($R(h^+)$ values) and heat transfer ($G(h^+)$ values) in turbulent flow is qualitatively the same as that predicted by our general correlation /5,6/, but it is more pronounced, the $G(h^+)$ values being lower than those of the general correlation. Both phenomena are very

likely due to the fact that the temperature profiles were not fully established in the present experiment, the test sections being too short (l/D was between 15 and 33).

The friction factors in laminar flow are 10% lower than the theoretical values for smooth annuli. This could be given by the uncertainty in the definition of the hydraulic diameter for a rough surface or by experimental error. If the data are corrected for the buoyancy effect, the temperature effect on friction factors both for upward and downward flow is accounted for by the use of the Reynolds number $Re_{\overline{W}}$ where the physical properties of air are evaluated at the temperature $T_{\overline{W}}$ average between the temperature of the inner rod surface and the outer smooth surface of the annulus, the average being weighted over the two surfaces. Also the heat transfer data in laminar flow are best correlated by the Graetz number $Gz_{\overline{W}}$ defined in the same way. The agreement of the laminar heat transfer data with the line suggested by McAdams for laminar flow in smooth tubes is reasonable.

Appendix I

Evaluation of the friction factor

For nonisothermal flow the acceleration due to temperature and pressure variation must be taken into account. For turbulent flow the equation

$$f = \frac{D}{2\Delta l \; p_m \; \gamma_m \; Ma_m^2} \left[p_1(1+\gamma_1 Ma_1^2) - p_2(1+\gamma_2 Ma_2^2) \right] \quad (15)$$

has been used (for its derivation see /25/).
Since the pressure differences in laminar flow are very small the error becomes substantial in single precision computation at the computer. Therefore the equation of Guggenheim /26/ has been used instead:

$$f = \frac{D}{2\Delta l} \left[\frac{\Delta p_{12}}{\rho_{Bm} u_{Bm}^2} - \frac{T_{B2}-T_{B1}}{T_{Bm}} - \ln \frac{p_1}{p_2} \right] \quad (16)$$

For nonisothermal vertical flow the measured pressure difference has to be corrected to allow for the difference between the gas density in the test section and that in the pressure tubes leading to the pressure transmitter. Depending on the direction of the flow a static balance gives

$$\Delta p_{12} = \Delta p_{measured} \pm g\Delta l(\rho_{Bm} - \rho_{PT}) \quad (17)$$

where + stands for downward and - for upward flow.

Acknowledgements

The authors acknowledge the help of P.Durand, F. Merschroth and K. Schorb in preparing the experimental apparatus and the test sections, in performing the experiments and in making some of the graphs.

Nomenclature

Geometrical parameters

A = cross section area of the annulus $[cm^2]$
b = width of the roughness $[cm]$
$D=2(r_2-r_1)$ = hydraulic diameter of the annulus $[cm]$
h = height of roughness rib $[cm]$
l = axial distance parallel to the flow $[cm]$
p = axial pitch of the repeated roughness ribs $[cm]$
r_1 = mean volumetric radius of the inner rough rod $[cm]$
r_2 = radius of outer smooth cylindrical surface of annulus $[cm]$
r_o = radius of the zero-shear-stress line in an annulus cross section $[cm]$
β = r_o/r_1
y = radial distance from the wall of the considered point $[cm]$
$\hat{y}$ = $r_o - r_1$ $[cm]$

Gas properties

c_p = specific heat at constant pressure $[cal/g^oC]$
k = thermal conductivity $[cal/cm\ s^oC]$
γ = specific heat ratio [dimensionless]
= kinematic viscosity $[cm^2/s]$
ρ = density $[g/cm^3]$

Temperatures $[^oK]$

T = temperature of the gas at the considered point
$T_B=T_E+(Q/Mc_p)$ = gas bulk temperature
T_E = gas temperature at test section entrance
T_W = wall temperature of the inner rough rod
T_{WM} = maximum wall temperature of the inner rough rod
$\bar{T_W}$ = average between the temperature of the inner rod surface and of the outer surface, weighted over the two surfaces
T_1 = gas bulk temperature of the inner region of the annulus

Other physical parameters

g = acceleration of gravity [cm/s^2]

h = convective heat transfer coefficient between inner tube surface and gas bulk [$cal/cm^2\ s^oC$]

M = mass flow rate of gas [g/s]

p = absolute static pressure of the gas [$dyne/cm^2$]

Q = quantity of heat given to the gas from entrance to the considered cross section of the annulus [cal/s]

q = heat flux at the inner rough surface [cal/cm^2s]

u = velocity of the gas [cm/s]

$u_B = M/A\rho_B$ = velocity of the bulk of the gas [cm/s]

u_1 = velocity of the bulk of the gas in the inner region of the annulus [cm/s]

u_2 = velocity of the bulk of the gas in the outer region of the annulus [cm/s]

$u^* = \sqrt{\tau/\rho}$ = friction velocity [cm/s]

τ = shear stress at the inner rough surface [$dyne/cm^2$]

Dimensionless Groups

A_s = slope of the logarithmic velocity profile relative to a smooth surface

$f = 2\tau/\rho_B u^2_B$ = friction coefficient (or friction factor) evaluated at the gas bulk temperature T_B

f_o = friction factor for circular smooth pipes (from Prandtl-Nikuradse universal law of friction for smooth tubes)

$G(h_W^+)$ = constant in the turbulent logarithmic temperature distribution, equal to dimensionless temperature at the tip of the roughness ribs

$G(h_W^+)^*$ = value of $G(h^+)$ defined in Ref./5,6/

$GPR = G(h_W^+)/Pr^{0.44}$

$GPR^* = G(h_W^+)^*/Pr^{0.44}$

GPR1 $= G(h_W^+) / \left[Pr^{0.44} (T_W/T_B)^{0.68} \right]$

GPRO1 $= G(h_W^+) / \left[Pr^{0.44} (T_W/T_B)^{0.68} \left(\frac{h}{0.01(r_2-r_1)} \right)^{0.053} \right]$

$Gz = \frac{1}{D\ Re\ Pr}$ = Graetz number

$Gz_{\bar{W}} = \frac{1}{D\ Re_{\bar{W}}\ Pr}$ = Graetz number evaluated at the temperature $T_{\bar{W}}$

$h^+ = \frac{h\ u^*}{\nu_B}$ = dimensionless height of roughness ribs= roughness cavity Reynolds number

$h_W^+ = \frac{h\ u^*}{\nu_W}$ = dimensionless height of roughness ribs evaluated at the wall temperature

$Ma = u_B / \sqrt{\gamma p / \rho_B}$ = Mach number evaluated at the gas bulk temperature T_B

$Nu_B = hD/k_B$ = Nusselt number evaluated at the gas bulk temperature T_B

$Pr = \frac{\nu_B \rho_B c_{PB}}{k_B}$ = Prandtl number evaluated at the gas bulk temperatur T_B

$Re = \frac{u_B\ D}{\nu_B}$ = Reynolds number evaluated at the gas bulk temperatur T_B

$Re_{\bar{W}} = \frac{u_B\ D}{\nu_{\bar{W}}}$ = Reynolds number evaluated at the temperature $T_{\bar{W}}$

$R(h^+)$ = constant in the turbulent logarithmic velocity distribution, equal to dimensionless velocity at the tip of the roughness ribs, isothermal flow

$R(h_W^+)$ = the same as before in nonisothermal flow

$R(h^+)1 = R(h_W^+) - \frac{0.055}{h/\hat{y}} \left(\frac{T_W}{T_1} \right)^{1.5}$

$R(h^+)01 = R(h^+)1 - 0.4 \ln \left(\frac{h/\hat{y}}{0.01} \right)$

$R(\infty)$ = value of $R(h^+)$ in the region of fully rough flow, where $R(h^+)$ is independent of h^+

$St = h/\rho_B c_{pB} u_B$ = Stanton number evaluated at the bulk gas temperature T_B

$t^+ = \frac{(T_W - T)\rho_B c_{pB} u^*}{q}$ = dimensionless gas temperature

$u^+ = u/u^*$ = dimensionless gas velocity

$y^+ = yu^*/\nu_B$ = dimensionless radial distance from the wall

Subscripts

No subscripts means generally that the gas physical properties have been evaluated at the gas bulk temperature T_B

B = gas properties evaluated at the gas bulk temperature T_B

W = gas properties evaluated at the wall temperature T_W

$\overline{W}$ = gas properties evaluated at the temperature $T_{\overline{W}}$ average between the temperature of the inner rod surface and the outer smooth surface, the average being weighted over the two surfaces

R = it refers to a rough surface

1,2 = it refers to the inner and outer regions respectively of an annulus.
In equations (15) and (16) it means two subsequent cross sections of annulus (in axial direction)

M = maximum

m = mean

PT = pressure tubing

REFERENCES

/1/ M.Dalle Donne and E.Meerwald, Heat Transfer from surfaces roughened by thread-type ribs at high temperatures, in Proceedings of the 1970 Heat Transfer and Fluid Mechanics Institute, Stanford Univ. Press, Stanford Calif., June 1970; see also "Zürich Club" Gas Cooled Fast Reactor Heat Transfer Meeting, Würenlingen, Switzerland.

/2/ E.Meerwald, Druckverlust und Wärmeübergang an glatten und rauhen Flächen bei hohen Temperaturen und turbulenter Strömung und deren Darstellung durch universelle Gesetze. KFK-Ext. 4/71-29 Kernforschungszentrum Karlsruhe, 1971.

/3/ M. Dalle Donne and E.Meerwald, Heat transfer from rough surfaces, latest results, ENEA Coordinating Group on Gas-Cooled Fast Reactor Development, Heat Transfer Specialist Meeting, Windscale, England, 1972.

/4/ M. Dalle Donne and E.Meerwald, Heat transfer and friction correlations for surfaces roughened by transversal ribs, NEA Coordinating Group on Gas-Cooled Fast Reactor Development, Core Performance Specialist Meeting, Studsvik, Sweden, 1973.

/5/ M.Dalle Donne, Wärmeübergang von rauhen Oberflächen, KFK 2397, EUR 5506d, Januar 1977.

/6/ M.Dalle Donne and L.Meyer, Turbulent convective heat transfer from rough surfaces with two-dimensional rectangular ribs, Int. J. Heat Mass Transfer, Vol.20, pp 583-620, 1977

/7/ M. Dalle Donne and L.Meyer, Experimental heat transfer and pressure drops of rods with three dimentional roughness in annuli, NEA Coordinating Group on Gas-Cooled Fast Reactor Development, Heat Transfer Specialist Meeting, Petten, Holland, 1975.

/8/ K. Maubach, Reibungsgesetze turbulenter Strömungen in geschlossenen glatten und rauhen Kanälen von beliebigem Querschnitt, KFK-Ext. 4/69-22, Kernforschungszentrum Karlsruhe, 1969.

/9/ M.Dalle Donne, J.Marek, A. Martelli and K.Rehme, BR2 bundle mockup heat transfer experiments, Nuclear Engineering and Design Vol.40, pp 143-156, January 1977.

/10/ K.Rehme, Experimentelle thermo-und fluiddynamische Untersuchungen an einem 19-Stabbündel mit künstlichen Oberflächenrauhigkeiten, KFK 2313, August 1976.

/11/ A.Martelli, Thermo-und fluiddynamische Analyse von gasgekühlten Brennelementbündeln, KFK 2436, EUR 5508d, März 1977.

/12/ A.Martelli, K.Rehme, Vergleich von Rechnungen und Messungen der Druck-und Wandtemperaturverteilung in einem gasgekühlten Stabbündel, Reaktortagung Mannheim, März 1977, Tagungsbericht S.19-22.

/13/ W.J. White, L. White, The effect of rib profile on heat transfer and pressure loss properties of transversely ribbed roughened surfaces, Proc. ASME Winter Meeting, New York Dec. 1970, Argumentation of Convective Heat and Mass Transfer.

/14/ W. Tiedt, Berechnung des laminaren und turbulenten Reibungswiderstandes konzentrischer und exzentrischer Ringspalte, Technischer Bericht Nr.4, Institut für Hydraulik und Hydrologie der TH Darmstadt, see also Chemiker Zeitung/ Chemische Apparatur 90. Jahrgang (1966) 91.Jahrgang (1967)

/15/ R.G. Deissler, Analytical investigation of fully developed laminar flow in tubes with heat transfer with fluid properties variable along the radius, NACA TN 2410, 1951

/16/ P.M. Worsoe-Schmidt and G.Leppert, Heat transfer and friction for laminar flow of gas in a circular tube at high heating rate, Int. J. Heat Mass Transfer, Vol.8, (1965), pp.1281-1301

/17/ R.W. Shumway and D.M. McEligot, Heated laminar gas flow in annuli with temperature-dependent transport properties, Nuclear Science and Engineering, 46, 394-407 (1971)

/18/ M. Dalle Donne, F.W. Bowditch, Experimental local transfer and friction coefficients for subsonic laminar transitional and turbulent flow of air or helium in a tube at high temperatures. Dragon Project Report 184, A.E.E. Winfrith, Dorchester, Dorset, England, 1963.

/19/ M.F. Taylor, A method of correlating local and average friction coefficients for both laminar and turbulent flow of gases through a smooth tube with surface to fluid bulk temperature ratios from 0.35 to 7.35, Int. Journal Heat Mass Transfer 10, 1123-1128, 1967.

/20/ A. Martelli, Thermo- und fluiddynamische Analyse von gasgekühlten Brennelementbündeln, KFK 2436, EUR 5508d, März 1977

/21/ A. Martelli, SAGAPO. A computer code for the thermo-fluiddynamic analysis of gas cooled fuel element bundles, KFK 2483, EUR 5510e, October 1977

/22/ J. Coney and M. El-Shaarawi, Finite difference analysis for laminar flow heat transfer in concentric annuli with simultaneously developing hydrodynamic and thermal boundary layers, Int. J. Numerical Methods in Engineering, 9, 17-38, 1975.

/23/ H. Heaton, W. Reynolds and W. Kays, Heat transfer in annular passages. Simultaneous development of velocity and temperature fields in laminar flow, Int. J. Heat Mass Transfer, 7, 763-781, 1964.

/24/ W. McAdams, Heat Transmission, pp.230-232, Third Edition, McGraw Hill, New York.

/25/ M. Dalle Donne and E. Meerwald, Experimental local heat transfer and average friction coefficients for subsonic turbulent flow of air in an annulus at high temperature, Int. J. Heat Mass Transfer, 9, 1361-1376, 1966.

/26/ E.A. Guggenheim, Compressible flow of perfect gas with heat input distributed symmetrically about middle of channel, Report MT-137, 1945, Reprinted July 1961 as Atomic Energy Canada Report No. AECL-1279.

Table I

Rod number	p [mm]	h=b [mm]	$\frac{p-b}{h}$	Rib edges	Rough rod length [mm]	Outer smooth tube diameter [mm]	r_1/r_2	l/D	R(∞)	$h/\hat{y}$	$\frac{h}{r_2-r_1}$
18	2.7	0.3	8	rounded	735	40.4	0.454	33.3	3.80	0.039	0.027
						50.0	0.367	23.2	3.40	0.028	0.019
19	2.7	0.3	8	sharp	436	40.4	0.454	21.6	3.42	0.040	0.027
						50.0	0.367	15.0	3.10	0.028	0.019

Table II

VERS.NR.	RE	F	F*RE	BETA	F2/F0	U2/U1	AS	RE2	RE1	F2	F1	F1/F0	H/Y	H+	R(H+)	RHC1
18-41- 1	1.36E+05	.00993	1351.7	.8330	1.0763	1.080	2.408	8.01E+04	2.59E+05	.00508.02074	5.577	.039	183.0	3.66	3.31
18-41- 2	1.06E+05	.01010	1067.4	.8280	1.0753	1.077	2.411	6.36E+04	1.98E+05	.00533.02073	5.290	.040	142.0	3.90	3.35
18-41- 3	8.16E+04	.01052	858.3	.8257	1.0749	1.077	2.413	4.97E+04	1.52E+05	.00563.02143	5.186	.040	111.5	3.76	3.20
18-41- 4	6.31E+04	.01080	681.3	.8212	1.0740	1.074	2.416	3.93E+04	1.16E+05	.00593.02163	4.953	.041	86.7	3.74	3.18
18-41- 5	4.93E+04	.01103	544.3	.8162	1.0732	1.071	2.418	3.14E+04	8.88E+04	.00624.02170	4.703	.041	67.9	3.77	3.20
18-41- 6	3.91E+04	.01126	440.7	.8113	1.0724	1.068	2.421	2.55E+04	6.93E+04	.00655.02173	4.466	.042	53.9	3.80	3.23
18-41- 7	3.14E+04	.01160	364.6	.8078	1.0719	1.066	2.423	2.08E+04	5.50E+04	.00688.02209	4.316	.042	43.7	3.75	3.17
18-41- 8	2.56E+04	.01172	300.5	.8018	1.0710	1.062	2.426	1.73E+04	4.39E+04	.00718.02180	4.051	.043	35.4	3.86	3.28
18-41- 9	2.14E+04	.01109	236.9	.7861	1.0689	1.048	2.430	1.53E+04	3.46E+04	.00740.01927	3.392	.045	27.9	4.59	3.99
18-41-10	1.69E+04	.01201	203.3	.7892	1.0693	1.053	2.432	1.20E+04	2.77E+04	.00787.02119	3.540	.044	23.1	4.10	3.50
18-41-11	1.37E+04	.01196	163.5	.7793	1.0682	1.045	2.435	1.01E+04	2.16E+04	.00824.02020	3.180	.046	18.3	4.41	3.81
18-41-12	2.31E+05	.00960	2221.7	.8427	1.0787	1.086	2.403	1.29E+05	4.55E+05	.00460.02075	6.198	.038	310.9	3.79	3.25
18-41-13	1.61E+05	.00984	1581.1	.8363	1.0771	1.082	2.406	9.29E+04	3.10E+05	.00492.02080	5.783	.039	216.3	3.82	3.28
18-41-14	1.21E+05	.01014	1226.1	.8322	1.0762	1.080	2.409	7.14E+04	2.30E+05	.00520.02112	5.549	.039	164.1	3.78	3.23
18-41-15	9.22E+04	.01039	958.2	.8277	1.0753	1.078	2.412	5.57E+04	1.73E+05	.00549.02131	5.292	.040	125.7	3.77	3.21
18-41-16	7.22E+04	.01070	772.0	.8241	1.0746	1.076	2.414	4.43E+04	1.33E+05	.00577.02166	5.109	.040	99.2	3.72	3.16
18-41-23	1.38E+05	.01010	1394.0	.8354	1.0769	1.083	2.408	8.03E+04	2.65E+05	.00508.02128	5.746	.039	187.9	3.72	3.17
18-41-24	1.02E+05	.01033	1049.8	.8297	1.0756	1.079	2.411	6.08E+04	1.91E+05	.00539.02135	5.412	.040	138.6	3.74	3.19
18-51- 1	3.34E+05	.00803	2681.7	.7999	1.0777	1.071	2.398	1.98E+05	7.04E+05	.00423.01850	5.975	.028	295.8	3.48	3.07
18-51- 2	2.46E+05	.00827	2031.0	.7945	1.0768	1.069	2.400	1.49E+05	5.09E+05	.00447.01871	5.703	.028	218.9	3.45	3.04
18-51- 3	1.90E+05	.00850	1613.5	.7903	1.0760	1.068	2.402	1.17E+05	3.88E+05	.00469.01897	5.504	.028	170.4	3.41	2.99
18-51- 4	1.49E+05	.00873	1301.6	.7862	1.0754	1.066	2.404	9.33E+04	3.01E+05	.00491.01921	5.313	.029	134.7	3.37	2.95
18-51- 5	1.20E+05	.00891	1066.5	.7816	1.0747	1.064	2.406	7.61E+04	2.38E+05	.00512.01931	5.108	.029	108.4	3.38	2.95
18-51- 6	9.63E+04	.00908	874.3	.7766	1.0740	1.061	2.408	6.24E+04	1.89E+05	.00535.01933	4.886	.029	87.3	3.40	2.97
18-51- 7	7.96E+04	.00924	736.0	.7722	1.0733	1.059	2.410	5.24E+04	1.54E+05	.00555.01937	4.700	.030	72.4	3.43	2.99
18-51- 8	6.37E+04	.00945	602.3	.7671	1.0726	1.057	2.412	4.27E+04	1.21E+05	.00581.01945	4.495	.030	58.0	3.44	3.00
18-51- 9	5.26E+04	.00960	505.3	.7617	1.0720	1.054	2.414	3.59E+04	9.82E+04	.00604.01937	4.287	.030	47.9	3.50	3.05
18-51-33	5.34E+04	.00972	519.1	.7646	1.0723	1.056	2.413	3.60E+04	1.01E+05	.00604.01984	4.414	.030	49.1	3.36	2.92
18-51-34	4.24E+04	.00998	423.0	.7592	1.0716	1.053	2.415	2.91E+04	7.85E+04	.00634.01995	4.213	.031	39.2	3.37	2.92
18-51-35	3.37E+04	.01008	340.1	.7506	1.0706	1.048	2.418	2.38E+04	6.07E+04	.00664.01950	3.895	.031	30.9	3.54	3.09
18-51-36	2.72E+04	.01016	276.3	.7416	1.0696	1.043	2.420	1.97E+04	4.75E+04	.00695.01856	3.586	.032	24.6	3.75	3.29
18-51-37	2.22E+04	.01018	226.3	.7314	1.0686	1.036	2.422	1.66E+04	3.75E+04	.00725.01821	3.265	.033	19.7	4.04	3.56
18-51-38	1.80E+04	.01010	182.1	.7177	1.0673	1.028	2.425	1.40E+04	2.90E+04	.00756.01702	2.875	.034	15.5	4.51	4.01
19-41- 1	1.21E+05	.01049	1268.5	.8364	1.0765	1.085	2.408	7.00E+04	2.33E+05	.00523.02222	5.852	.039	168.1	3.50	2.96
19-41- 2	8.90E+04	.01089	969.0	.8325	1.0761	1.083	2.411	5.26E+04	1.69E+05	.00556.02276	5.630	.039	125.2	3.42	2.87
19-41- 3	7.02E+04	.01118	785.1	.8289	1.0754	1.082	2.413	4.22E+04	1.32E+05	.00584.02309	5.431	.040	99.5	3.38	2.83
19-41- 4	5.37E+04	.01143	614.3	.8236	1.0744	1.078	2.416	3.31E+04	9.91E+04	.00617.02315	5.135	.040	76.3	3.40	2.85
19-41- 5	4.30E+04	.01168	502.9	.8195	1.0737	1.076	2.419	2.70E+04	7.82E+04	.00647.02331	4.917	.041	61.3	3.40	2.84
19-41- 6	3.42E+04	.01196	409.5	.8150	1.0730	1.073	2.422	2.19E+04	6.13E+04	.00679.02346	4.695	.041	49.0	3.41	2.84
19-41- 7	2.79E+04	.01219	340.5	.8106	1.0723	1.070	2.424	1.82E+04	4.92E+04	.00710.02352	4.485	.042	40.0	3.43	2.86
19-41- 8	2.24E+04	.01236	277.3	.8046	1.0714	1.066	2.427	1.50E+04	3.88E+04	.00745.02328	4.205	.042	32.0	3.52	2.95
19-41- 9	1.82E+04	.01259	229.6	.7993	1.0707	1.062	2.430	1.25E+04	3.09E+04	.00781.02320	3.978	.043	26.0	3.58	3.00
19-41-10	1.50E+04	.01264	189.4	.7921	1.0697	1.056	2.433	1.05E+04	2.48E+04	.00815.02260	3.676	.044	21.1	3.76	3.17
19-41-11	1.19E+04	.01269	151.4	.7829	1.0686	1.049	2.436	8.67E+03	1.91E+04	.00858.02180	3.328	.045	16.6	4.01	3.41
19-41-12	9.82E+03	.01235	121.2	.7693	1.0671	1.037	2.439	7.48E+03	1.50E+04	.00892.01954	2.865	.047	13.1	4.56	3.94
19-41-13	8.14E+03	.01248	101.5	.7618	1.0664	1.032	2.442	6.35E+03	1.21E+04	.00932.01944	2.643	.048	10.7	4.76	4.13
19-41-14	7.01E+03	.01227	86.0	.7507	1.0655	1.023	2.444	5.67E+03	9.96E+03	.00962.01813	2.344	.050	9.0	5.22	4.58
19-41-15	6.19E+03	.01234	76.4	.7447	1.0651	1.018	2.446	5.10E+03	8.60E+03	.00991.01768	2.198	.051	7.8	5.41	4.75
19-41-16	5.44E+03	.01193	64.9	.7298	1.0643	1.007	2.447	4.68E+03	7.13E+03	.01015.01584	1.871	.054	6.6	6.17	5.50
19-41-17	4.77E+03	.01146	54.7	.7117	1.0633	0.994	2.448	4.31E+03	5.79E+03	.01039.01380	1.540	.058	5.4	7.18	6.48

Table II (contd.)

VERS.NR.	RE	F	F*RE	BETA	F2/F0	U2/U1	AS	RE2	RE1	F2	F1	F1/F0	H/Y	H+	R(H+)	RHO1
19-41-18	4.07E+03	.01063	43.3	.6803	1.0619	0.974	2.447	3.97E+03	4.28E+03	.01063	.01066	1.091	.066	4.1	9.24	8.49
19-41-20	3.00E+05	.01000	2995.8	.8532	1.0816	1.096	2.398	1.59E+05	6.10E+05	.00443	.02243	7.063	.037	418.1	3.34	2.81
19-41-21	2.05E+05	.01019	2090.8	.8465	1.0796	1.092	2.402	1.13E+05	4.09E+05	.00474	.02236	6.547	.038	285.8	3.40	2.87
19-41-22	1.44E+05	.01039	1497.8	.8399	1.0779	1.087	2.406	8.20E+04	2.81E+05	.00506	.02228	6.081	.039	200.6	3.46	2.92
19-41-23	1.09E+05	.01061	1155.9	.8349	1.0767	1.084	2.409	6.36E+04	2.09E+05	.00534	.02236	5.765	.039	151.9	3.48	2.94
19-41-24	8.60E+04	.01088	935.8	.8315	1.0760	1.083	2.411	5.10E+04	1.63E+05	.00560	.02267	5.565	.039	120.7	3.44	2.89
19-41-25	6.82E+04	.01112	758.4	.8273	1.0751	1.080	2.414	4.13E+04	1.27E+05	.00587	.02281	5.330	.040	96.1	3.44	2.89
19-51- 1	2.24E+05	.00865	1941.8	.7987	1.0777	1.073	2.400	1.34E+05	4.71E+05	.00457	.01989	5.978	.028	205.9	3.11	2.70
19-51- 2	1.78E+05	.00889	1582.4	.7952	1.0769	1.072	2.402	1.08E+05	3.70E+05	.00477	.02019	5.805	.028	164.7	3.06	2.65
19-51- 3	1.43E+05	.00907	1300.4	.7910	1.0763	1.070	2.404	8.81E+04	2.94E+05	.00497	.02033	5.597	.028	133.1	3.05	2.64
19-51- 4	1.15E+05	.00927	1065.4	.7868	1.0756	1.068	2.405	7.18E+04	2.32E+05	.00519	.02049	5.393	.029	107.1	3.04	2.62
19-51- 5	9.35E+04	.00940	878.1	.7813	1.0747	1.065	2.407	5.96E+04	1.86E+05	.00540	.02037	5.131	.029	86.9	3.11	2.68
19-51- 6	7.44E+04	.00965	718.5	.7770	1.0741	1.064	2.409	4.82E+04	1.46E+05	.00566	.02062	4.951	.029	69.7	3.08	2.65
19-51- 7	6.23E+04	.00993	619.0	.7748	1.0738	1.063	2.411	4.07E+04	1.21E+05	.00588	.02105	4.868	.029	59.0	2.99	2.56
19-51- 8	4.93E+04	.01001	493.4	.7665	1.0726	1.058	2.414	3.31E+04	9.34E+04	.00616	.02057	4.506	.030	46.2	3.16	2.72
19-51- 9	3.14E+05	.00832	2609.7	.8032	1.0788	1.075	2.398	1.83E+05	6.68E+05	.00429	.01939	6.206	.028	284.3	3.21	2.80
19-51-10	3.60E+04	.01019	367.0	.7558	1.0713	1.052	2.417	2.50E+04	6.59E+04	.00657	.02011	4.088	.031	33.4	3.35	2.90
19-51-11	4.06E+04	.01038	421.7	.7647	1.0722	1.058	2.415	2.74E+04	7.65E+04	.00643	.02123	4.457	.030	38.6	3.02	2.58
19-51-12	3.22E+04	.01057	340.5	.7575	1.0714	1.054	2.418	2.23E+04	5.93E+04	.00676	.02103	4.177	.031	30.5	3.12	2.67
19-51-13	2.64E+04	.01069	282.6	.7503	1.0706	1.049	2.420	1.87E+04	4.75E+04	.00705	.02067	3.910	.031	24.9	3.25	2.80
19-51-14	2.12E+04	.01080	228.6	.7411	1.0696	1.043	2.422	1.54E+04	3.69E+04	.00739	.02013	3.596	.032	19.7	3.45	2.98
19-51-15	1.78E+04	.01077	191.9	.7313	1.0686	1.037	2.424	1.33E+04	3.00E+04	.00766	.01928	3.282	.033	16.3	3.74	3.27
19-51-16	1.45E+04	.01075	155.4	.7188	1.0674	1.029	2.427	1.12E+04	2.34E+04	.00801	.01822	2.922	.034	12.9	4.13	3.64
19-51-17	1.16E+04	.01086	125.8	.7075	1.0664	1.022	2.429	9.23E+03	1.80E+04	.00842	.01751	2.635	.035	10.2	4.43	3.93
19-51-18	9.57E+03	.01077	103.1	.6927	1.0652	1.013	2.431	7.91E+03	1.41E+04	.00877	.01622	2.295	.037	8.1	4.97	4.45
19-51-19	7.80E+03	.01092	85.2	.6816	1.0647	1.006	2.433	6.62E+03	1.10E+04	.00920	.01561	2.072	.038	6.5	5.29	4.75
19-51-20	6.52E+03	.01053	68.7	.6568	1.0633	0.991	2.434	5.84E+03	8.36E+03	.00952	.01328	1.639	.041	5.1	6.47	5.90
19-51-21	5.28E+03	.01030	54.3	.6310	1.0617	0.976	2.435	4.99E+03	6.07E+03	.00994	.01128	1.274	.046	3.8	7.77	7.16
19-51-22	4.29E+03	.01049	45.0	.6160	1.0610	0.968	2.436	4.17E+03	4.62E+03	.01047	.01059	1.109	.048	3.0	8.45	7.82

Table III

VERS.NR.	RE*E4	REW*E4	F	RE*F	ST	TW/TE	TW/TB	TW/T1	BETA	AS	H/Y	H+	H+W	RH+	RH+1	RH+01	GPR	GPR*	GPR1	GPR01
18-41- 1	32.480	20.516	.00896	2909.5	.00395	1.36	1.30	1.28	.8406	2.400	.039	411.9	267.7	4.15	3.94	3.40	19.8	20.2	16.5	15.6
18-41- 2	21.850	13.815	.00933	2038.4	.00432	1.36	1.30	1.29	.8360	2.403	.039	281.5	182.3	4.03	3.81	3.27	18.0	18.0	15.0	14.3
18-41- 3	15.174	9.512	.00950	1441.2	.00460	1.37	1.31	1.29	.8283	2.407	.040	194.1	125.1	4.12	3.91	3.36	16.3	16.4	13.6	12.9
18-41- 4	11.020	6.839	.00975	1074.1	.00496	1.39	1.32	1.29	.8225	2.410	.040	141.2	90.3	4.12	3.90	3.35	14.7	14.6	12.2	11.6
18-41- 5	8.507	5.329	.01006	856.0	.00520	1.38	1.31	1.29	.8189	2.412	.041	109.9	71.1	4.05	3.85	3.28	13.9	13.8	11.5	10.9
18-41- 6	6.635	4.096	.01031	684.2	.00533	1.40	1.32	1.30	.8143	2.415	.041	85.9	54.9	4.04	3.83	3.26	13.4	13.4	11.1	10.5
18-41- 7	5.359	3.321	.01052	563.6	.00552	1.40	1.32	1.29	.8099	2.417	.042	69.4	44.6	4.05	3.85	3.28	12.7	12.7	10.5	10.0
18-41-12	12.679	8.053	.00956	1212.6	.00476	1.36	1.30	1.28	.8240	2.409	.040	161.3	105.6	4.20	4.00	3.45	15.4	15.5	12.9	12.2
18-41-13	15.418	9.704	.00937	1444.2	.00454	1.37	1.31	1.29	.8270	2.407	.040	195.5	126.5	4.23	4.02	3.46	16.4	16.4	13.7	13.0
18-41-14	19.031	12.078	.00920	1750.5	.00440	1.36	1.30	1.28	.8302	2.406	.040	239.9	157.0	4.26	4.06	3.51	16.9	17.2	14.1	13.4
18-41-15	25.157	15.914	.00916	2304.2	.00407	1.36	1.30	1.28	.8366	2.403	.039	319.2	208.8	4.15	3.94	3.40	18.9	19.5	15.8	15.0
18-41-16	31.826	20.258	.00904	2877.7	.00391	1.35	1.30	1.28	.8412	2.400	.038	405.8	265.8	4.10	3.89	3.35	20.2	20.6	16.9	16.0
18-41-25	5.313	3.306	.01044	554.7	.00545	1.39	1.31	1.27	.8058	2.418	.042	66.6	44.3	4.30	4.12	3.54	11.8	12.9	9.8	9.3
18-41-26	4.383	2.727	.01060	464.5	.00554	1.39	1.31	1.28	.8028	2.419	.043	55.7	36.5	4.25	4.06	3.48	12.1	12.5	10.0	9.5
18-41-27	3.642	2.257	.01065	388.0	.00563	1.40	1.32	1.27	.7958	2.422	.044	45.4	30.0	4.44	4.27	3.68	11.2	12.1	9.3	8.8
18-41-28	2.966	1.811	.01086	322.0	.00572	1.42	1.33	1.28	.7915	2.424	.044	37.1	24.1	4.44	4.25	3.65	11.2	11.8	9.3	8.8
18-41- 8	28.775	10.351	.00855	2459.9	.00380	2.03	1.83	1.75	.8285	2.402	.040	337.8	131.1	4.61	3.71	3.16	20.1	20.4	13.3	12.6
18-41- 9	19.575	7.095	.00875	1713.1	.00402	2.04	1.82	1.74	.8210	2.405	.041	228.6	89.9	4.66	3.80	3.24	18.6	18.9	12.4	11.7
18-41-10	13.387	4.806	.00897	1201.3	.00428	2.07	1.83	1.74	.8130	2.408	.042	155.2	60.9	4.71	3.87	3.30	17.0	17.2	11.3	10.7
18-41-11	10.007	3.638	.00918	918.4	.00451	2.07	1.82	1.72	.8069	2.411	.042	115.6	46.2	4.73	3.94	3.36	15.8	16.0	10.5	10.0
18-41-17	7.626	2.805	.00967	737.7	.00462	2.05	1.80	1.68	.8027	2.413	.043	87.7	36.6	4.68	3.97	3.38	15.3	16.1	10.2	9.7
18-41-18	6.175	2.253	.00937	578.6	.00459	2.07	1.81	1.67	.7894	2.417	.045	67.4	28.4	5.24	4.57	3.97	14.5	15.4	9.7	9.2
18-41-19	5.092	1.875	.00957	487.0	.00470	2.06	1.80	1.66	.7854	2.418	.045	55.6	23.7	5.24	4.60	3.99	14.0	14.9	9.4	8.9
18-41-29	8.176	2.980	.00946	773.6	.00458	2.07	1.81	1.70	.8034	2.413	.043	94.2	38.4	4.71	3.96	3.38	15.5	16.0	10.3	9.8
18-41-20	27.879	7.355	.00803	2237.3	.00341	2.56	2.22	2.03	.8132	2.404	.042	291.9	90.0	5.46	4.10	3.52	21.6	22.7	12.6	11.9
18-41-21	18.619	4.844	.00824	1533.6	.00355	2.61	2.24	2.02	.8034	2.408	.043	190.9	59.4	5.61	4.30	3.72	20.3	21.5	11.7	11.1
18-41-22	12.659	3.293	.00839	1062.6	.00373	2.64	2.24	1.99	.7923	2.411	.044	126.4	40.2	5.83	4.61	4.01	18.6	19.9	10.8	10.2
18-41-31	2.937	0.763	.00916	269.0	.00401	2.74	2.24	1.94	.7472	2.424	.051	27.0	9.0	6.75	5.78	5.12	15.9	17.1	9.2	8.7
18-51-10	32.506	19.815	.00755	2454.1	.00401	1.36	1.33	1.30	.7852	2.400	.029	264.7	168.3	4.12	3.81	3.39	16.2	16.7	13.3	12.9
18-51-11	24.244	14.838	.00785	1904.1	.00423	1.36	1.33	1.29	.7815	2.401	.029	199.7	127.9	4.00	3.70	3.27	15.1	15.7	12.5	12.0
18-51-12	18.681	11.435	.00812	1516.8	.00444	1.36	1.33	1.29	.7780	2.403	.029	155.4	99.6	3.90	3.60	3.17	14.3	14.8	11.8	11.4
18-51-13	14.704	8.980	.00833	1224.7	.00459	1.37	1.33	1.29	.7734	2.405	.030	122.8	78.7	3.87	3.57	3.14	13.6	14.1	11.2	10.8
18-51-14	11.745	7.141	.00847	995.2	.00472	1.37	1.33	1.29	.7677	2.407	.030	97.9	62.5	3.91	3.62	3.18	13.0	13.5	10.7	10.3
18-51-15	9.448	5.710	.00863	815.8	.00499	1.38	1.34	1.30	.7622	2.408	.030	78.5	50.1	3.95	3.66	3.21	11.8	12.3	9.7	9.4
18-51-16	7.639	4.646	.00882	673.4	.00515	1.38	1.33	1.29	.7570	2.410	.031	63.5	40.8	3.97	3.69	3.24	11.2	11.7	9.2	8.9
18-51-17	6.113	3.715	.00896	547.8	.00527	1.38	1.33	1.29	.7502	2.412	.031	50.5	32.6	4.06	3.79	3.33	10.7	11.1	8.8	8.5
18-51-17	6.129	3.706	.00897	550.1	.00522	1.38	1.34	1.29	.7504	2.412	.031	50.6	32.5	4.05	3.78	3.32	10.8	11.4	8.9	8.6
18-51-18	5.070	3.065	.00913	462.9	.00533	1.38	1.34	1.29	.7447	2.414	.032	41.7	26.9	4.12	3.85	3.39	10.3	10.9	8.5	8.2
18-51-19	33.453	20.179	.00755	2525.6	.00391	1.37	1.34	1.30	.7860	2.399	.029	272.3	171.7	4.11	3.79	3.37	16.7	17.4	13.7	13.3
18-51-20	32.250	10.601	.00707	2279.7	.00366	2.06	1.93	1.80	.7669	2.400	.030	233.3	86.4	4.86	3.56	3.12	17.4	18.0	11.2	10.8
18-51-21	23.738	7.900	.00736	1746.9	.00387	2.05	1.91	1.78	.7628	2.402	.031	173.5	65.3	4.72	3.48	3.03	16.4	16.9	10.5	10.2
18-51-22	18.151	6.110	.00759	1377.1	.00406	2.04	1.90	1.76	.7575	2.404	.031	132.7	51.0	4.69	3.51	3.06	15.3	16.0	9.9	9.6
18-51-23	14.224	4.786	.00777	1105.1	.00421	2.05	1.90	1.75	.7514	2.405	.031	103.4	40.1	4.72	3.58	3.12	14.4	15.1	9.3	9.0
18-51-24	11.383	3.794	.00789	897.9	.00429	2.07	1.91	1.75	.7448	2.407	.032	82.0	31.7	4.80	3.67	3.21	13.9	14.6	9.0	8.7
18-51-25	9.141	3.045	.00807	737.4	.00438	2.07	1.91	1.75	.7390	2.409	.032	65.6	25.5	4.83	3.74	3.26	13.5	14.2	8.7	8.4
18-51-26	7.382	2.461	.00819	604.9	.00442	2.08	1.91	1.74	.7319	2.410	.033	52.4	20.6	4.95	3.89	3.41	13.2	13.9	8.5	8.2
18-51-27	5.896	1.967	.00826	487.1	.00446	2.08	1.91	1.73	.7220	2.412	.034	40.9	16.3	5.20	4.19	3.70	12.7	13.4	8.2	7.9
18-51-28	4.881	1.610	.00831	405.4	.00439	2.10	1.92	1.72	.7116	2.414	.035	32.9	13.1	5.51	4.55	4.04	12.6	13.5	8.1	7.8
18-51-29	31.204	7.096	.00668	2085.7	.00340	2.67	2.42	2.16	.7484	2.401	.032	200.9	55.8	5.65	3.50	3.04	18.2	19.0	10.0	9.7
18-51-30	23.188	5.315	.00694	1609.8	.00356	2.67	2.41	2.13	.7435	2.403	.032	149.8	42.3	5.55	3.49	3.02	17.3	18.1	9.5	9.2

Table III (contd.)

VERS.NR.	RE*E4	REW*E4	F	RE*F	ST	TW/TE	TW/TB	TW/TI	BETA	AS	H/Y	H+	H+W	RH+	RH+1	RH+01	GPR	GPR*	GPR1	GPR01
18-51-31	17.701	4.055	.00718	1270.8	.00367	2.68	2.41	2.12	.7382	2.404	.033	114.3	32.6	5.50	3.50	3.03	16.8	17.6	9.2	8.9
18-51-32	13.908	3.220	.00738	1026.4	.00378	2.68	2.39	2.10	.7328	2.406	.033	89.6	26.1	5.50	3.58	3.11	16.1	17.0	8.9	8.6
18-51-39	5.193	2.993	.00912	473.4	.00521	1.43	1.37	1.32	.7454	2.413	.032	42.7	26.3	4.09	3.78	3.31	10.9	11.4	8.8	8.5
18-51-40	4.098	2.397	.00928	380.4	.00537	1.42	1.36	1.31	.7375	2.415	.033	33.4	21.0	4.22	3.93	3.46	10.2	10.7	8.2	8.0
18-51-41	3.292	1.925	.00939	309.2	.00538	1.42	1.36	1.31	.7291	2.417	.033	26.6	16.7	4.39	4.11	3.63	10.0	10.5	8.1	7.8
18-51-42	2.625	1.534	.00942	247.3	.00537	1.42	1.36	1.30	.7162	2.420	.034	20.5	13.0	4.78	4.52	4.03	9.4	10.1	7.7	7.4
19-41- 1	28.309	16.755	.00969	2742.4	.00417	1.39	1.35	1.33	.8458	2.399	.038	375.0	229.7	3.63	3.36	2.82	19.5	20.1	15.9	15.1
19-41- 2	19.088	11.477	.00989	1687.8	.00449	1.38	1.34	1.31	.8385	2.403	.039	252.0	157.1	3.69	3.44	2.90	17.5	18.0	14.4	13.6
19-41- 3	13.479	8.045	.01011	1362.1	.00477	1.39	1.35	1.32	.8317	2.407	.039	177.2	110.2	3.75	3.50	2.95	16.0	16.5	13.0	12.4
19-41- 4	10.387	6.243	.01036	1075.7	.00502	1.38	1.34	1.31	.8273	2.409	.040	137.0	86.0	3.73	3.50	2.94	14.9	15.4	12.2	11.5
19-41- 5	8.023	4.777	.01049	841.6	.00531	1.39	1.35	1.31	.8210	2.412	.041	104.8	65.6	3.83	3.59	3.03	13.5	14.1	11.0	10.4
19-41- 6	30.243	9.964	.00908	2744.9	.00395	2.05	1.93	1.82	.8355	2.399	.039	365.4	132.4	4.14	3.10	2.55	20.1	20.7	12.9	12.2
19-41- 7	20.644	6.815	.00921	1901.2	.00422	2.06	1.92	1.81	.8269	2.403	.040	245.5	90.2	4.27	3.27	2.72	18.2	18.8	11.6	11.0
19-41- 8	14.007	4.601	.00943	1320.8	.00449	2.07	1.93	1.80	.8184	2.407	.041	164.5	60.9	4.35	3.39	2.82	16.5	17.1	10.6	10.0
19-41- 9	10.496	3.477	.00959	1006.6	.00474	2.07	1.92	1.78	.8115	2.409	.042	122.0	46.0	4.43	3.52	2.95	15.2	15.8	9.7	9.2
19-41-10	7.751	2.574	.00981	760.7	.00492	2.07	1.92	1.77	.8043	2.412	.043	89.1	34.1	4.50	3.64	3.06	14.2	15.0	9.2	8.7
19-41-11	6.437	2.156	.00988	636.0	.00505	2.07	1.91	1.75	.7985	2.414	.043	73.0	28.4	4.63	3.81	3.22	13.5	14.3	8.7	8.3
19-41-12	26.847	6.102	.00882	2367.3	.00376	2.66	2.42	2.21	.8247	2.401	.041	300.6	80.0	4.53	2.72	2.16	21.0	21.7	11.5	10.9
19-41-13	18.115	4.096	.00885	1602.5	.00401	2.69	2.43	2.18	.8122	2.405	.042	194.3	53.0	4.85	3.17	2.59	18.7	19.6	10.2	9.7
19-41-14	12.820	2.904	.00902	1156.8	.00417	2.70	2.43	2.15	.8034	2.408	.043	134.8	37.6	4.98	3.39	2.81	17.5	18.5	9.6	9.1
19-41-15	9.608	2.205	.00917	881.0	.00438	2.70	2.41	2.11	.7950	2.411	.044	98.7	28.5	5.13	3.68	3.08	16.1	17.2	8.9	8.4
19-41-16	7.050	1.633	.00927	653.4	.00455	2.69	2.40	2.06	.7832	2.414	.046	69.5	21.0	5.47	4.16	3.55	14.9	16.1	8.2	7.8
19-41-17	5.827	1.359	.00938	546.8	.00463	2.69	2.39	2.03	.7766	2.416	.047	56.3	17.4	5.62	4.39	3.77	14.3	15.6	7.9	7.5
19-41-18	6.266	3.776	.01079	676.0	.00558	1.38	1.34	1.30	.8171	2.414	.041	82.4	52.2	3.78	3.56	2.99	12.6	13.1	10.3	9.8
19-41-19	6.232	3.773	.01089	678.6	.00552	1.38	1.34	1.30	.8183	2.414	.041	82.6	52.5	3.71	3.49	2.92	13.0	13.5	10.7	10.1
19-41-20	4.879	2.952	.01102	537.7	.00572	1.38	1.34	1.30	.8119	2.417	.042	64.2	40.9	3.80	3.59	3.02	12.1	12.6	10.0	9.5
19-41-21	3.825	2.330	.01130	432.2	.00592	1.38	1.33	1.29	.8070	2.420	.042	50.4	32.4	3.81	3.61	3.03	11.5	12.0	9.5	9.0
19-41-22	3.025	1.831	.01148	347.2	.00611	1.38	1.34	1.29	.8002	2.423	.043	39.4	25.4	3.92	3.72	3.14	10.7	11.4	8.8	8.3
19-41-22	3.926	2.339	.01123	440.9	.00594	1.40	1.35	1.30	.8065	2.419	.042	51.3	32.5	3.85	3.64	3.06	11.3	11.9	9.2	8.7
19-41-23	2.509	1.497	.01160	291.1	.00621	1.40	1.35	1.29	.7943	2.425	.044	32.4	20.7	4.03	3.83	3.24	10.2	11.0	8.4	7.9
19-41-24	2.181	1.314	.01155	251.9	.00625	1.39	1.34	1.29	.7882	2.427	.045	27.7	17.9	4.22	4.03	3.43	9.9	10.6	8.1	7.7
19-41-25	1.741	1.061	.01164	202.6	.00631	1.38	1.33	1.28	.7797	2.430	.046	21.8	14.3	4.43	4.26	3.65	9.5	10.2	7.8	7.4
19-41-26	1.366	0.808	.01144	156.3	.00615	1.41	1.35	1.28	.7647	2.433	.048	16.3	10.5	5.00	4.82	4.19	9.1	10.1	7.4	7.0
19-41-27	1.081	0.662	.01163	125.6	.00612	1.37	1.33	1.26	.7560	2.436	.049	12.7	8.5	5.22	5.07	4.43	8.9	10.0	7.4	7.0
19-41-28	0.899	0.547	.01156	103.9	.00604	1.38	1.33	1.26	.7448	2.439	.051	10.3	6.9	5.64	5.49	4.84	8.7	9.8	7.2	6.8
19-41-29	0.737	0.450	.01171	86.3	.00603	1.38	1.33	1.25	.7353	2.441	.053	8.3	5.6	5.93	5.80	5.13	8.3	9.6	6.9	6.5
19-41-30	0.587	0.356	.01169	68.7	.00575	1.38	1.33	1.25	.7202	2.444	.056	6.3	4.3	6.56	6.43	5.74	8.5	9.9	7.0	6.6
19-51- 1	21.707	12.745	.00834	1810.1	.00439	1.38	1.36	1.31	.7857	2.401	.029	183.0	114.5	3.61	3.28	2.86	14.6	15.9	11.8	11.5
19-51- 2	17.209	10.046	.00844	1452.0	.00460	1.39	1.36	1.31	.7791	2.403	.029	143.8	90.0	3.71	3.38	2.95	13.4	14.6	10.8	10.5
19-51- 3	13.598	7.725	.00867	1178.9	.00467	1.41	1.39	1.33	.7745	2.405	.030	113.8	69.7	3.68	3.33	2.90	13.1	14.4	10.5	10.2
19-51- 4	11.249	6.294	.00882	992.0	.00505	1.43	1.40	1.33	.7695	2.406	.030	93.6	57.0	3.70	3.35	2.92	11.4	12.7	9.1	8.8
19-51- 5	8.984	5.040	.00898	806.6	.00523	1.42	1.39	1.33	.7635	2.408	.030	74.5	45.6	3.76	3.42	2.98	10.7	11.9	8.5	8.3
19-51- 6	7.532	4.259	.00922	694.8	.00540	1.42	1.39	1.32	.7610	2.409	.031	62.9	38.9	3.68	3.35	2.91	10.2	11.5	8.2	7.9
19-51- 7	6.109	3.456	.00937	572.4	.00556	1.42	1.39	1.32	.7546	2.411	.031	50.7	31.5	3.76	3.45	3.00	9.6	10.8	7.7	7.4
19-51- 8	4.665	2.664	.00957	446.5	.00574	1.41	1.38	1.31	.7461	2.414	.032	38.4	24.2	3.88	3.59	3.13	8.8	10.2	7.1	6.9
19-51- 9	20.860	6.578	.00797	1663.2	.00418	2.06	1.97	1.78	.7659	2.402	.030	153.3	57.8	4.33	3.08	2.64	15.2	16.6	9.6	9.2
19-51-10	16.909	5.351	.00812	1373.7	.00441	2.06	1.97	1.76	.7603	2.403	.031	123.2	47.2	4.37	3.18	2.73	13.9	15.3	8.8	8.5
19-51-11	13.418	4.146	.00819	1098.6	.00452	2.09	2.00	1.89	.7622	2.406	.031	105.4	35.9	4.33	2.81	2.36	12.7	14.2	7.9	7.7
19-51-12	11.009	3.349	.00826	909.8	.00467	2.11	2.01	1.76	.7423	2.407	.032	76.1	29.2	4.77	3.64	3.17	12.1	13.6	7.5	7.3
19-51-13	8.573	2.625	.00822	704.3	.00476	2.11	2.00	1.73	.7278	2.409	.034	56.6	22.4	5.25	4.21	3.73	11.1	12.7	6.9	6.7

Table III (contd.)

VERS.NR.	RE*E4	REW*E4	F	RE*F	ST	TW/TE	TW/TB	TW/T1	BETA	AS	H/Y	H+	H+W	RH+	RH+1	RH+01	GPR	GPR*	GPR1	GPR01
19-51-14	29.778	10.221	.00751	2237.4	.00400	1.95	1.88	1.72	.7702	2.400	.030	217.4	87.3	4.57	3.45	3.01	15.6	17.0	10.1	9.8
19-51-15	22.511	7.828	.00781	1757.7	.00423	1.94	1.87	1.70	.7667	2.402	.030	166.0	67.8	4.44	3.37	2.93	14.5	15.9	9.5	9.2
19-51-16	3.406	1.117	.00871	296.5	.00510	2.03	1.93	1.61	.6863	2.417	.038	20.5	9.2	6.32	5.62	5.09	8.6	10.5	5.5	5.3
19-51-17	31.917	19.483	.00798	2548.5	.00413	1.35	1.33	1.29	.7925	2.398	.028	268.3	172.7	3.67	3.37	2.95	15.9	17.1	13.1	12.7
19-51-18	3.597	2.145	.00960	345.2	.00588	1.38	1.35	1.31	.7395	2.417	.032	30.5	19.0	4.09	3.79	3.32	7.8	9.2	6.4	6.2
19-51-19	6.812	2.229	.00857	583.9	.00501	2.03	1.93	1.68	.7269	2.411	.034	46.2	19.3	5.03	4.11	3.63	10.4	12.0	6.6	6.4
19-51-20	5.762	1.890	.00862	496.8	.00506	2.03	1.93	1.66	.7187	2.412	.034	38.3	16.2	5.25	4.39	3.89	9.9	11.6	6.3	6.1
19-51-21	4.579	1.503	.00872	399.5	.00512	2.03	1.93	1.64	.7073	2.414	.036	29.5	12.8	5.56	4.76	4.25	9.4	11.1	6.0	5.8
19-51-22	30.687	6.786	.00714	2189.8	.00371	2.60	2.46	2.10	.7509	2.401	.032	194.5	56.5	5.43	3.41	2.95	16.7	18.3	9.1	8.8
19-51-23	20.889	4.740	.00744	1554.2	.00398	2.57	2.42	2.05	.7420	2.403	.032	131.2	39.9	5.44	3.62	3.15	15.0	16.7	8.2	8.0
19-51-24	16.095	3.721	.00767	1233.8	.00420	2.55	2.40	2.00	.7354	2.405	.033	100.1	31.6	5.46	3.79	3.31	13.8	15.5	7.6	7.4
19-51-25	12.892	2.914	.00778	1003.1	.00426	2.59	2.43	2.00	.7263	2.407	.034	78.0	24.7	5.67	4.04	3.55	13.3	15.1	7.3	7.0
19-51-26	10.168	2.297	.00786	799.0	.00438	2.60	2.43	1.97	.7143	2.409	.035	59.2	19.3	6.00	4.51	4.01	12.3	14.3	6.7	6.5
19-51-27	8.333	1.865	.00791	659.0	.00445	2.62	2.44	1.94	.7025	2.410	.036	46.6	15.5	6.38	4.99	4.48	11.6	13.6	6.3	6.1
19-51-28	6.642	1.489	.00799	531.0	.00452	2.62	2.44	1.90	.6894	2.412	.038	35.6	12.2	6.81	5.55	5.02	10.9	13.1	5.9	5.7
19-51-29	5.646	1.264	.00795	449.0	.00451	2.63	2.44	1.87	.6750	2.413	.039	28.6	10.1	7.41	6.28	5.73	10.3	12.6	5.6	5.4
19-51-30	4.447	0.999	.00797	354.4	.00453	2.63	2.44	1.82	.6548	2.414	.042	20.9	7.8	8.29	7.32	6.75	9.4	11.8	5.1	4.9
19-51-31	3.427	0.765	.00804	275.6	.00447	2.64	2.44	1.77	.6319	2.416	.046	14.8	5.8	9.35	8.54	7.94	8.7	11.4	4.7	4.6
19-51-32	3.999	2.377	.00987	394.7	.00591	1.38	1.35	1.28	.7460	2.415	.032	33.7	21.9	3.72	3.46	2.99	8.7	9.9	7.1	6.8
19-51-33	3.195	1.877	.00993	317.2	.00601	1.39	1.36	1.28	.7352	2.417	.033	26.3	17.0	3.99	3.73	3.26	8.0	9.3	6.5	6.3
19-51-34	2.607	1.528	.00995	259.5	.00597	1.39	1.36	1.32	.7305	2.420	.033	22.1	13.6	4.15	3.84	3.37	7.6	9.0	6.2	6.0
19-51-35	2.098	1.229	.00987	207.1	.00592	1.39	1.36	1.27	.7095	2.422	.035	16.2	10.7	4.80	4.57	4.07	7.2	8.7	5.9	5.7
19-51-36	1.746	1.020	.01000	174.6	.00590	1.39	1.36	1.27	.7008	2.423	.036	13.3	8.8	5.02	4.80	4.29	7.1	8.6	5.7	5.5
19-51-37	1.423	0.828	.01004	142.9	.00585	1.40	1.37	1.27	.6876	2.425	.038	10.5	7.0	5.45	5.25	4.72	6.7	8.4	5.4	5.2
19-51-38	1.162	0.671	.01011	117.4	.00573	1.40	1.37	1.27	.6745	2.427	.039	8.3	5.5	5.89	5.70	5.15	6.6	8.4	5.4	5.2
19-51-39	0.953	0.541	.01040	99.2	.00572	1.42	1.39	1.27	.6659	2.429	.040	6.7	4.5	6.05	5.86	5.31	6.6	8.4	5.3	5.1
19-51-40	0.736	0.416	.01083	79.8	.00551	1.42	1.39	1.27	.6571	2.431	.042	5.2	3.4	6.17	5.99	5.42	7.2	9.1	5.8	5.6
19-51-41	0.640	0.364	.01097	70.2	.00554	1.42	1.38	1.26	.6484	2.432	.043	4.4	3.0	6.46	6.29	5.71	6.8	8.8	5.4	5.3
19-51-46	3.964	1.272	.00879	348.4	.00506	2.06	1.95	1.65	.6999	2.415	.036	25.1	10.7	5.76	4.96	4.44	9.4	11.2	6.0	5.8
19-51-47	3.108	0.990	.00885	275.2	.00505	2.07	1.96	1.63	.6842	2.417	.038	18.7	8.2	6.29	5.56	5.03	8.9	10.9	5.6	5.4
19-51-48	2.551	0.810	.00891	227.2	.00502	2.07	1.96	1.61	.6706	2.419	.040	14.7	6.6	6.78	6.12	5.56	8.5	10.6	5.4	5.2
19-51-49	2.048	0.653	.00902	184.8	.00502	2.07	1.96	1.59	.6561	2.420	.042	11.3	5.2	7.30	6.71	6.14	8.0	10.2	5.1	4.9
19-51-50	1.724	0.543	.00911	157.1	.00497	2.09	1.97	1.57	.6425	2.421	.044	9.1	4.3	7.86	7.31	6.72	7.7	10.1	4.8	4.7
19-51-51	1.405	0.435	.00935	131.3	.00496	2.11	1.99	1.56	.6303	2.422	.046	7.2	3.4	8.28	7.77	7.16	7.4	10.0	4.7	4.5
19-51-52	1.132	0.351	.00980	110.9	.00493	2.12	1.99	1.55	.6245	2.424	.047	5.8	2.8	8.31	7.83	7.21	7.6	10.3	4.7	4.6
19-51-61	3.905	0.855	.00816	318.5	.00445	2.67	2.47	1.83	.6508	2.415	.043	18.2	6.7	8.34	7.36	6.78	9.8	12.4	5.3	5.1
19-51-62	3.041	0.664	.00832	253.0	.00441	2.68	2.47	1.79	.6323	2.417	.046	13.3	5.1	9.14	8.31	7.70	9.3	12.1	5.0	4.8
19-51-63	2.478	0.540	.00851	210.9	.00440	2.69	2.48	1.74	.6167	2.417	.049	10.2	4.1	9.86	9.14	8.50	8.8	11.8	4.7	4.6
19-51-64	1.990	0.432	.00862	171.5	.00437	2.71	2.48	1.68	.5921	2.418	.054	7.4	3.1	11.24	10.67	10.00	7.9	11.2	4.2	4.1
19-51-65	1.662	0.365	.00894	148.6	.00439	2.70	2.47	1.63	.5816	2.419	.057	6.0	2.7	11.73	11.24	10.55	7.5	11.1	4.0	3.9

Table IV

VERS.NR.	RE	F	F*RE
18-41- 5	2.43E+03	.00962	23.3
18-41- 6	1.93E+03	.01083	20.9
18-41- 7	1.63E+03	.01249	20.3
18-41- 8	1.19E+03	.01507	18.0
18-41- 3	2.79E+03	.00921	25.7
18-41- 4	2.43E+03	.00992	24.1
18-41- 5	2.14E+03	.01074	23.0
18-41- 6	1.83E+03	.01258	23.0
18-41- 7	1.65E+03	.01334	22.0
18-41- 8	1.36E+03	.01446	19.7

Table V

VERS.NR.	RE*E4	$\overline{RE}$*E4	F	RE*F	ST	TW/TE	TW/TB	GRAEZ	NUB
18-41- 3	0.320	0.295	.01070	34.2	.00441	1.24	1.20	.01106	9.96
18-41- 4	0.296	0.272	.01061	31.4	.00414	1.24	1.20	.01195	8.66
18-41- 5	0.249	0.230	.01023	25.5	.00401	1.23	1.19	.01418	7.07
18-41- 6	0.217	0.200	.01163	25.2	.00426	1.23	1.19	.01633	6.51
18-41- 8	0.165	0.153	.01436	23.7	.00513	1.23	1.19	.02145	5.97
18-41- 9	0.388	0.332	.01113	43.2	.00453	1.47	1.37	.00916	12.37
18-41-10	0.340	0.291	.01129	38.3	.00432	1.47	1.37	.01047	10.31
18-41-11	0.298	0.254	.01106	32.9	.00400	1.47	1.37	.01194	8.38
18-41-12	0.256	0.218	.01161	29.7	.00375	1.46	1.37	.01388	6.76
18-41-13	0.226	0.193	.01243	28.1	.00397	1.46	1.36	.01576	6.30
18-41-15	0.174	0.150	.01472	25.6	.00467	1.47	1.36	.02043	5.72
18-41-16	0.150	0.130	.01438	21.6	.00518	1.47	1.35	.02372	5.46
18-41-17	0.127	0.111	.01931	24.5	.00565	1.47	1.34	.02813	5.02
18-41-18	0.190	0.162	.01152	21.8	.00445	1.46	1.36	.01877	5.92
18-41-19	0.430	0.315	.00977	42.0	.00391	1.93	1.69	.00833	11.75
18-41-20	0.373	0.272	.00985	36.7	.00384	1.95	1.70	.00961	10.01
18-41-21	0.320	0.235	.01085	34.7	.00385	1.93	1.68	.01119	8.61
18-41-22	0.278	0.202	.01132	31.4	.00365	1.94	1.68	.01291	7.08
18-41-23	0.248	0.179	.01217	30.2	.00349	1.94	1.67	.01447	6.04
18-41-24	0.210	0.154	.01385	29.1	.00369	1.94	1.65	.01710	5.41
18-41-25	0.177	0.131	.01568	27.8	.00412	1.95	1.63	.02031	5.08
18-41-26	0.154	0.115	.01749	26.9	.00437	1.94	1.61	.02345	4.66
18-41-27	0.134	0.102	.02096	28.0	.00484	1.95	1.58	.02698	4.49
18-41-28	0.114	0.088	.02539	29.0	.00545	1.95	1.55	.03165	4.31
18-41-29	0.097	0.076	.02934	28.6	.00606	1.94	1.52	.03715	4.08
18-41-30	0.083	0.066	.03390	28.2	.00666	1.94	1.49	.04349	3.83
18-41-31	0.224	0.205	.01101	24.6	.00411	1.24	1.20	.01581	6.49
18-41-39	0.172	0.158	.01325	22.7	.00489	1.24	1.19	.02063	5.93

Table V (contd.)

VERS.NR.	RE*E4	RE$\bar{W}$*E4	F	RE*F	ST	TW/TE	TW/TB	GRAEZ	NUB
18-41- 7	0.289	0.254	.01017	29.4	.00388	1.36	1.30	.01227	7.90
18-41- 8	0.244	0.216	.01068	26.1	.00415	1.36	1.29	.01453	7.13
18-41- 9	0.214	0.189	.01156	24.7	.00448	1.36	1.29	.01662	6.73
18-41-10	0.183	0.163	.01294	23.6	.00502	1.37	1.28	.01946	6.45
18-41-11	0.474	0.317	.01048	49.7	.00333	2.17	1.85	.00759	11.01
18-41-12	0.431	0.288	.01075	46.4	.00331	2.17	1.84	.00835	9.94
18-41-13	0.388	0.260	.01099	42.6	.00333	2.16	1.83	.00929	8.99
18-41-14	0.355	0.239	.01136	40.3	.00338	2.16	1.82	.01015	8.34
18-41-15	0.317	0.215	.01177	37.4	.00341	2.17	1.81	.01135	7.53
18-41-16	0.285	0.192	.01213	34.6	.00346	2.17	1.80	.01265	6.86
18-41-17	0.258	0.174	.01255	32.4	.00357	2.17	1.78	.01396	6.41
18-41-18	0.218	0.149	.01402	30.6	.00390	2.17	1.75	.01655	5.91
18-41-19	0.184	0.128	.01590	29.2	.00442	2.15	1.70	.01972	5.61
18-41-20	0.160	0.113	.01798	28.8	.00479	2.15	1.68	.02264	5.30
18-41-21	0.138	0.101	.02020	28.0	.00522	2.17	1.65	.02622	4.99
18-41-22	0.124	0.092	.02200	27.3	.00588	2.17	1.61	.02930	5.03
18-41-23	0.447	0.238	.01105	49.4	.00256	2.80	2.15	.00813	7.90
18-41-24	0.398	0.212	.01157	46.0	.00263	2.80	2.12	.00915	7.21
18-41-25	0.346	0.186	.01234	42.7	.00277	2.79	2.08	.01053	6.61
18-41-26	0.306	0.168	.01301	39.8	.00288	2.81	2.05	.01191	6.06
18-41-27	0.247	0.135	.01528	37.7	.00321	2.80	1.98	.01481	5.43
18-41-28	0.216	0.120	.01684	36.3	.00339	2.80	1.94	.01694	5.02
18-41-29	0.187	0.107	.01855	34.6	.00371	2.82	1.89	.01963	4.74
18-41-30	0.164	0.096	.02060	33.8	.00407	2.80	1.84	.02235	4.56
18-41-31	0.135	0.082	.02414	32.7	.00481	2.80	1.76	.02708	4.45
18-41-32	0.235	0.206	.01067	25.1	.00408	1.36	1.29	.01510	6.74
18-41-33	0.212	0.187	.01149	24.4	.00437	1.35	1.28	.01674	6.52
18-41-34	0.192	0.170	.01232	23.6	.00473	1.35	1.28	.01853	6.37
18-41-35	0.171	0.152	.01359	23.2	.00518	1.34	1.26	.02083	6.21
18-41-36	0.154	0.138	.01492	23.0	.00558	1.34	1.26	.02305	6.05
18-41-37	0.139	0.125	.01547	21.5	.00603	1.34	1.26	.02560	5.88
18-41-38	0.126	0.114	.01742	22.0	.00652	1.34	1.25	.02821	5.77

Table V (contd.)

VERS.NR.	RE*E4	$\overline{RE}$*E4	F	RE*F	ST	TW/TE	TW/TB	GRAEZ	NUB
19-41-32	0.394	0.332	.01166	45.9	.00527	1.40	1.36	.00901	14.61
19-41-33	0.328	0.277	.01071	35.2	.00482	1.40	1.36	.01081	11.14
19-41-34	0.266	0.225	.01071	28.5	.00458	1.39	1.35	.01332	8.59
19-41-35	0.218	0.185	.01300	28.4	.00527	1.38	1.34	.01628	8.10
19-41-36	0.172	0.147	.01475	25.3	.00627	1.38	1.33	.02072	7.56
19-41-37	0.138	0.119	.01945	26.9	.00723	1.38	1.32	.02576	7.01
19-51-43	0.428	0.361	.01106	47.3	.00565	1.42	1.38	.00577	17.05
19-51-44	0.341	0.287	.01093	37.3	.00535	1.41	1.38	.00724	12.87
19-51-45	0.278	0.234	.01179	32.8	.00534	1.41	1.38	.00887	10.49
19-51-54	0.741	0.473	.01026	76.0	.00512	2.11	1.97	.00335	26.68
19-51-55	0.614	0.388	.01073	65.9	.00527	2.12	1.97	.00404	22.76
19-51-56	0.501	0.313	.01150	57.6	.00546	2.13	1.97	.00496	19.23
19-51-57	0.406	0.253	.01234	50.1	.00587	2.12	1.95	.00613	16.74
19-51-58	0.327	0.200	.01351	44.1	.00582	2.12	1.93	.00762	13.35
19-51-59	0.261	0.158	.01651	43.0	.00567	2.12	1.92	.00956	10.36
19-51-60	0.213	0.132	.01973	42.1	.00613	2.11	1.89	.01169	9.15
19-51-68	0.880	0.432	.01013	89.2	.00441	2.74	2.45	.00284	27.21
19-51-69	0.706	0.340	.01098	77.5	.00447	2.73	2.43	.00354	22.06
19-51-70	0.585	0.277	.01180	69.1	.00458	2.74	2.41	.00427	18.74
19-51-71	0.473	0.221	.01307	61.8	.00489	2.77	2.39	.00529	16.17
19-51-72	0.383	0.177	.01468	56.2	.00528	2.77	2.35	.00656	14.09
19-51-73	0.302	0.137	.01717	51.9	.00541	2.76	2.31	.00832	11.37
19-51-74	0.244	0.111	.01882	45.9	.00530	2.75	2.27	.01032	8.99

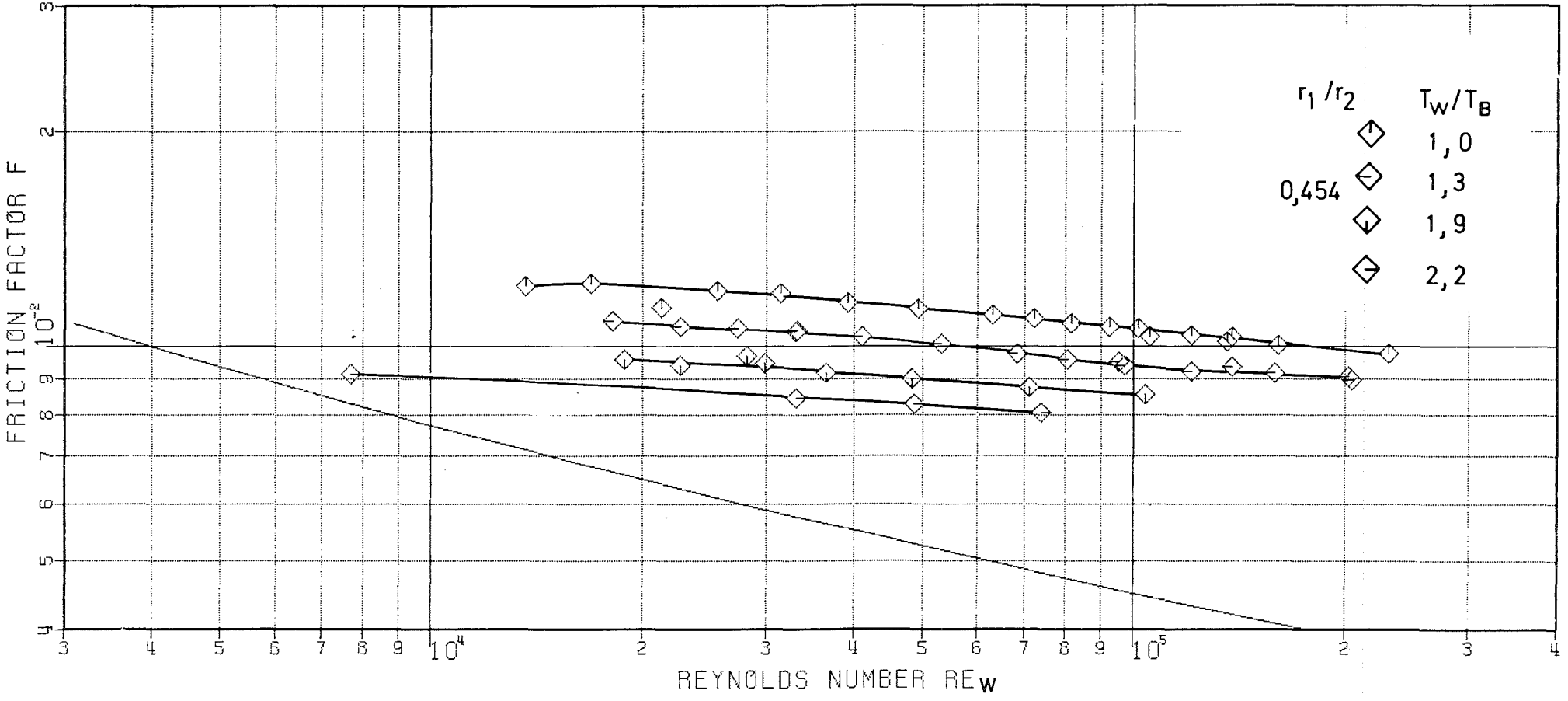

Fig. 1: Untransformed friction factor of annulus vs. Re_W ($Re_W \geq 3000$), test section "18" in tube of 40.4 mm I.D.

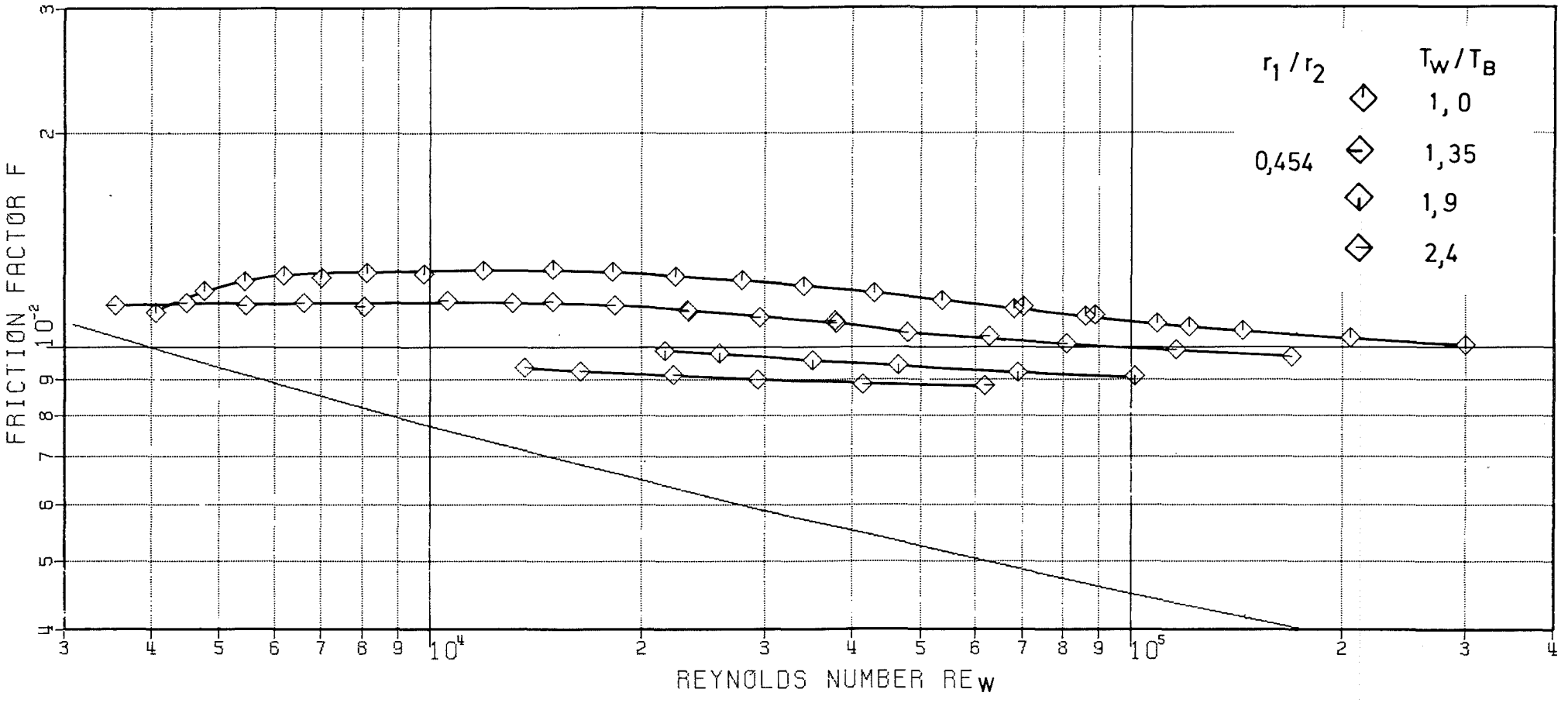

Fig. 2: Untransformed friction factor of annulus vs. Re_W ($Re_W \geqslant 3000$), test section "19" in tube of 40.4 mm I.D.

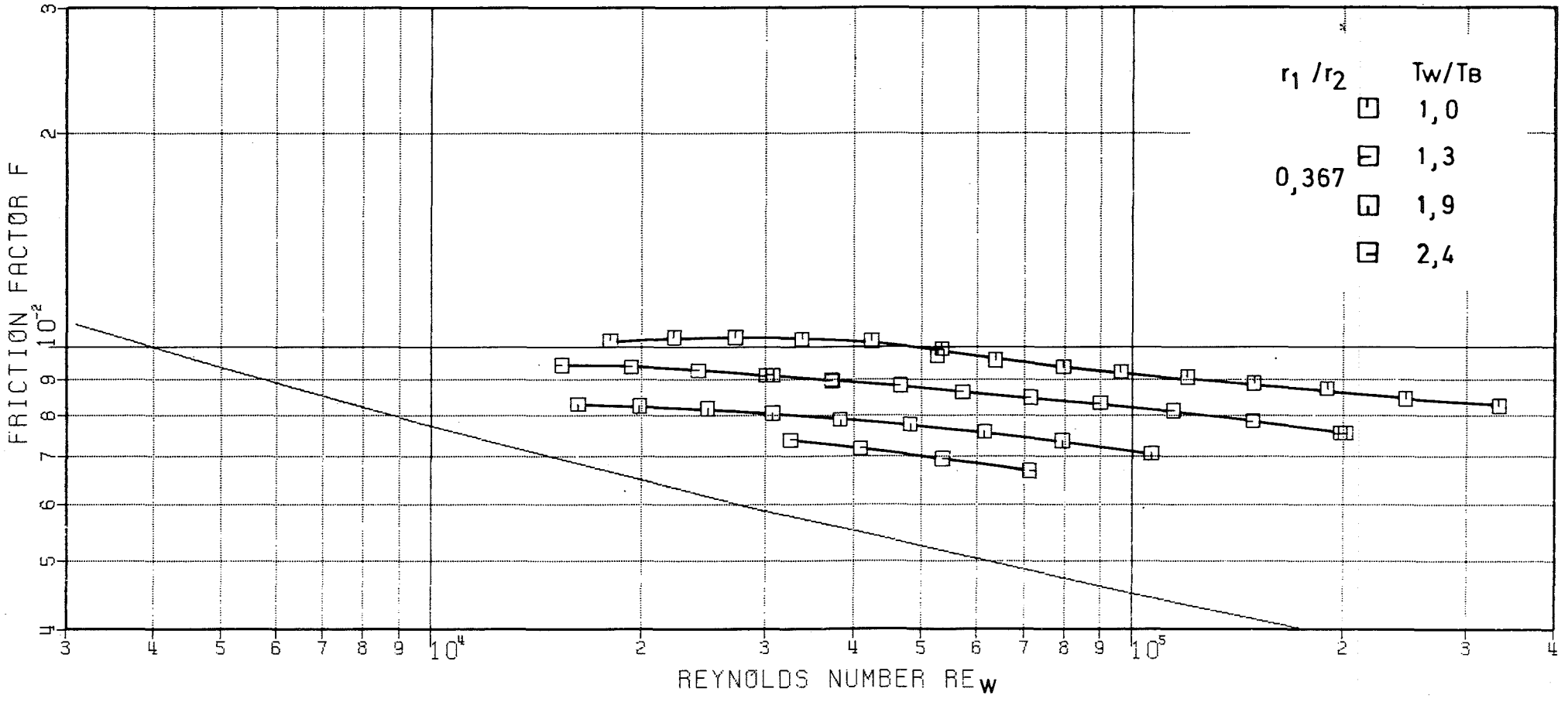

Fig. 3: Untransformed friction factor of annulus vs. Re_W ($Re_W \geqslant 3000$), test section "18" in tube of 50 mm I.D.

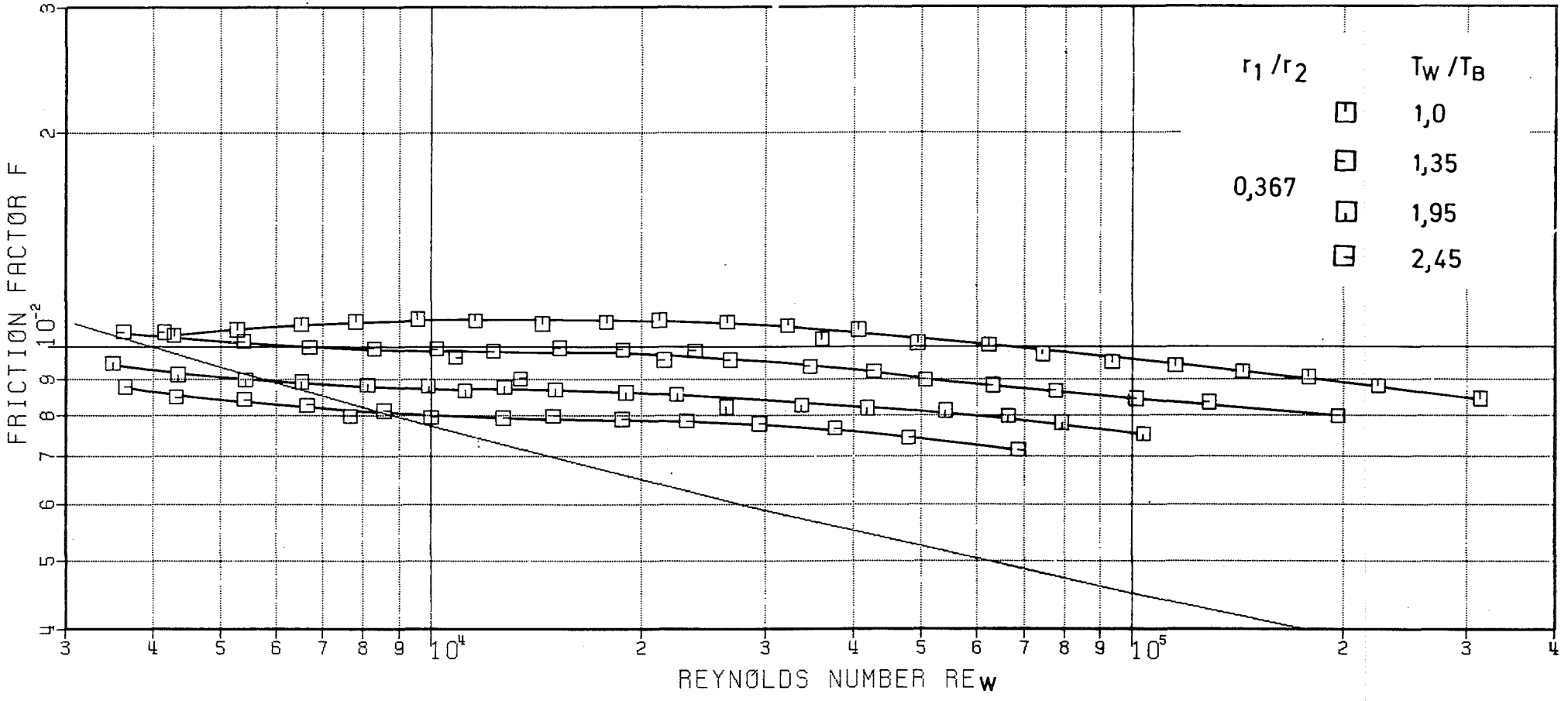

Fig. 4: Untransformed friction factor of annulus vs. Re_W ($Re_W \geqslant 3000$), test section "19" in tube of 50 mm I.D.

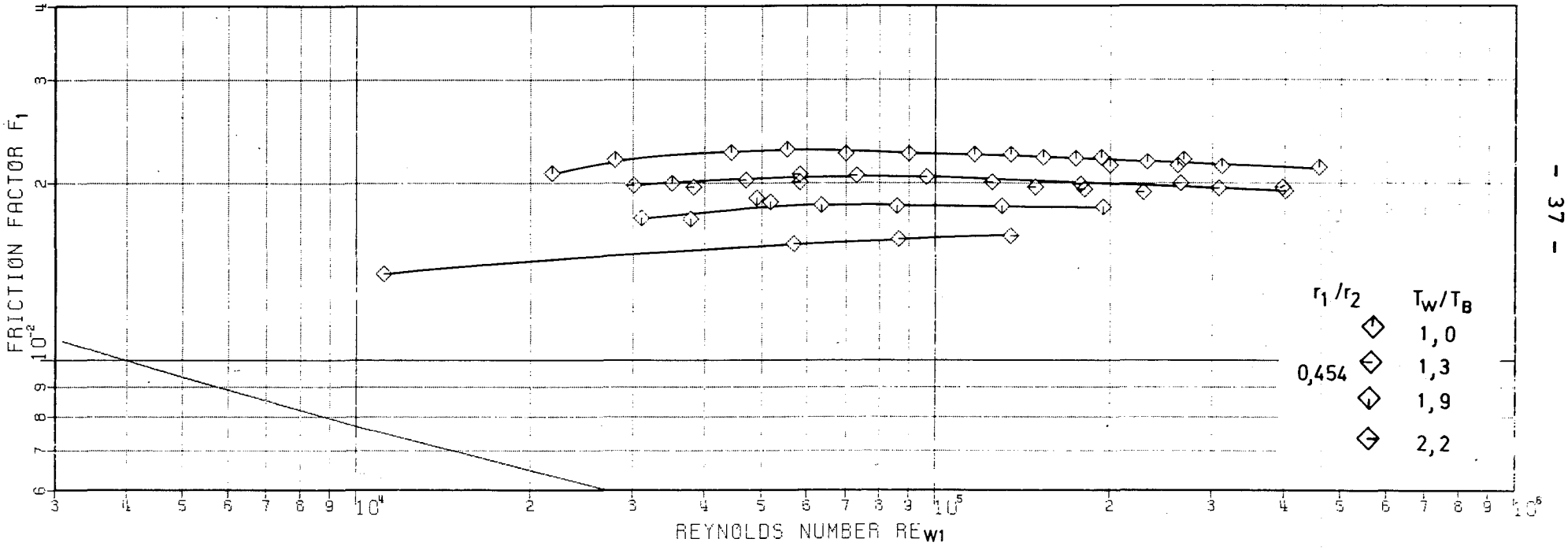

Fig. 5: Transformed friction factor vs. Re_{W1} ($Re_W \geq 3000$), test section "18" in tube of 40.4 mm I.D.

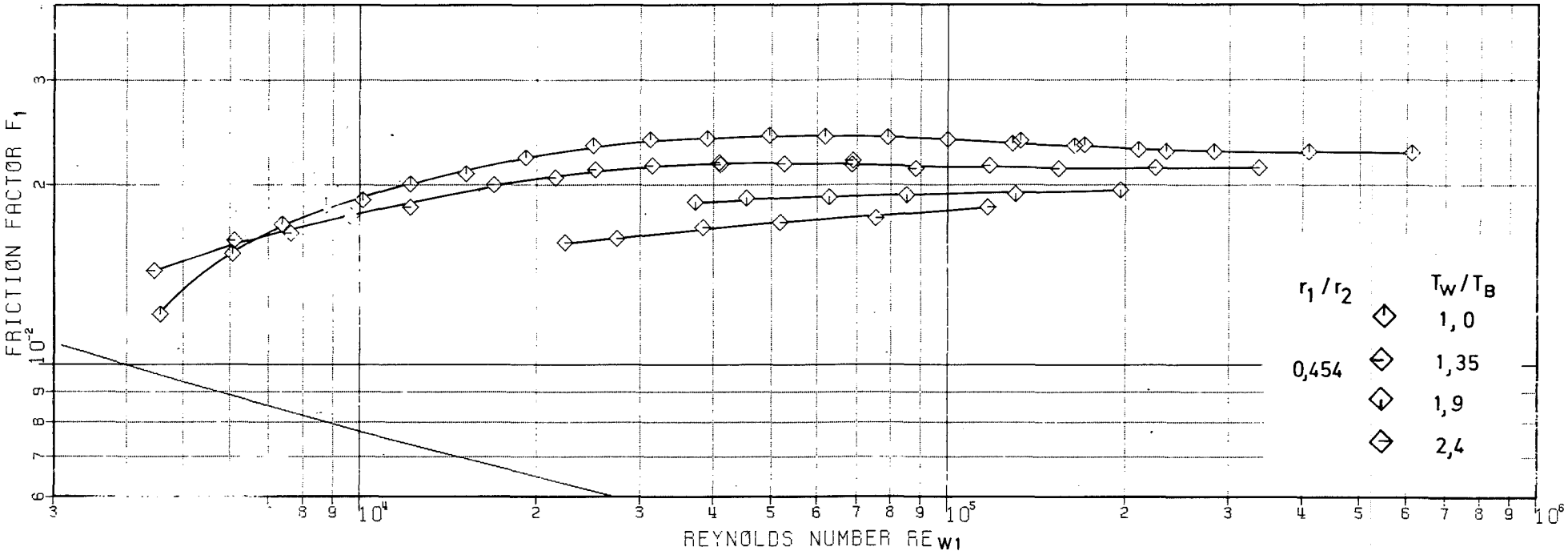

Fig. 6: Transformed friction factor vs. Re_{W1} ($Re_W \geq 3000$), test section "19" in tube of 40.4 mm I.D.

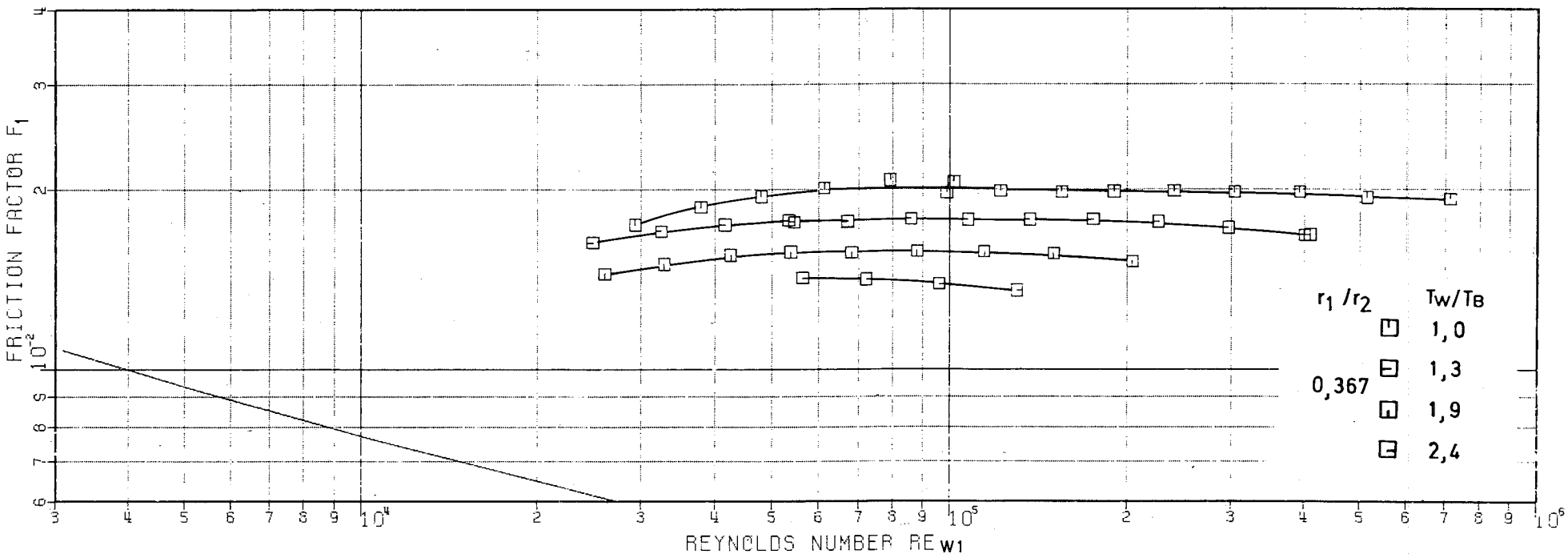

Fig. 7: Transformed friction factor vs. Re_{W1} ($Re_W \geqslant 3000$), test section "18" in tube of 50 mm I.D.

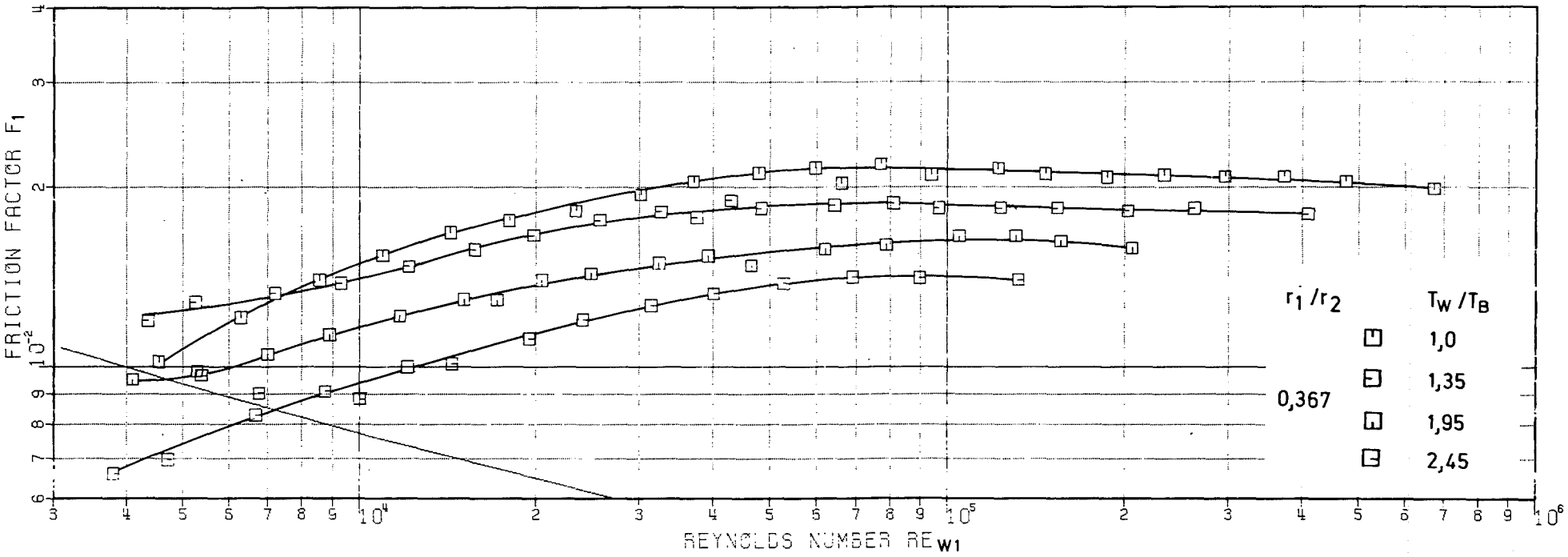

Fig. 8: Transformed friction factor vs. Re_{W1} ($Re_W \geqslant 3000$), test section "19" in tube of 50 mm I.D.

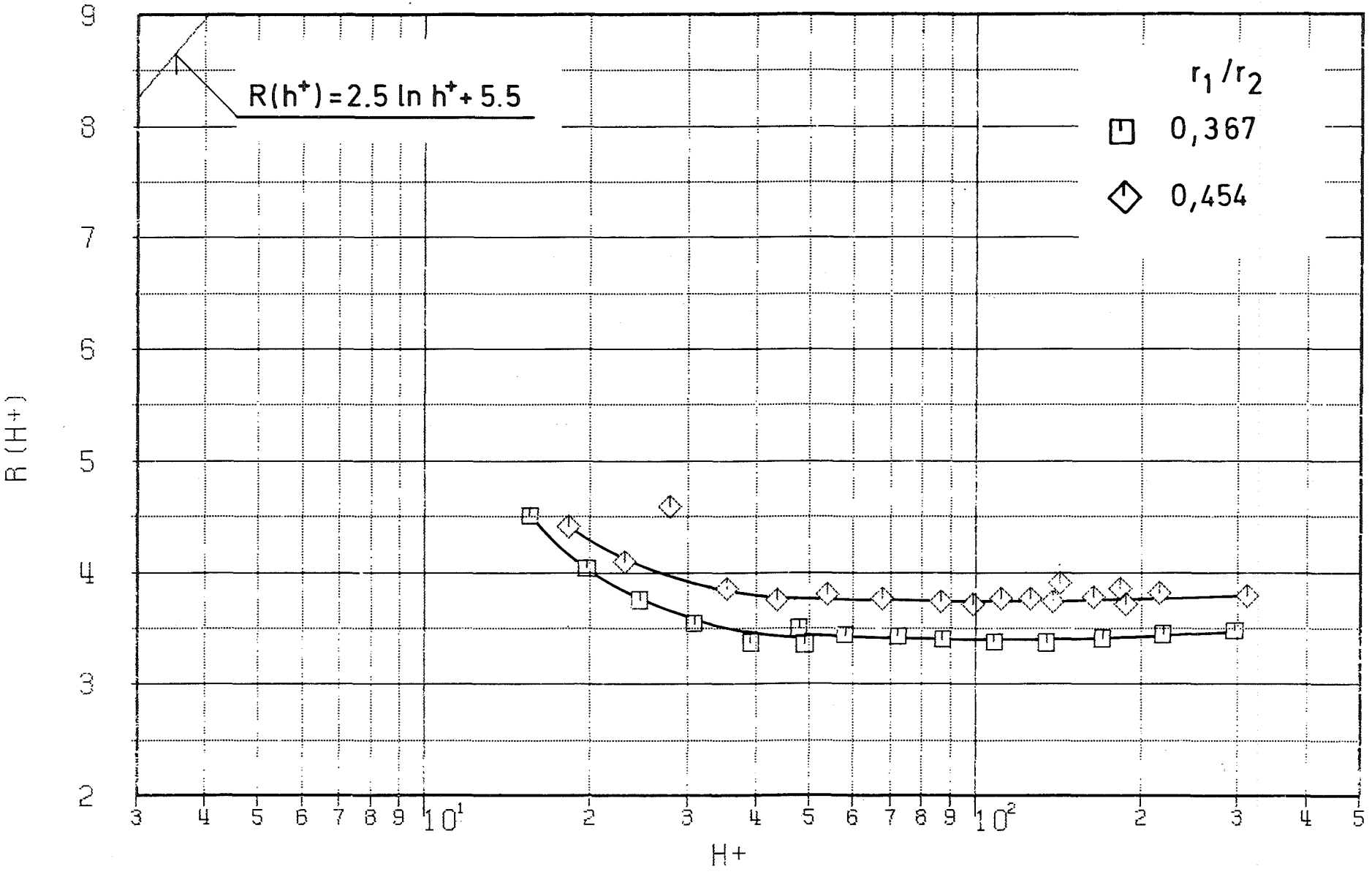

Fig. 9: $R(h^+)$ vs. h^+, isothermal runs. Rod "18".

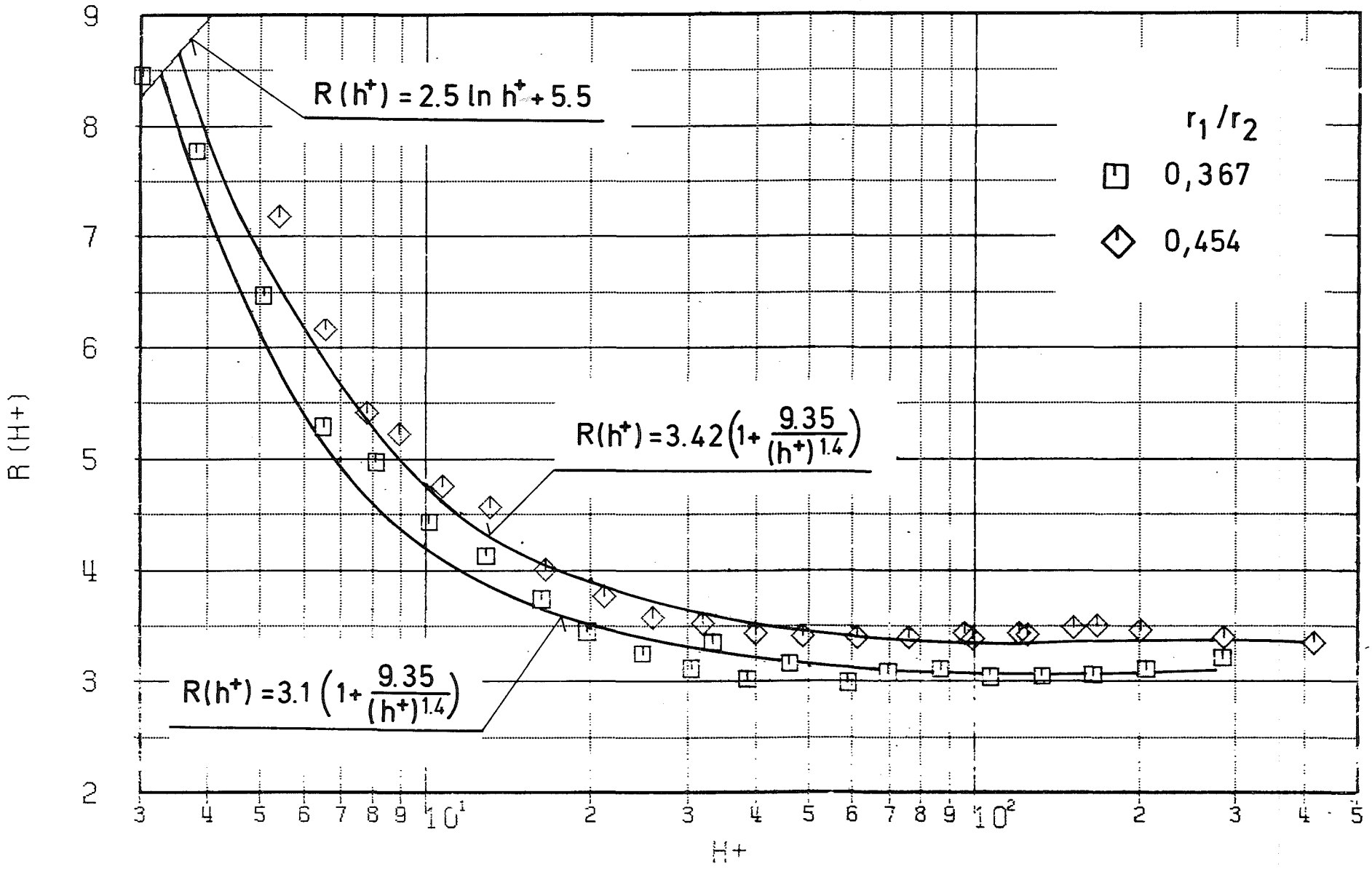

Fig.10: $R(h^+)$ vs. h^+, isothermal runs. Rod "19".

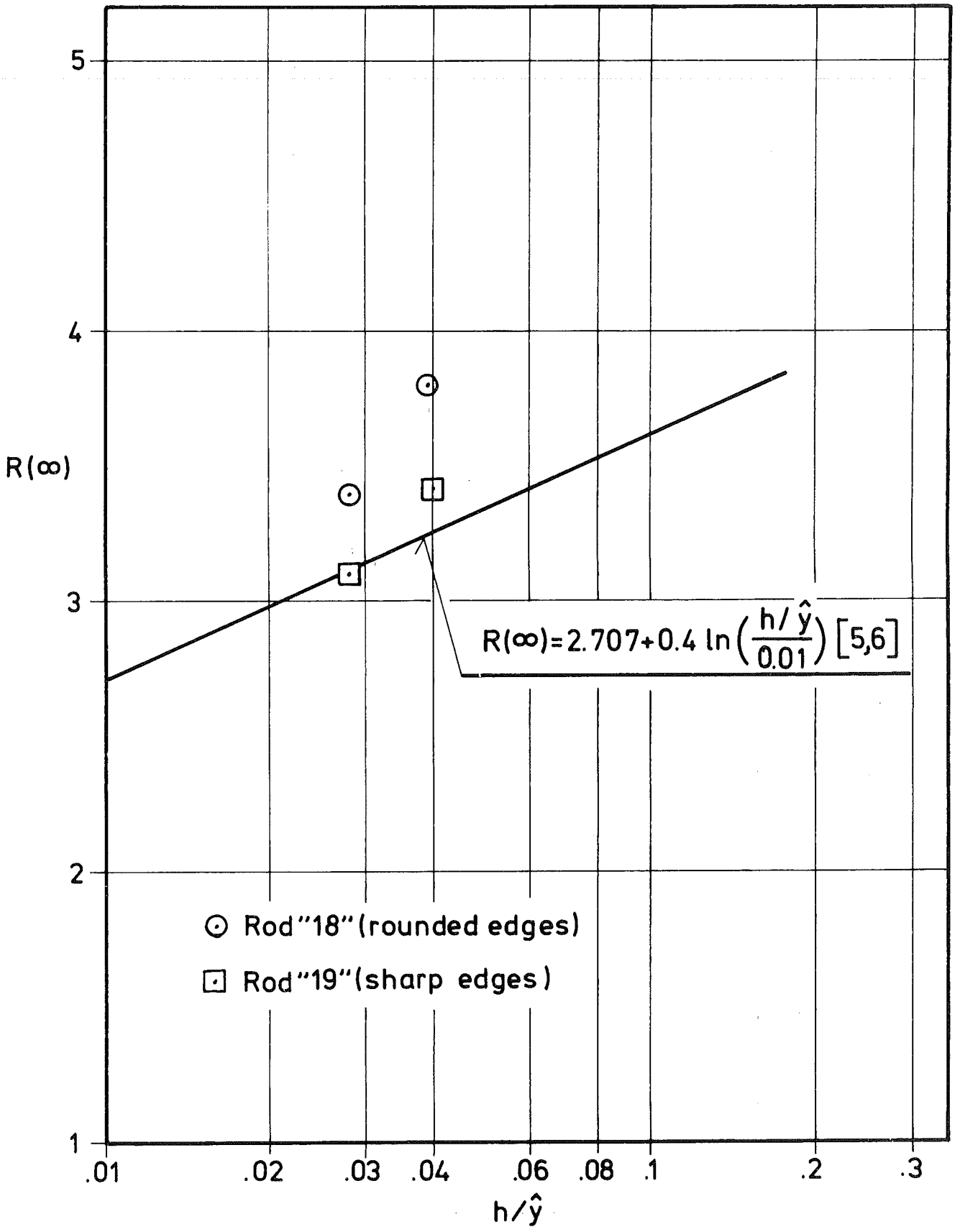

Fig.11: Fully rough flow values of $R(h^+)$ vs. $h/\hat{y}$.

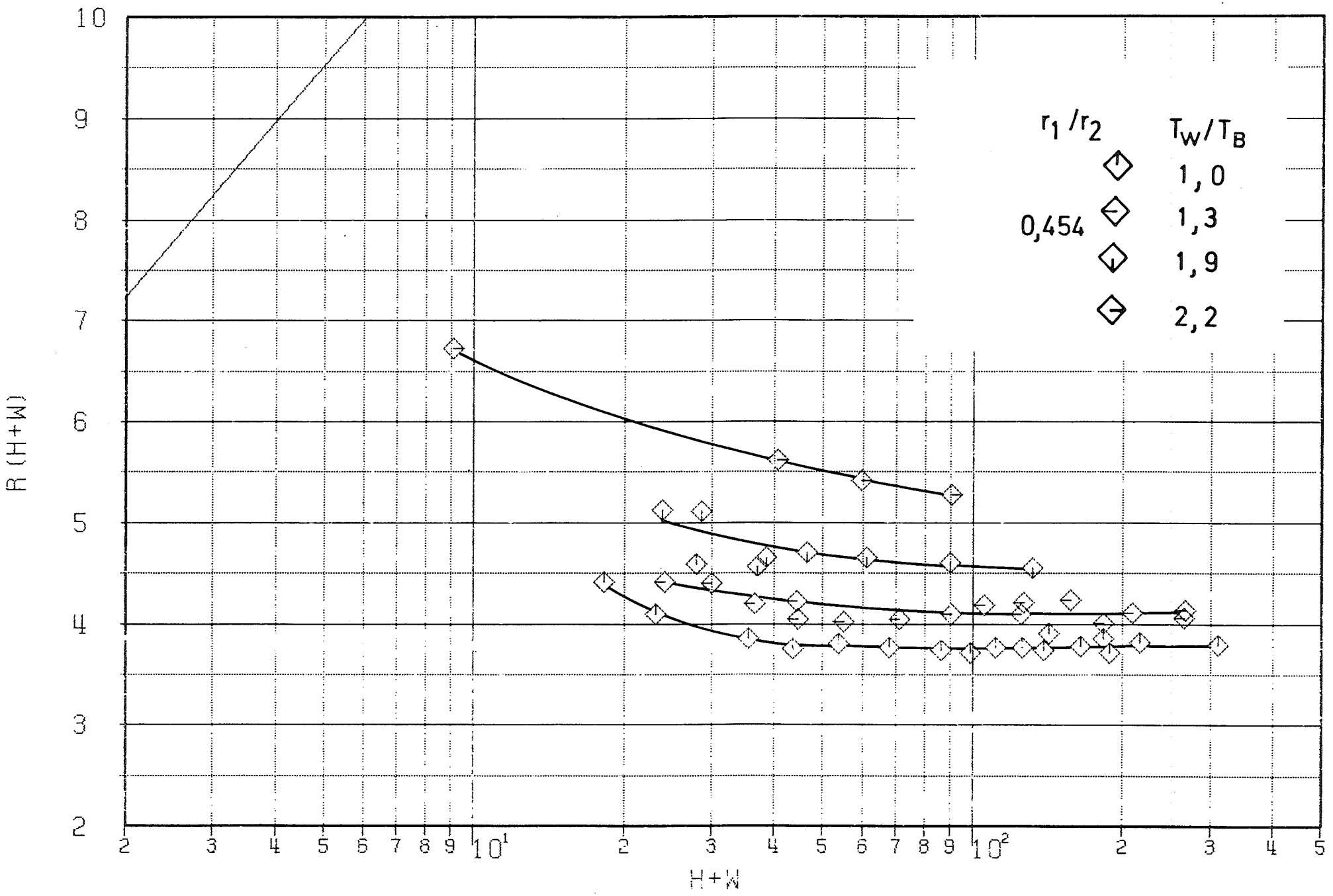

Fig.12: $R(h_W^+)$ vs. h_W^+ ($Re_W \geqslant 3000$), thermal runs, test section "18" in tube of 40.4 mm I.D.

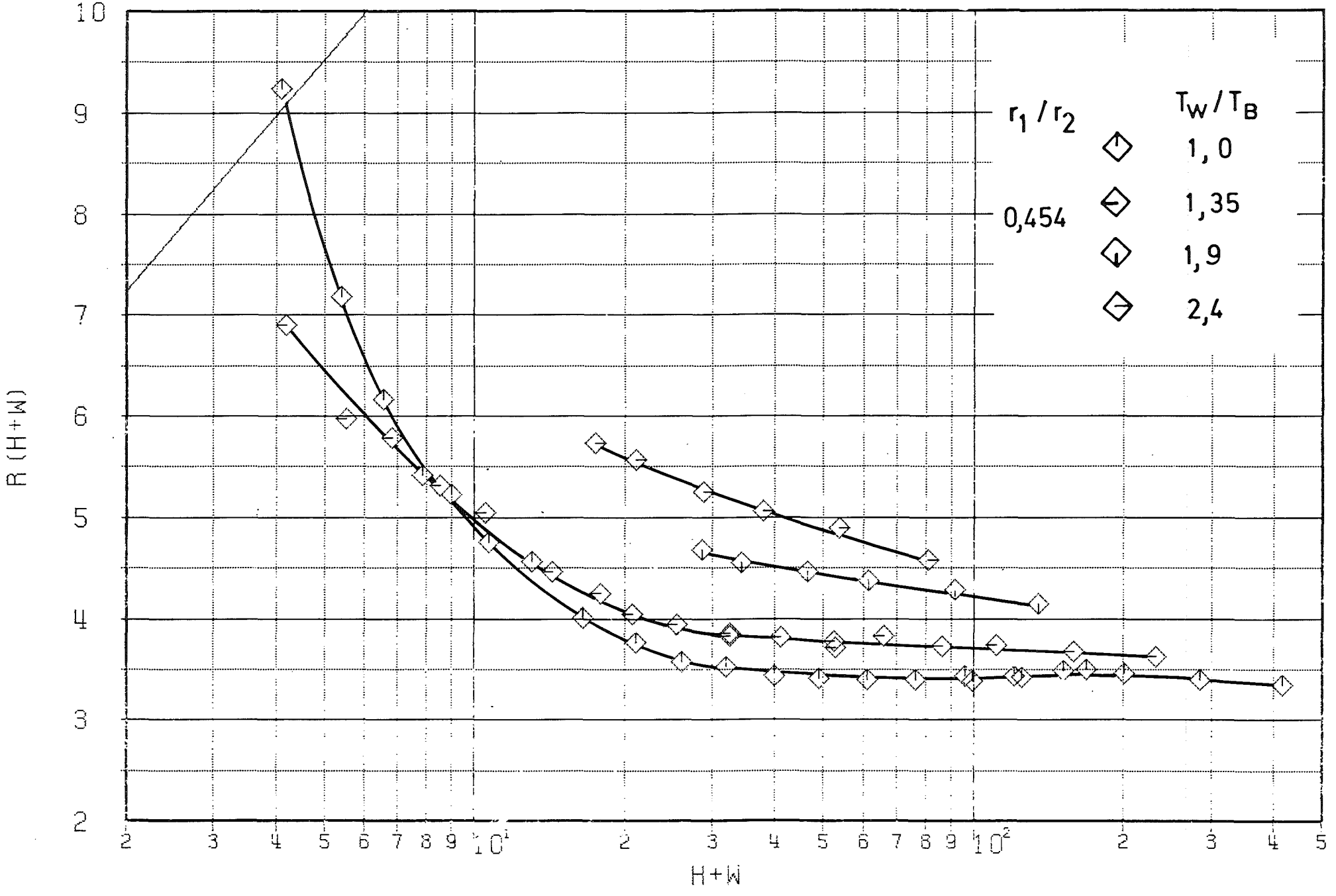

Fig.13: $R(h_W^+)$ vs. h_W^+ ($Re_W \geqslant 3000$), thermal runs, test section "19" in tube of 40.4 mm I.D.

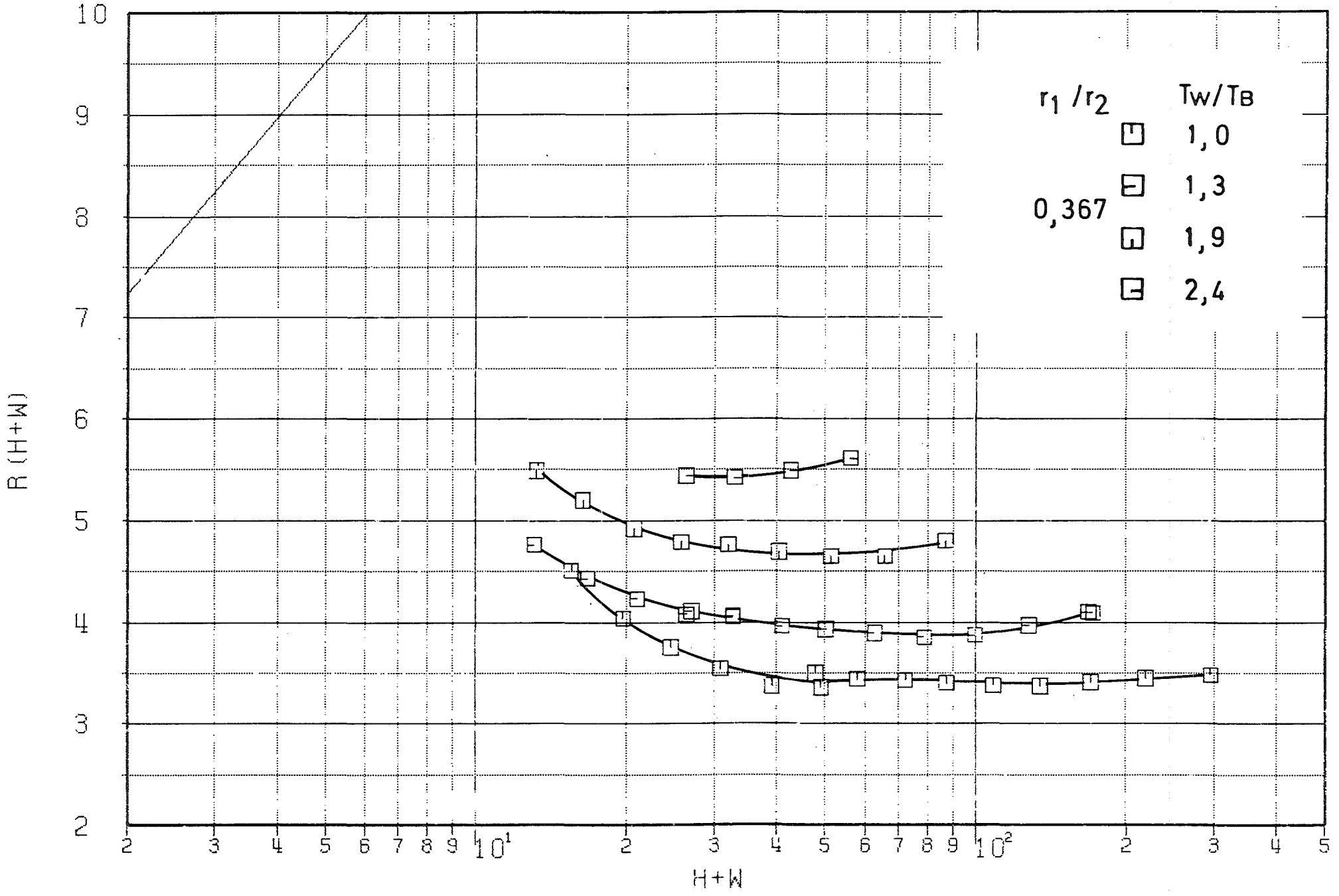

Fig.14: $R(h_W^+)$ vs. h_W^+ ($Re_W \geqslant 3000$), thermal runs, test section "18" in tube of 50 mm I.D.

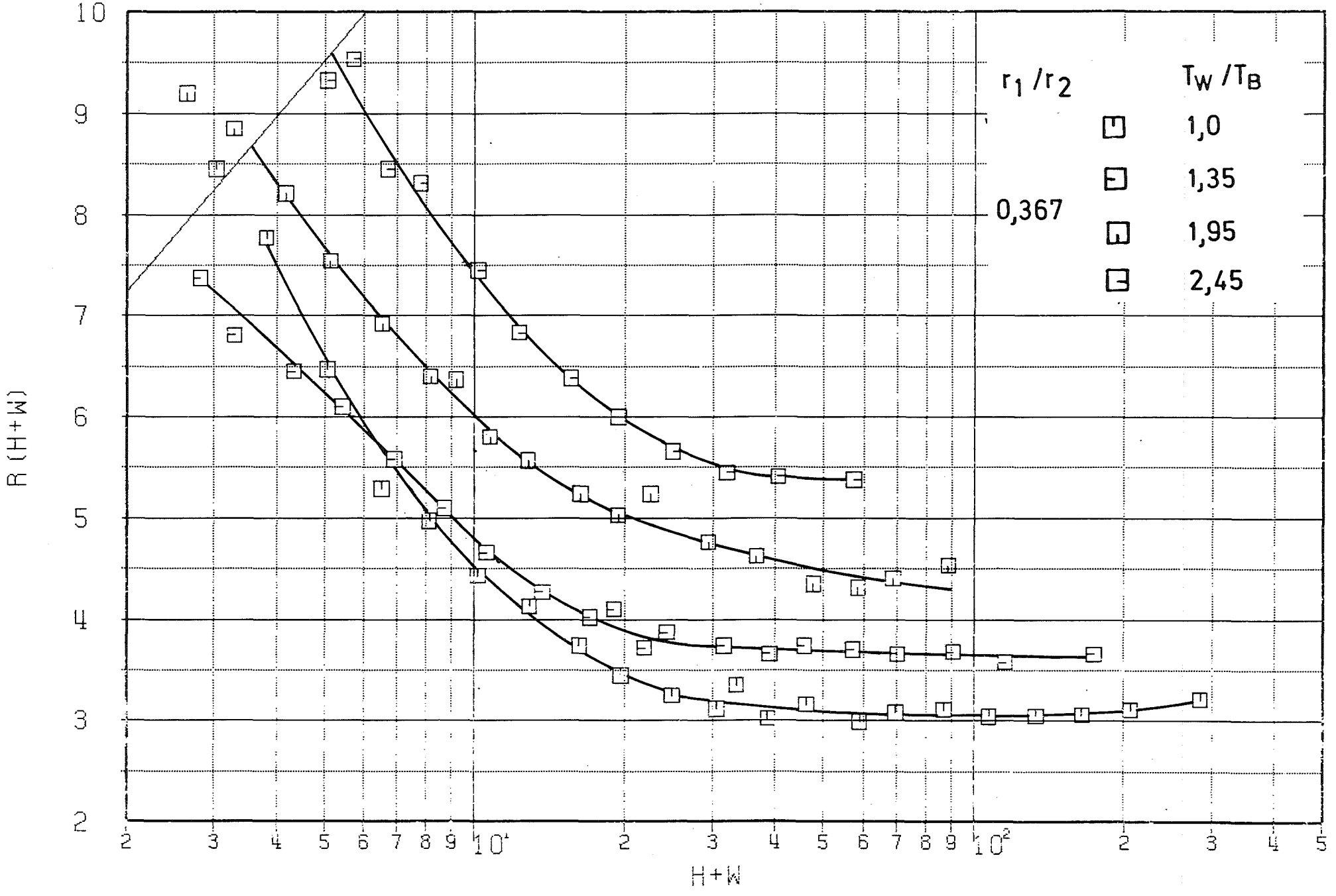

Fig.15: $R(h_W^+)$ vs. h_W^+ ($Re_W \geqslant 3000$), thermal runs, test section "19" in tube of 50 mm I.D.

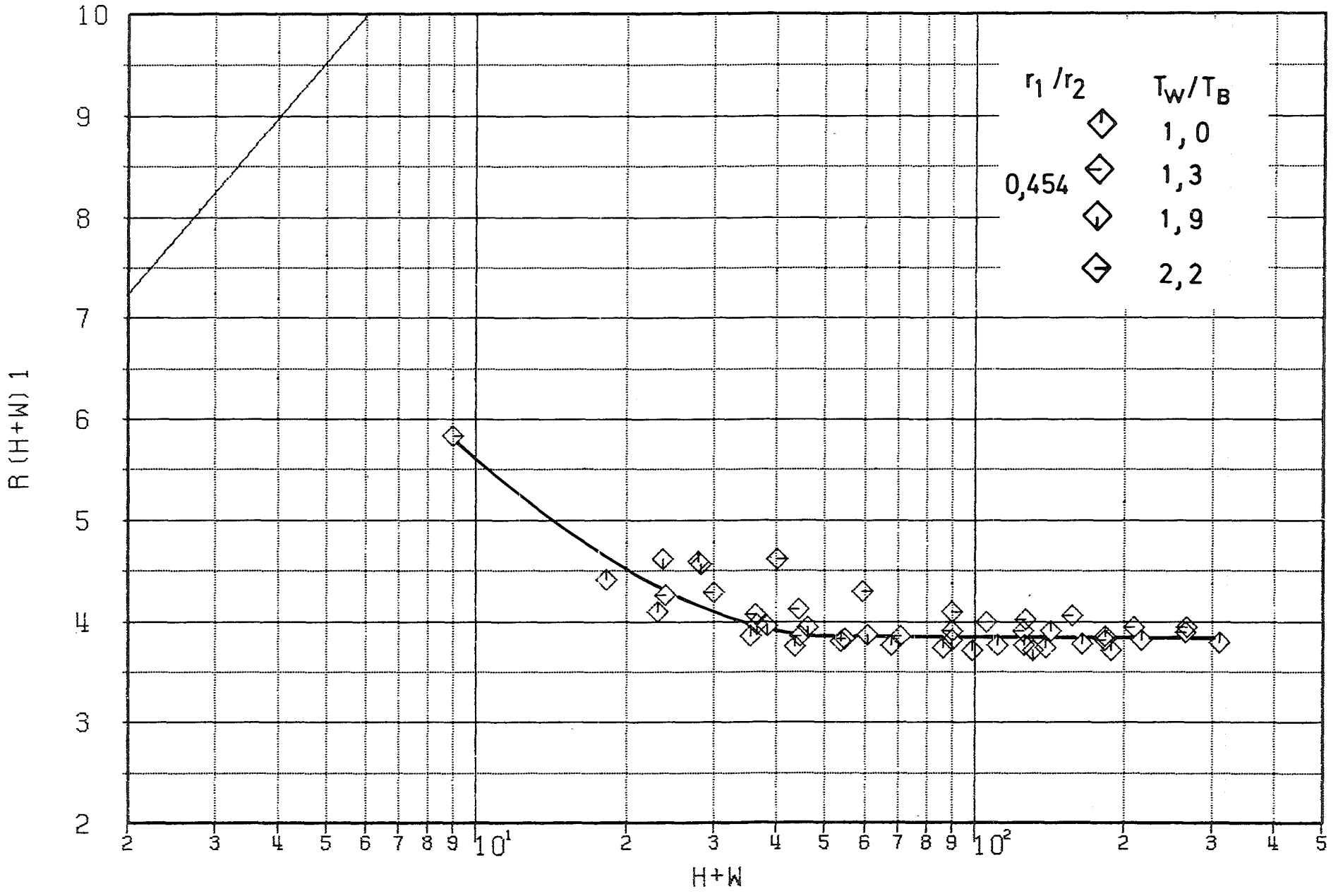

TESTSTRECKE 18

Fig.16: $R(h_W^+) - \frac{0.55}{h/\hat{y}} \left(\frac{T_W}{T_1}\right)^{1.5}$ vs. h_w^+ ($Re_W \geqslant 3000$), test section "18" in tube of 40.4 mm I.D.

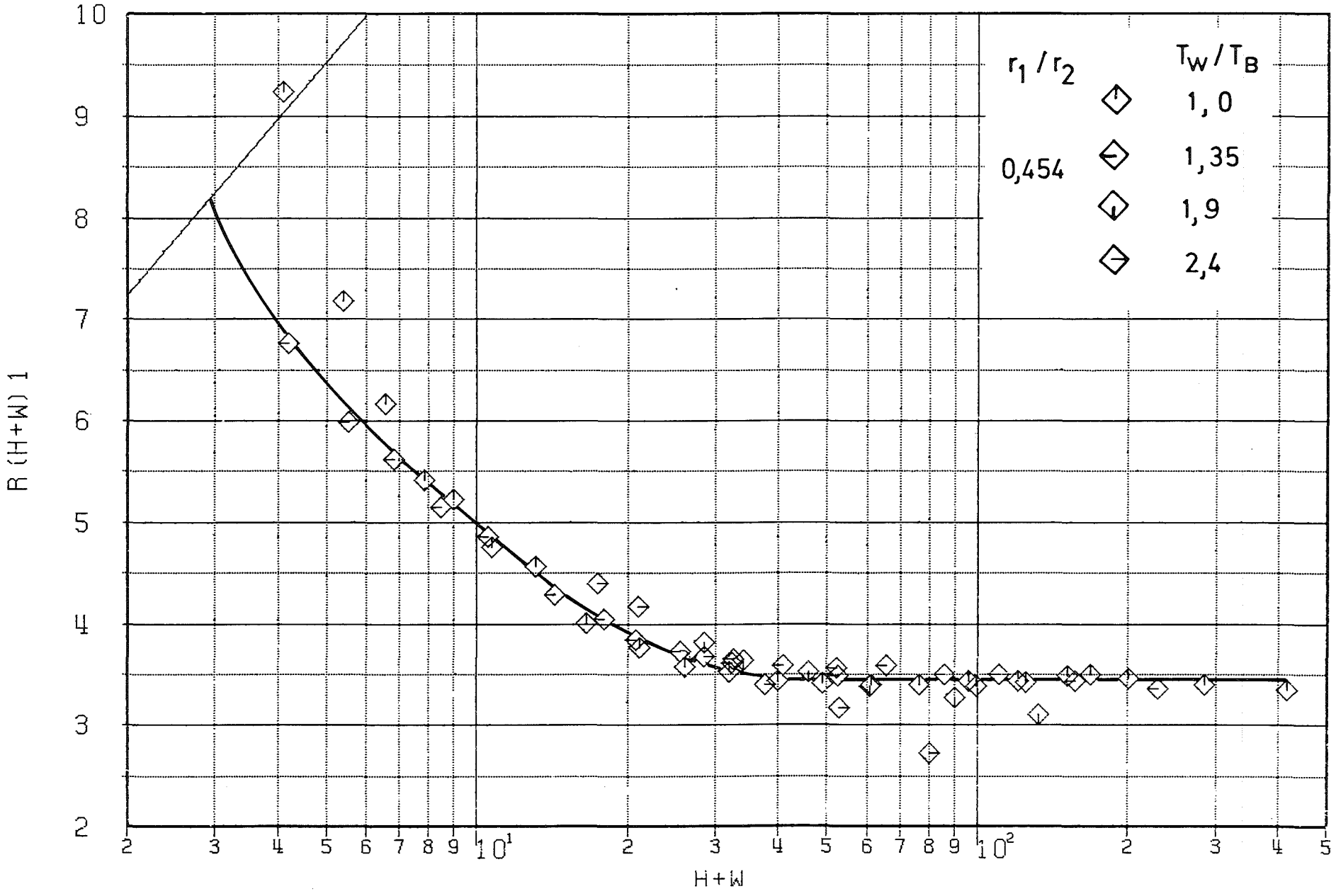

Fig.17: $R(h_W^+) - \frac{0.55}{h/\hat{y}} \left(\frac{T_W}{T_1} \right)^{1.5}$ vs. h_W^+ ($Re_W \geqslant 3000$), test section "19" in tube of 40.4 mm I.D.

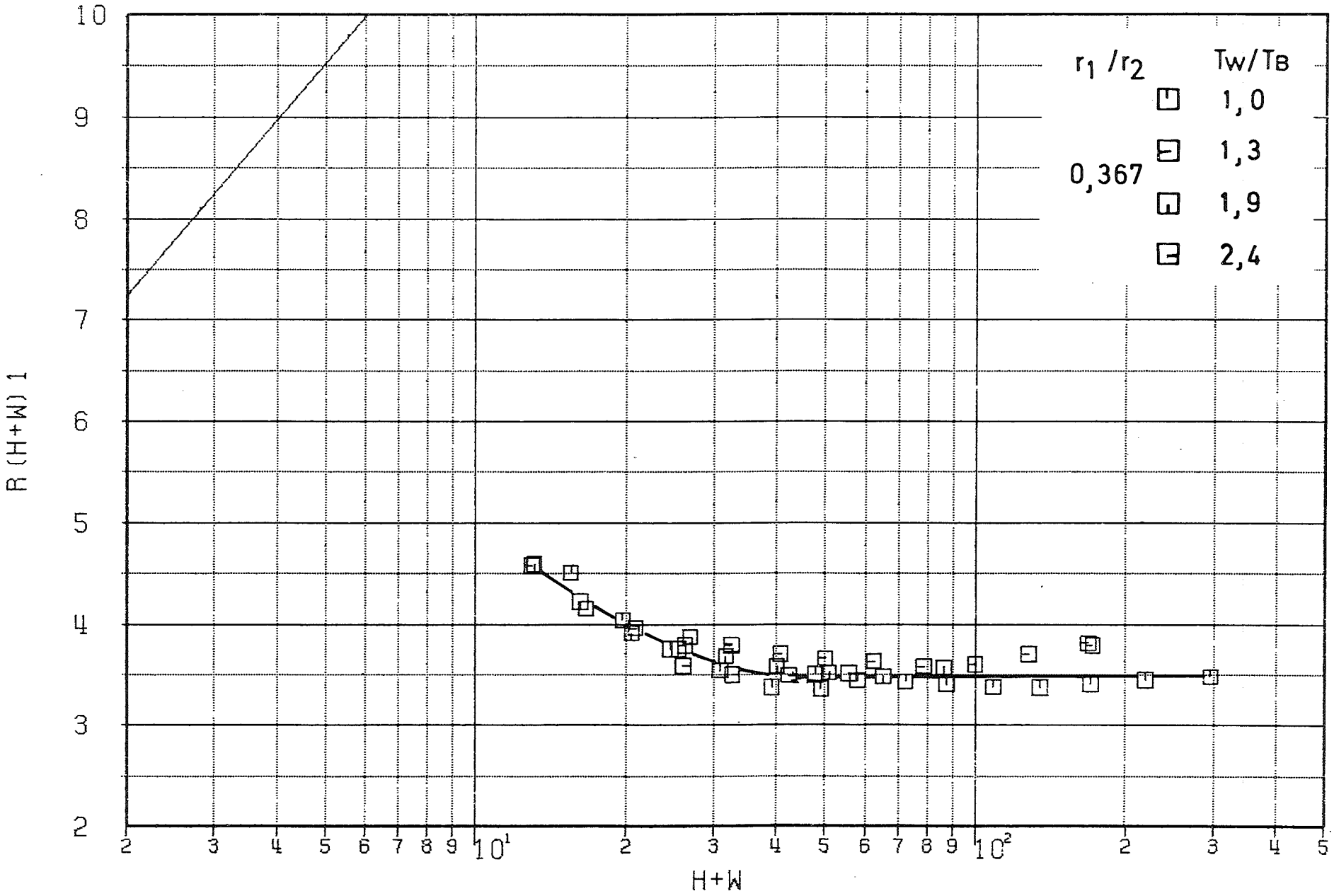

Fig.18: $R(h_W^+) - \frac{0.55}{h/\tilde{y}} \left(\frac{T_W}{T_1}\right)^{1.5}$ vs. h_W^+ ($Re_W \geqslant 3000$), test section "18" in tube of 50 mm I.D.

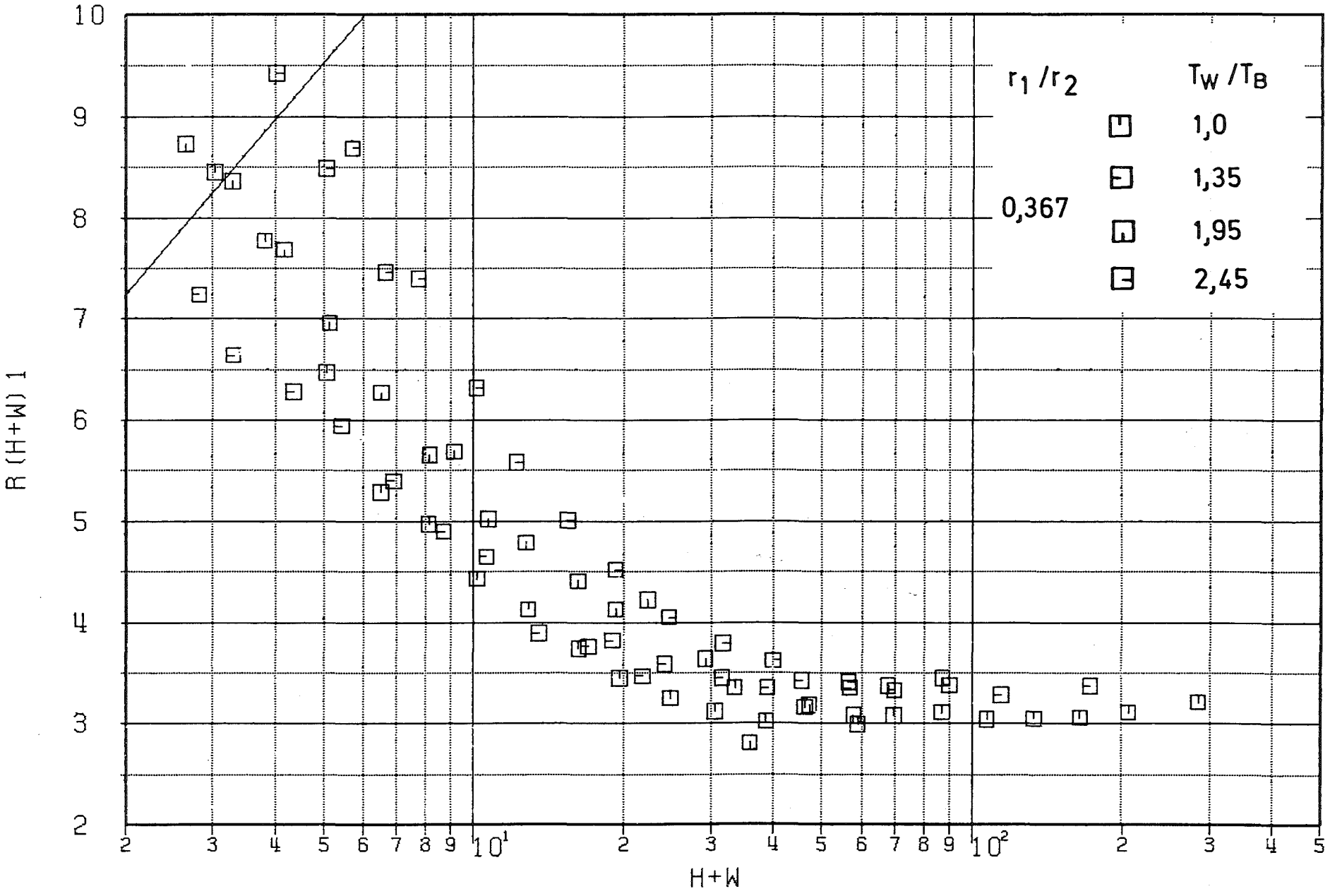

TESTSTRECKE 19

Fig.19: $R(h_W^+) - \frac{0.55}{h/\hat{y}} \left(\frac{T_W}{T_1}\right)^{1.5}$ vs. h_W^+ ($Re_W \geqslant 3000$), test section "19" in tube of 50 mm I.D.

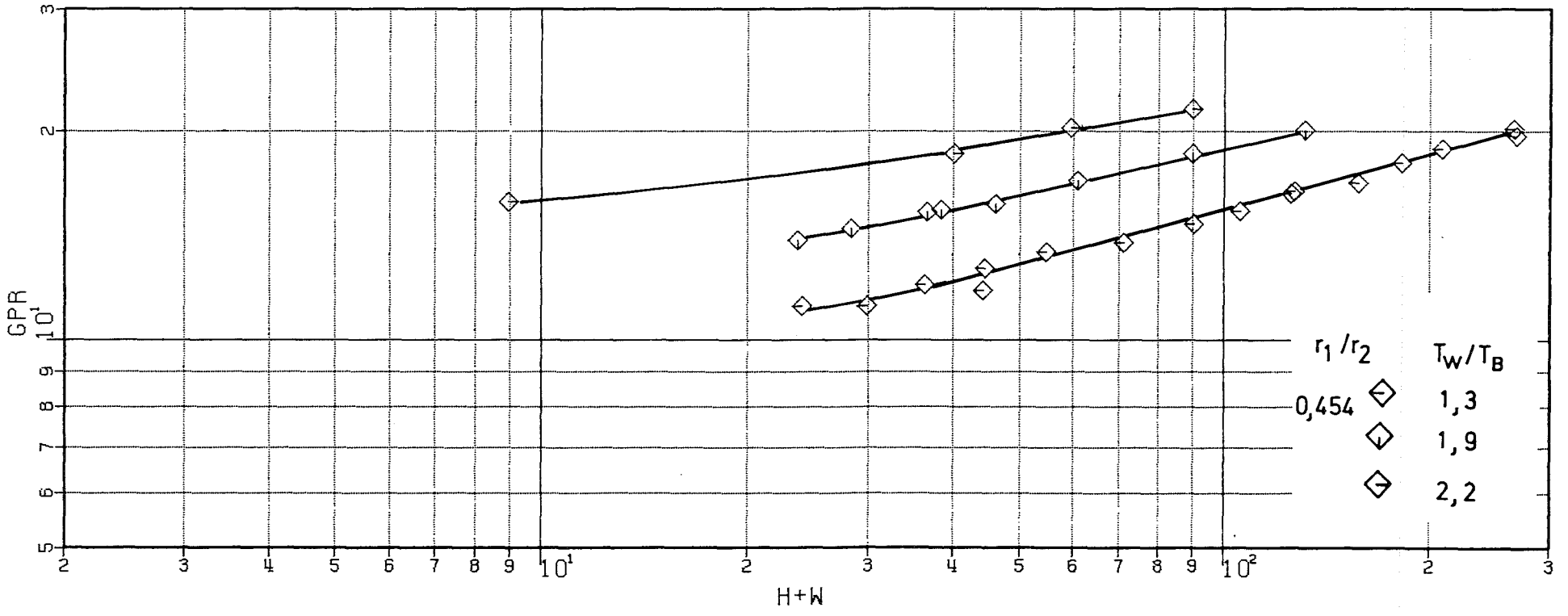

Fig.20: $G(h_W^+)$ vs. h_W^+ ($Re_W \geqslant 3000$), test section "18" in tube of 40.4 mm I.D.

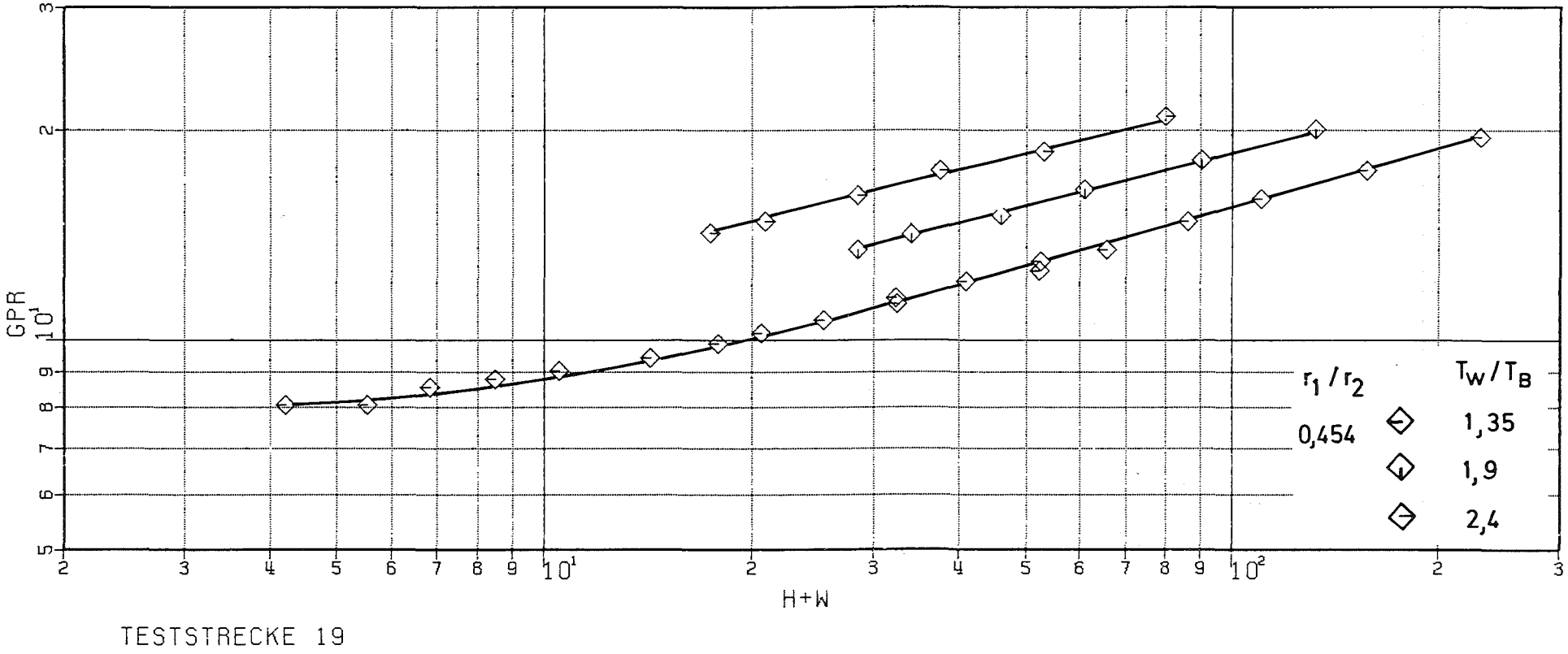

Fig.21: $G(h_W^+)$ vs. h_W^+ ($Re_W \geqslant 3000$), test section "19" in tube of 40.4 mm I.D.

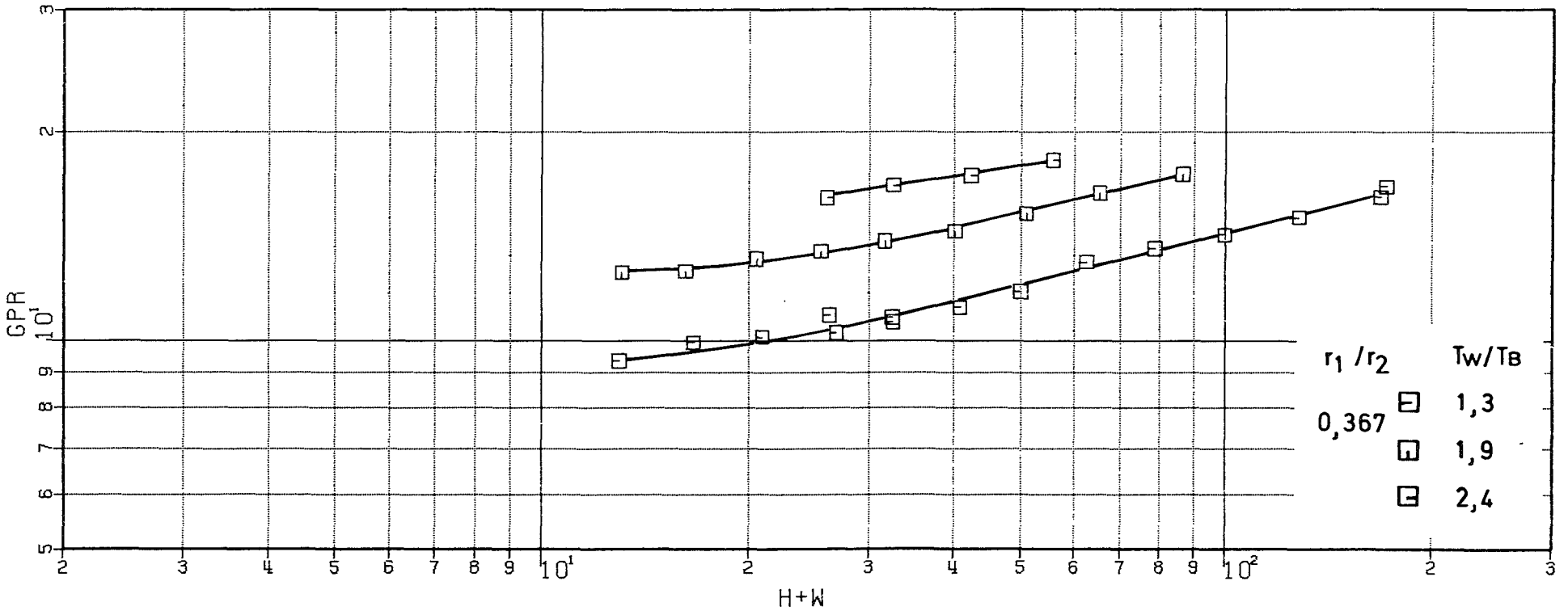

Fig.22: $G(h_W^+)$ vs. h_W^+ ($Re_W \geqslant 3000$), test section "18" in tube of 50 mm I.D.

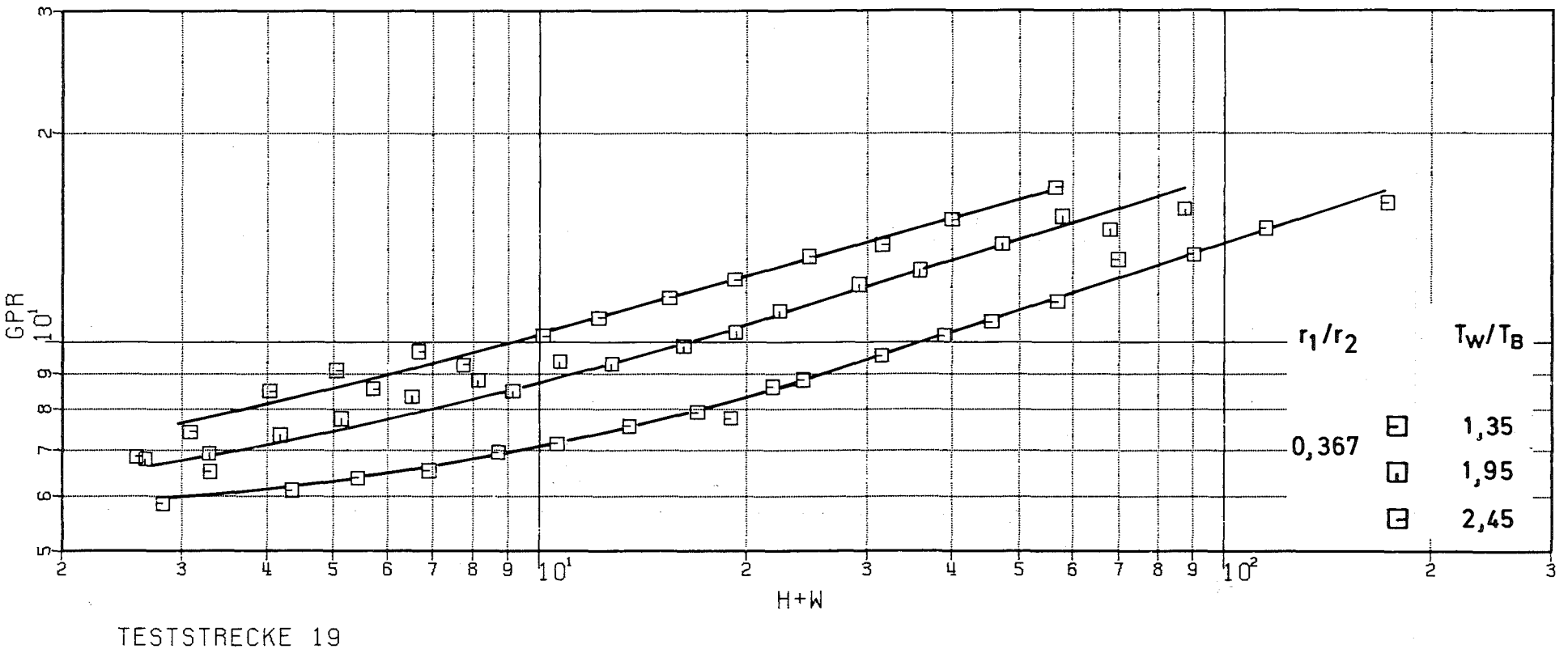

Fig.23: $G(h_W^+)$ vs. h_W^+ ($Re_W \geqslant 3000$), test section "19" in tube of 50 mm I.D.

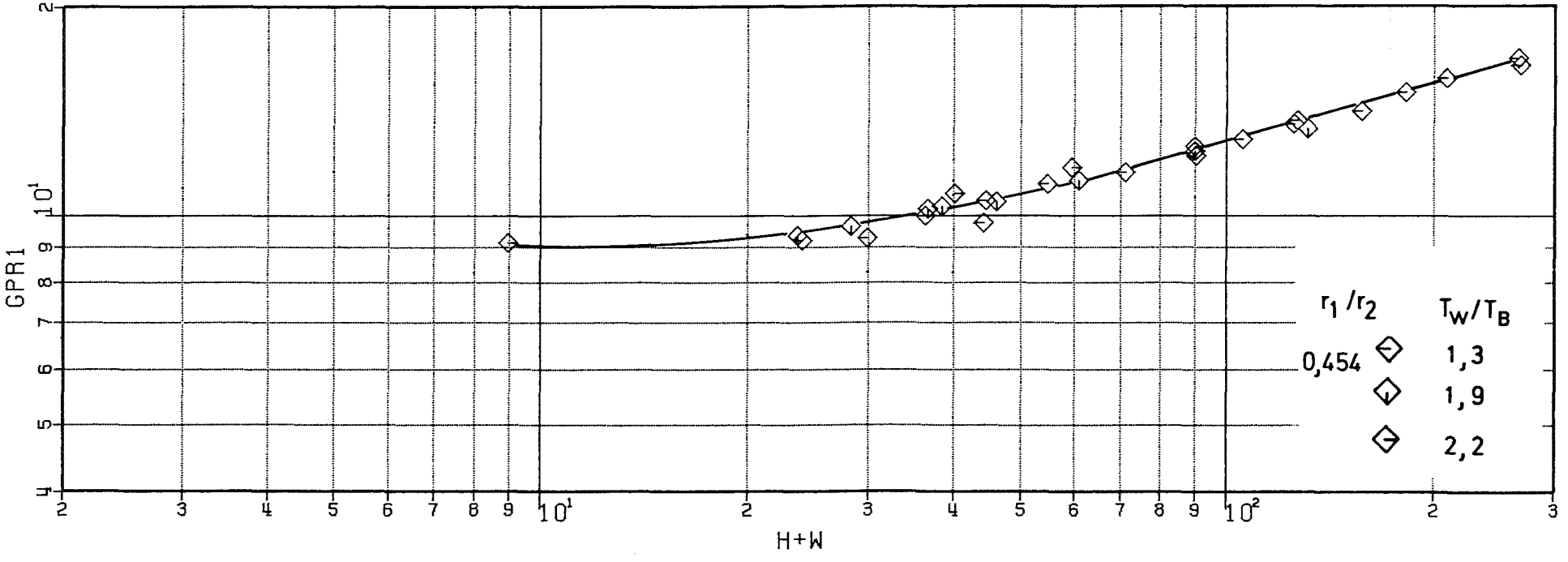

Fig.24: GPR1= $\frac{G(h_W^+)}{Pr^{0.44}} \left(\frac{T_W}{T_B}\right)^{-0.68}$ vs. h_W^+, test section "18" in tube of 40.4 mm I.D.

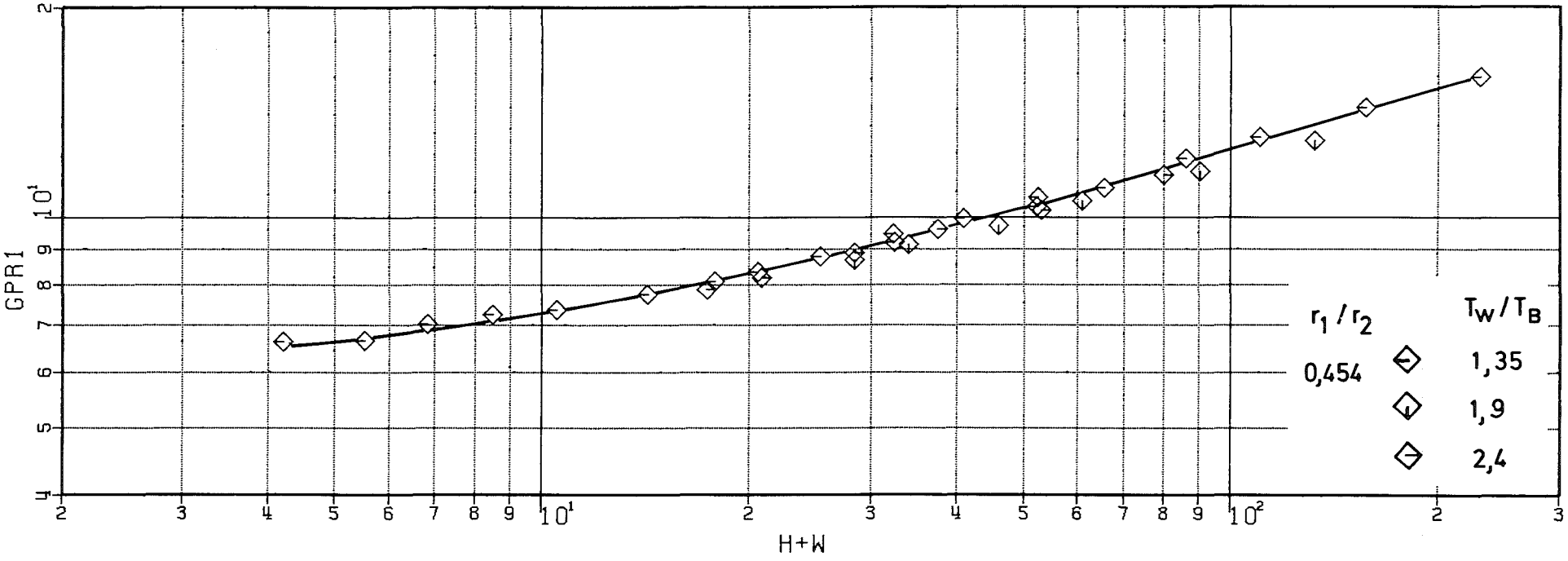

Fig.25: $GPR1 = \frac{G(h_W^+)}{Pr^{0.44}} \left(\frac{T_W}{T_B} \right)^{-0.68}$ vs. h_W^+, test section "19" in tube of 40.4 mm I.D.

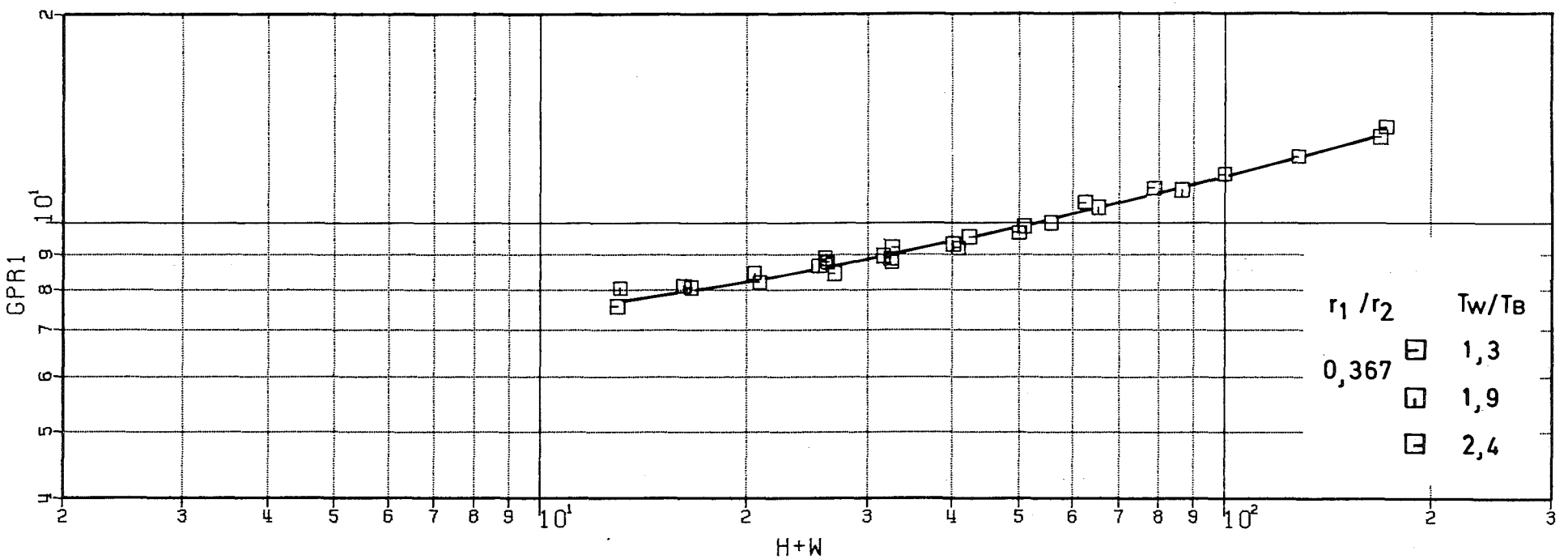

TESTSTRECKE 18

Fig.26: GPR1= $\frac{G(h_W^+)}{Pr^{0.44}} \left(\frac{T_W}{T_B}\right)^{-0.68}$ vs. h_W^+, test section "18" in tube of 50 mm I.D.

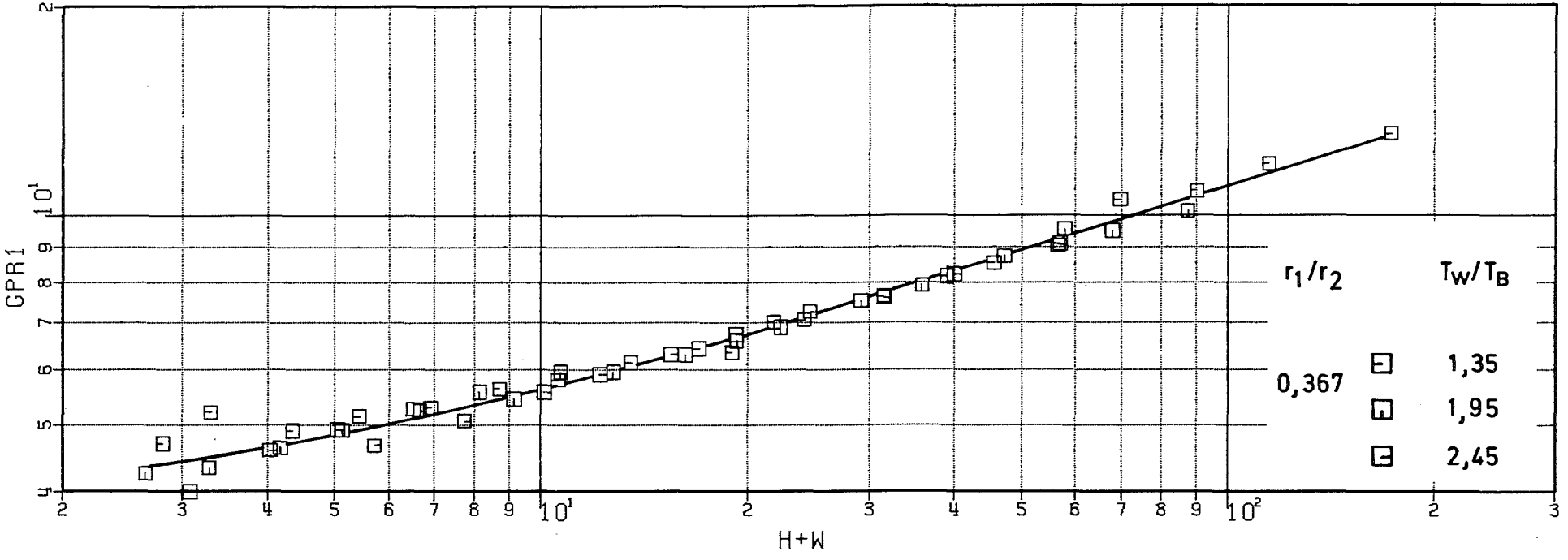

Fig.27: $GPR1 = \frac{G(h_W^+)}{Pr^{0.44}} \left(\frac{T_W}{T_B} \right)^{-0.68}$ vs. h_W^+, test section "19" in tube of 50 mm I.D.

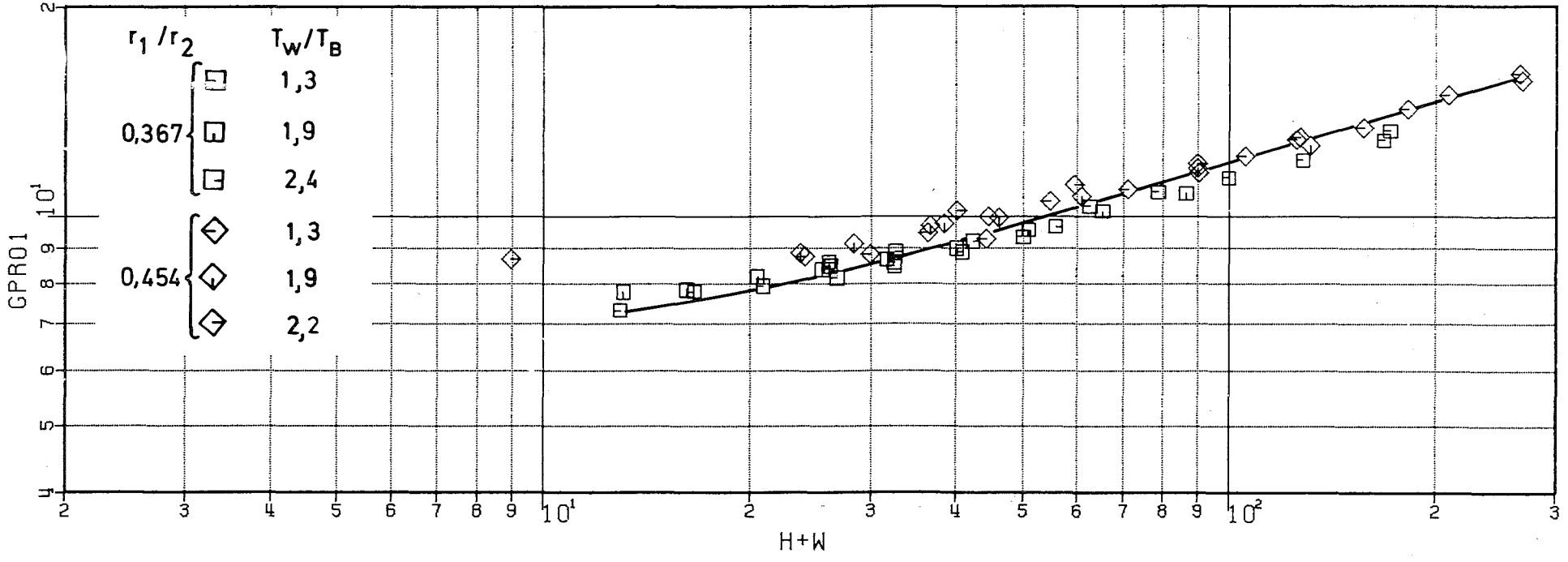

Fig.28: $GPRO1 = \frac{G(h_W^+)}{Pr^{0.44}} \left(\frac{T_W}{T_B}\right)^{-0.68} \left(\frac{h}{0.01(r_2-r_1)}\right)^{-0.053}$ vs. h_W^+ for rough rod "18"

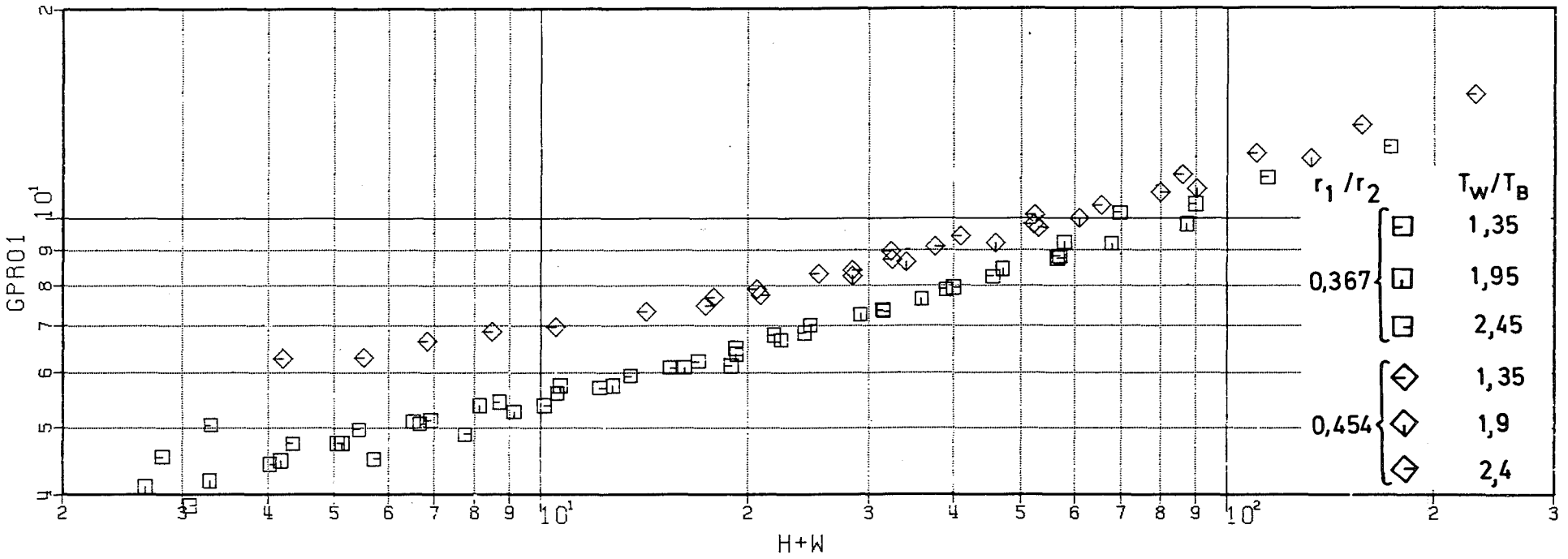

Fig.29: $GPRO1 = \frac{G(h_W^+)}{Pr^{0.44}} \left(\frac{T_W}{T_B}\right)^{-0.68} \left(\frac{h}{0.01(r_2-r_1)}\right)^{-0.053}$ vs. h_W^+ for rough rod "19"

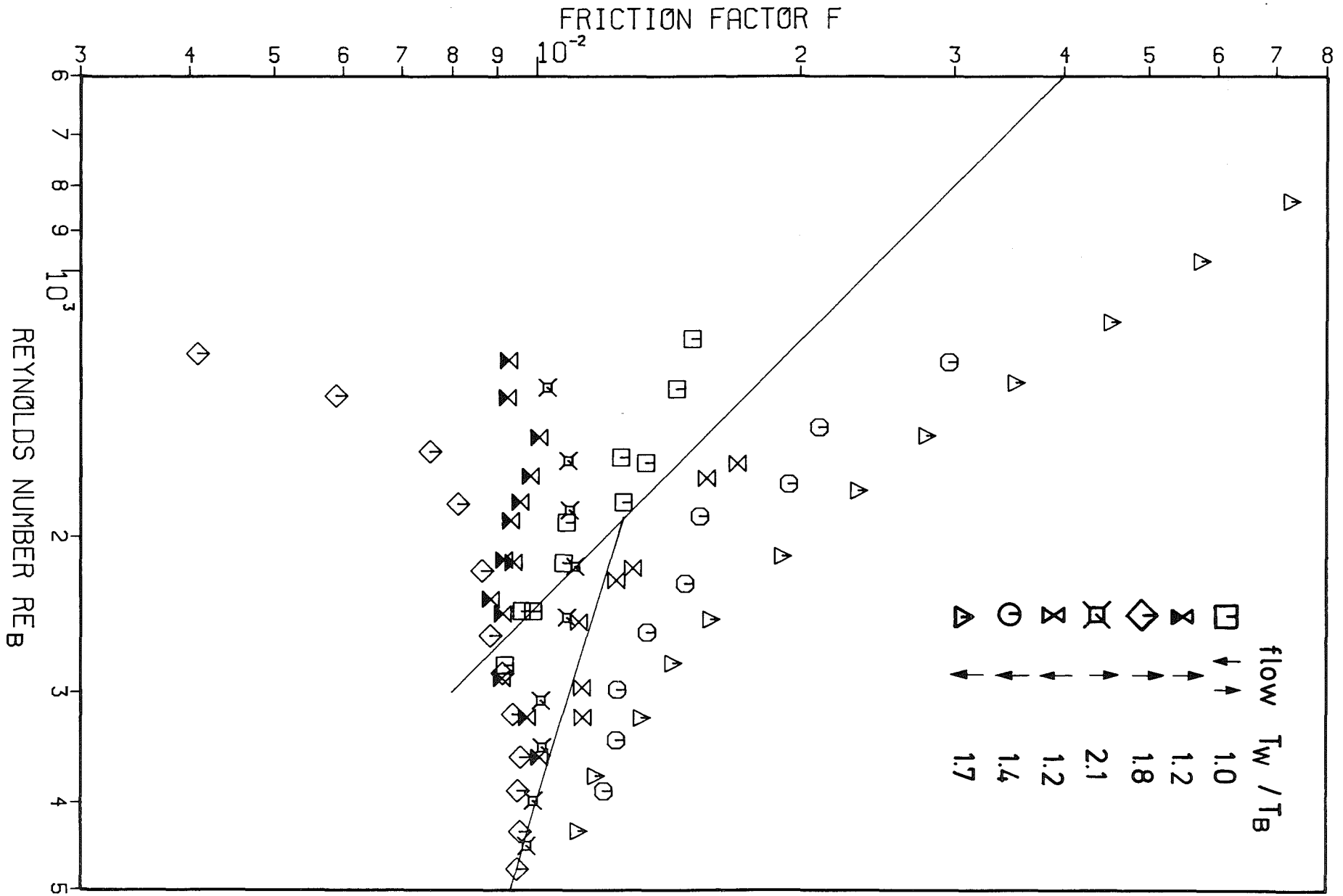

Fig.30: Friction factor vs. Reynolds number, laminar flow, rod "18"
Δp not corrected for buoyancy effect.

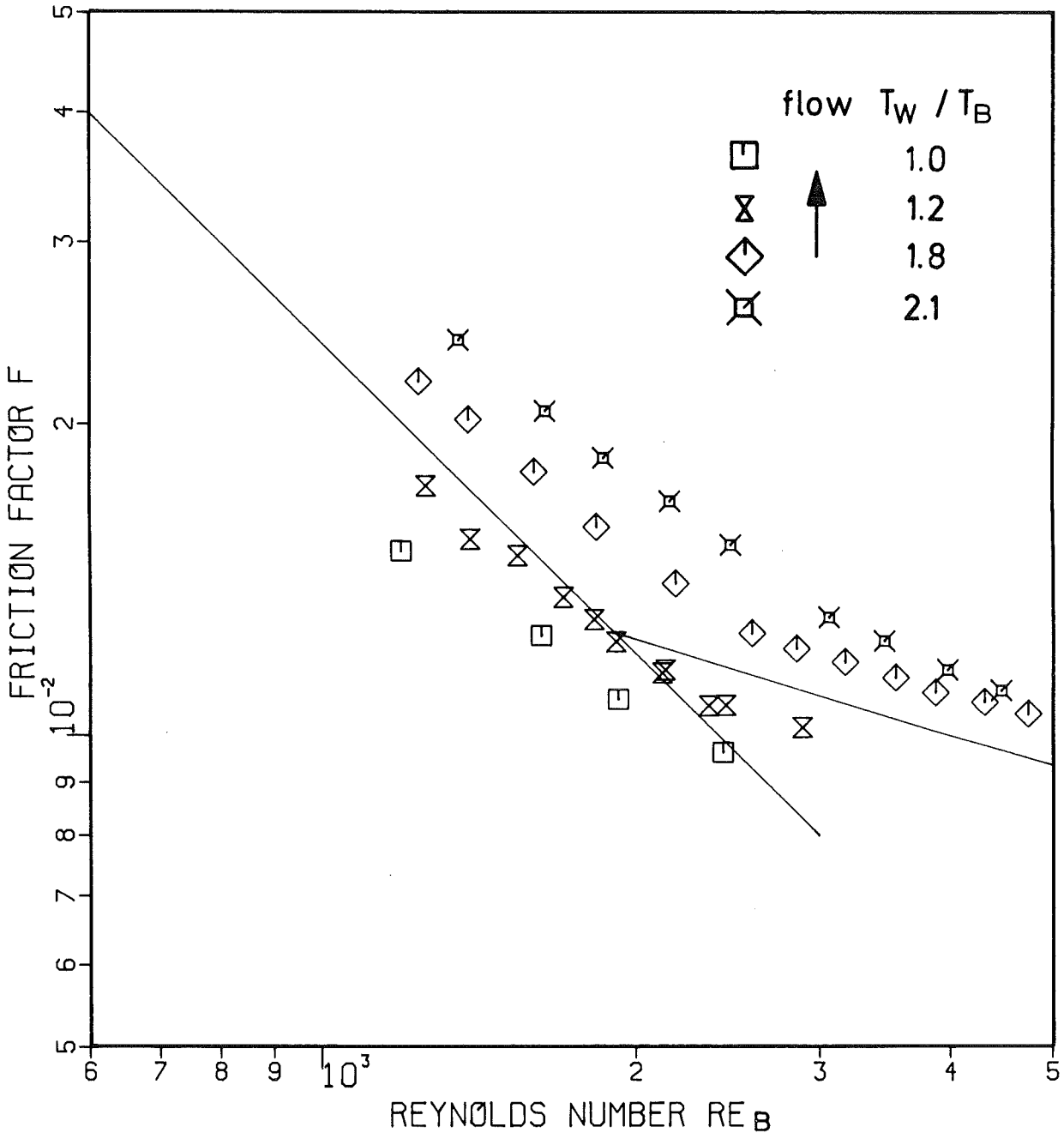

Fig.31: Friction factor vs. Reynolds number, laminar flow, rod "18" upward flow, Δp corrected for buoyancy effect.

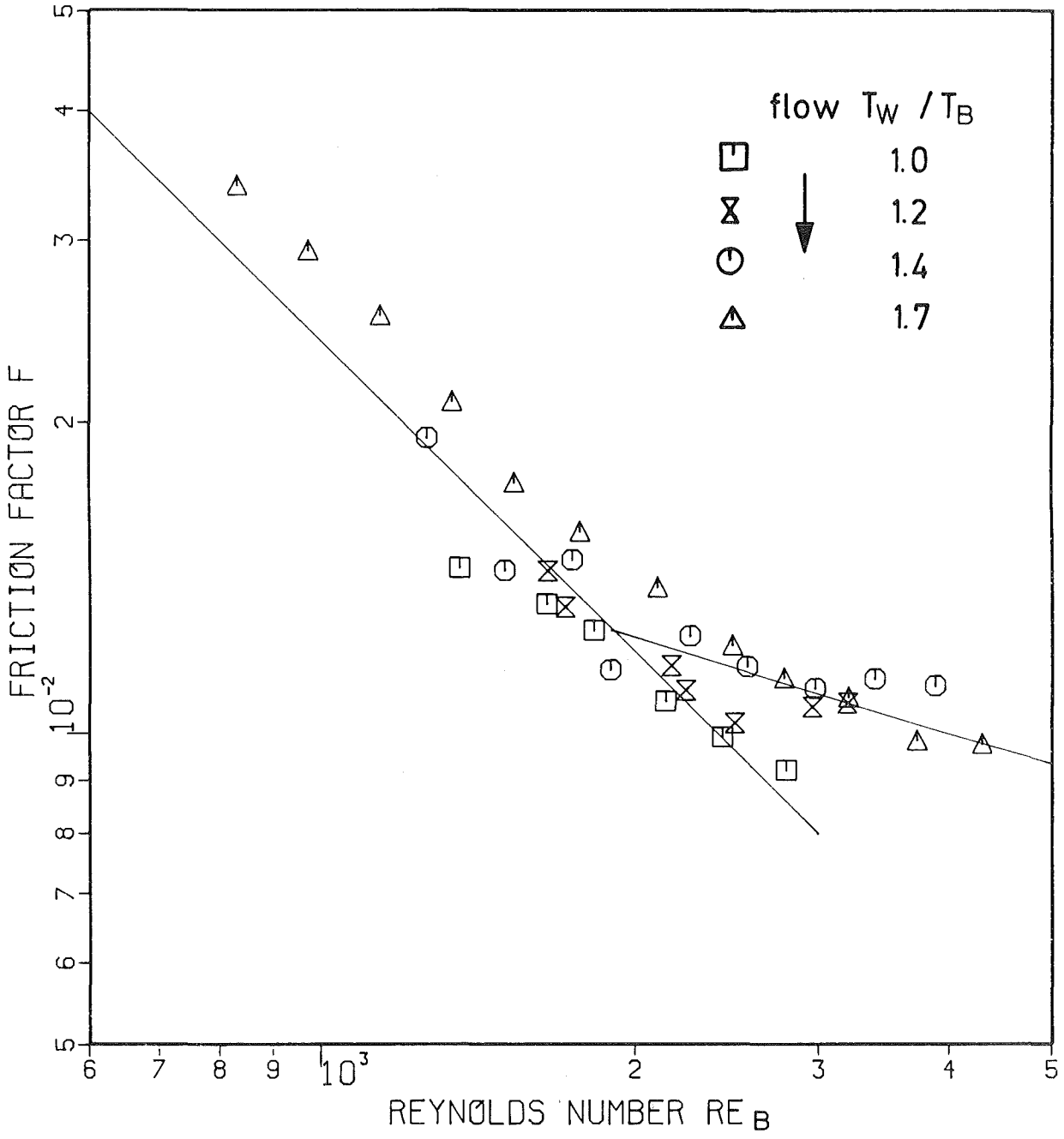

Fig.32: Friction factor vs. Reynolds number, laminar flow, rod "18" downward flow, Δp corrected for buoyancy effect.

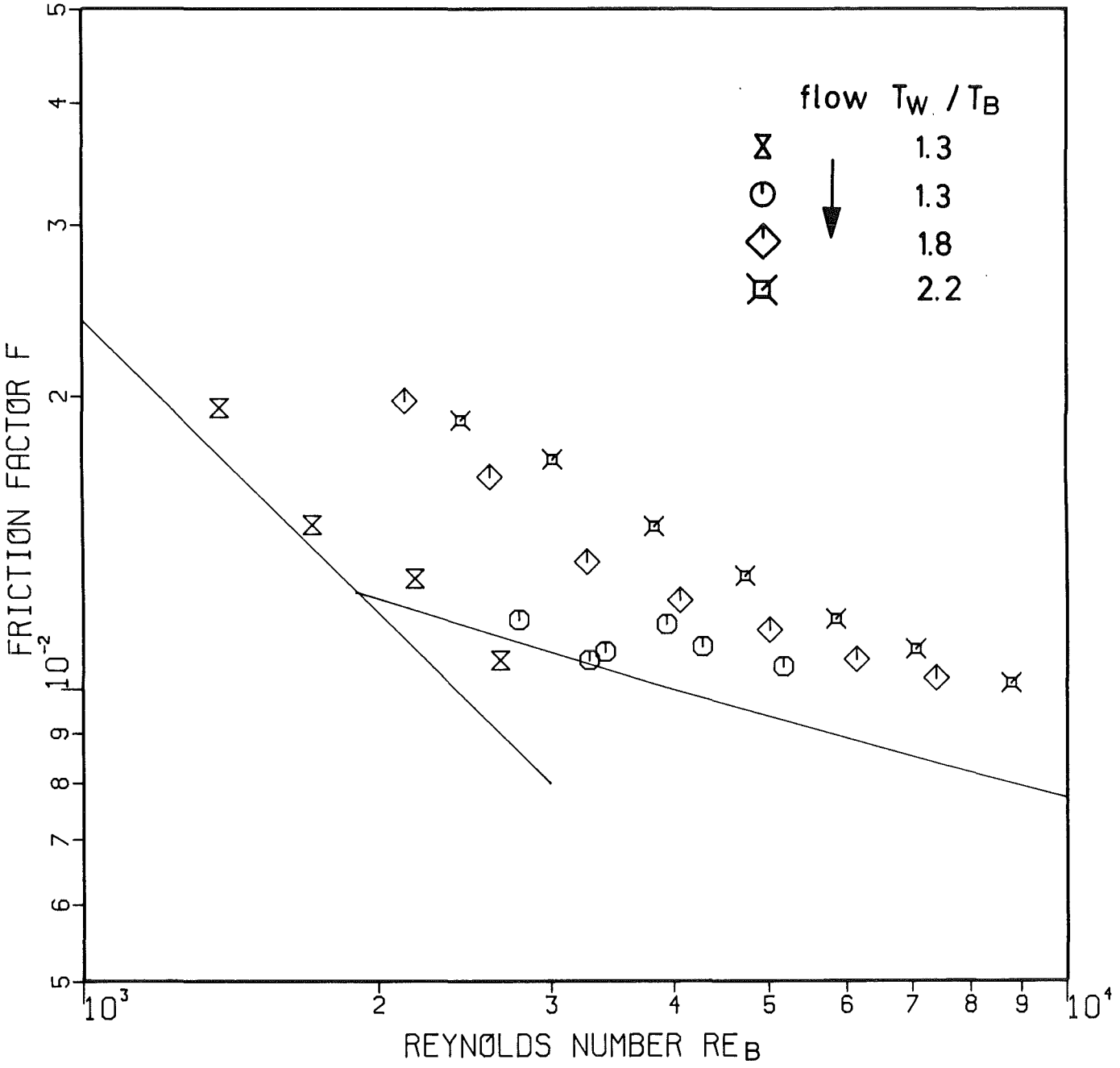

Fig.33: Friction factor vs. Reynolds number, laminar flow, rod "19"
Δp corrected for buoyancy effect.

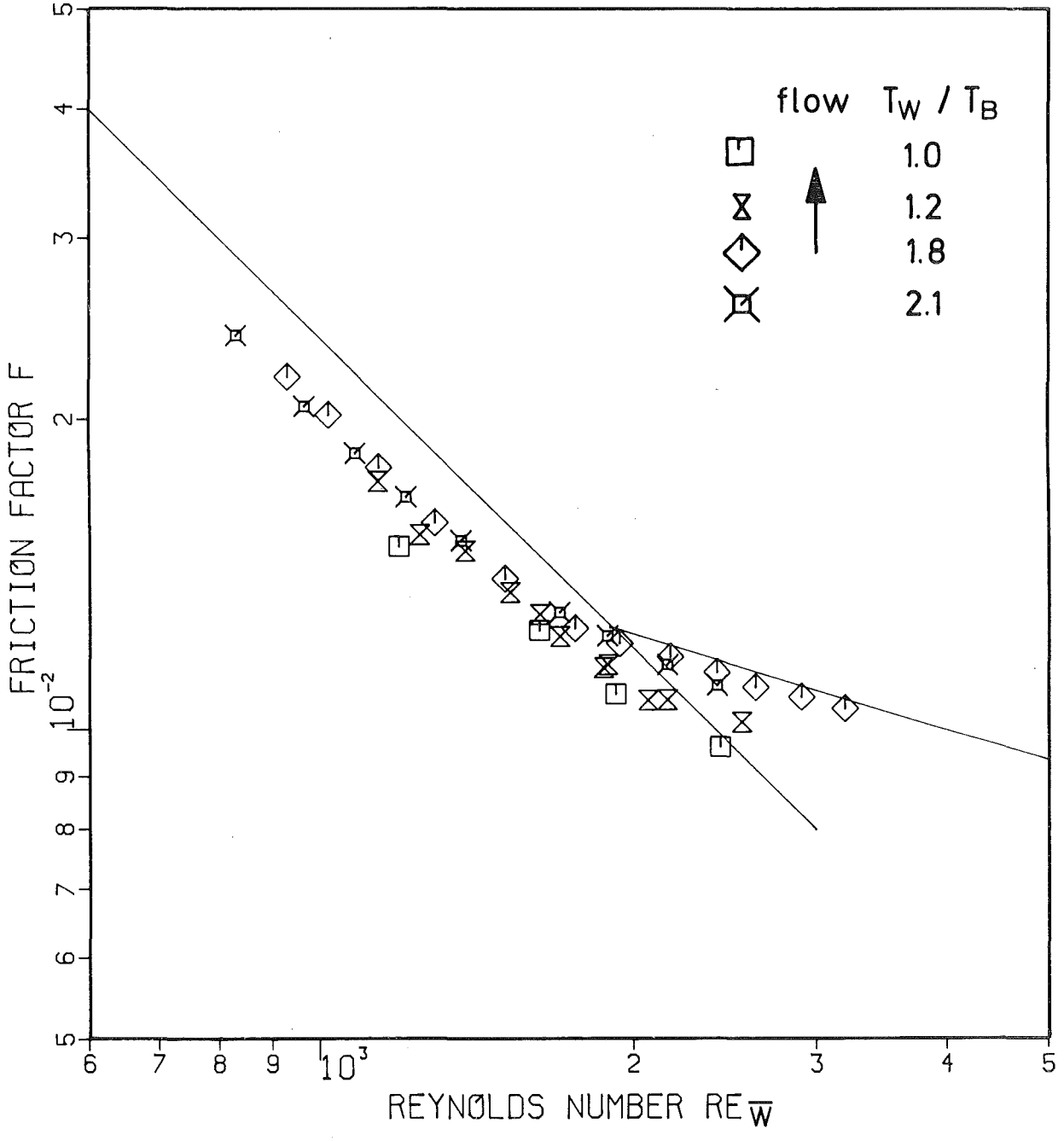

Fig.34: Friction factor vs. Reynolds number based on average wall temperature, rod "18" upwards laminar flow.

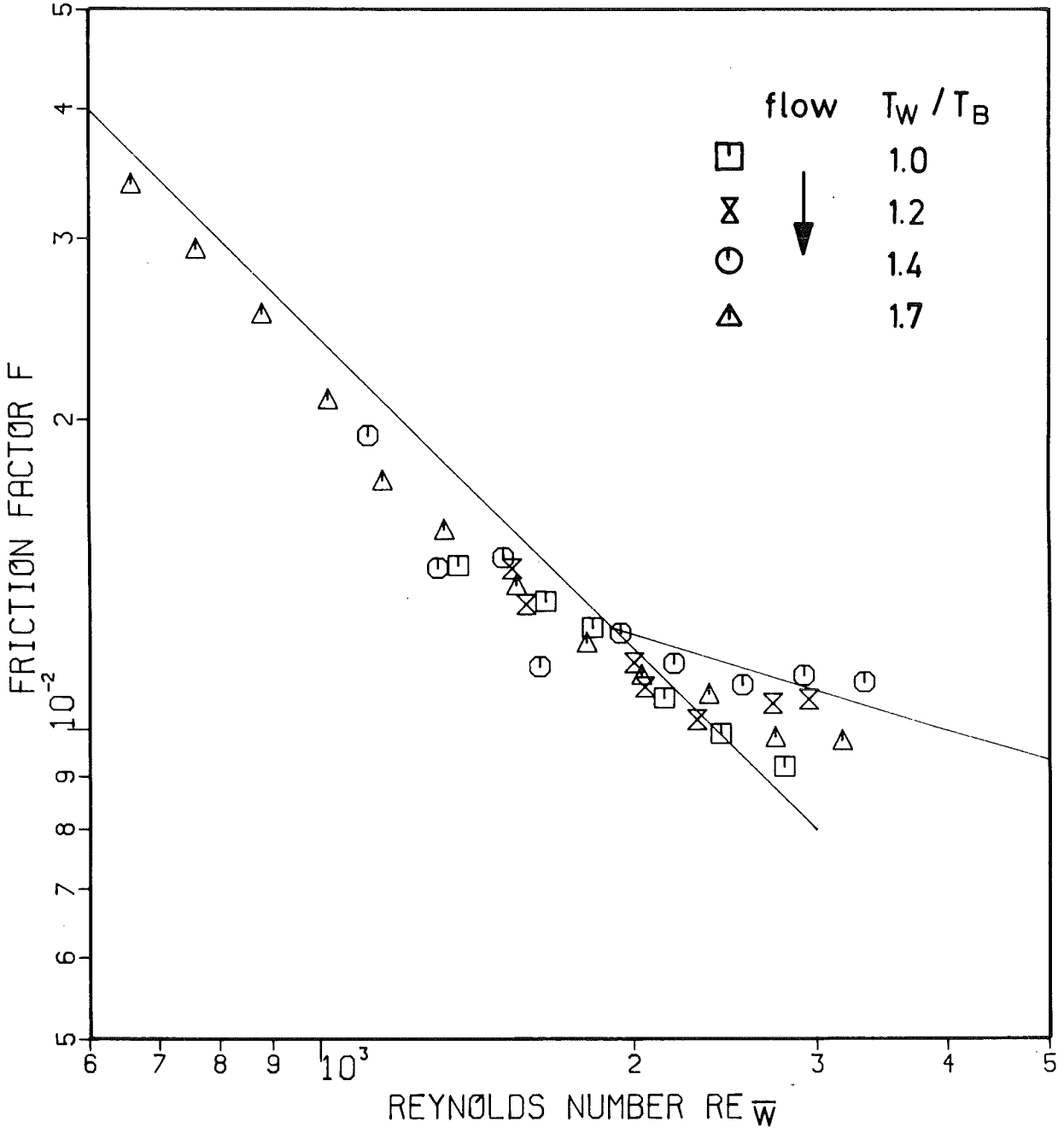

Fig.35: Friction factor vs. Reynolds number based on average wall temperature, rod "18", downwards laminar flow.

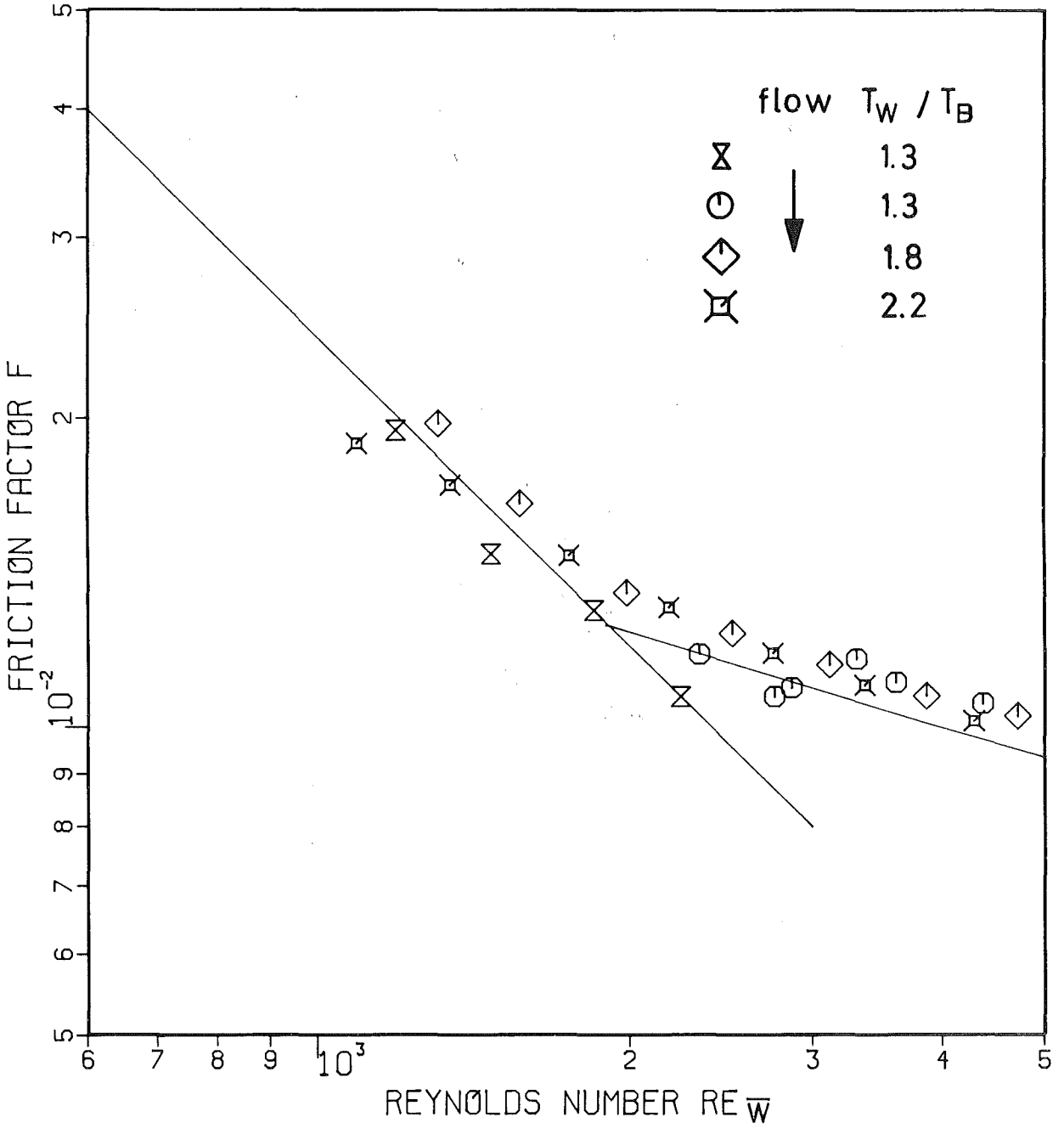

Fig.36: Friction factor vs. Reynolds number based on average wall temperature, rod "19", laminar flow.

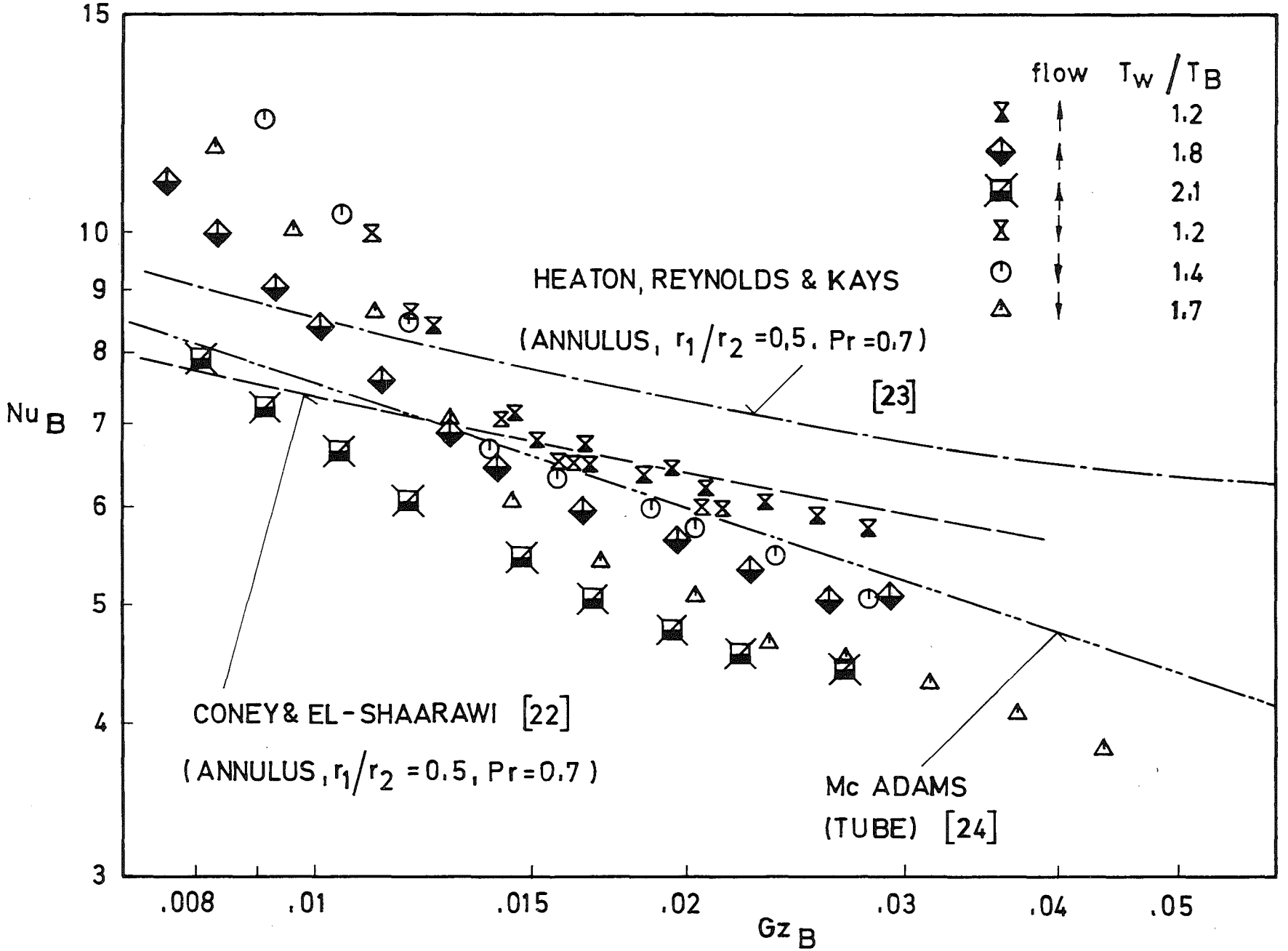

Fig.37: Nusselt number Nu_B vs. Graetz number Gz_B for test section 18/40.4 and $Re_W \leqslant 3000$.

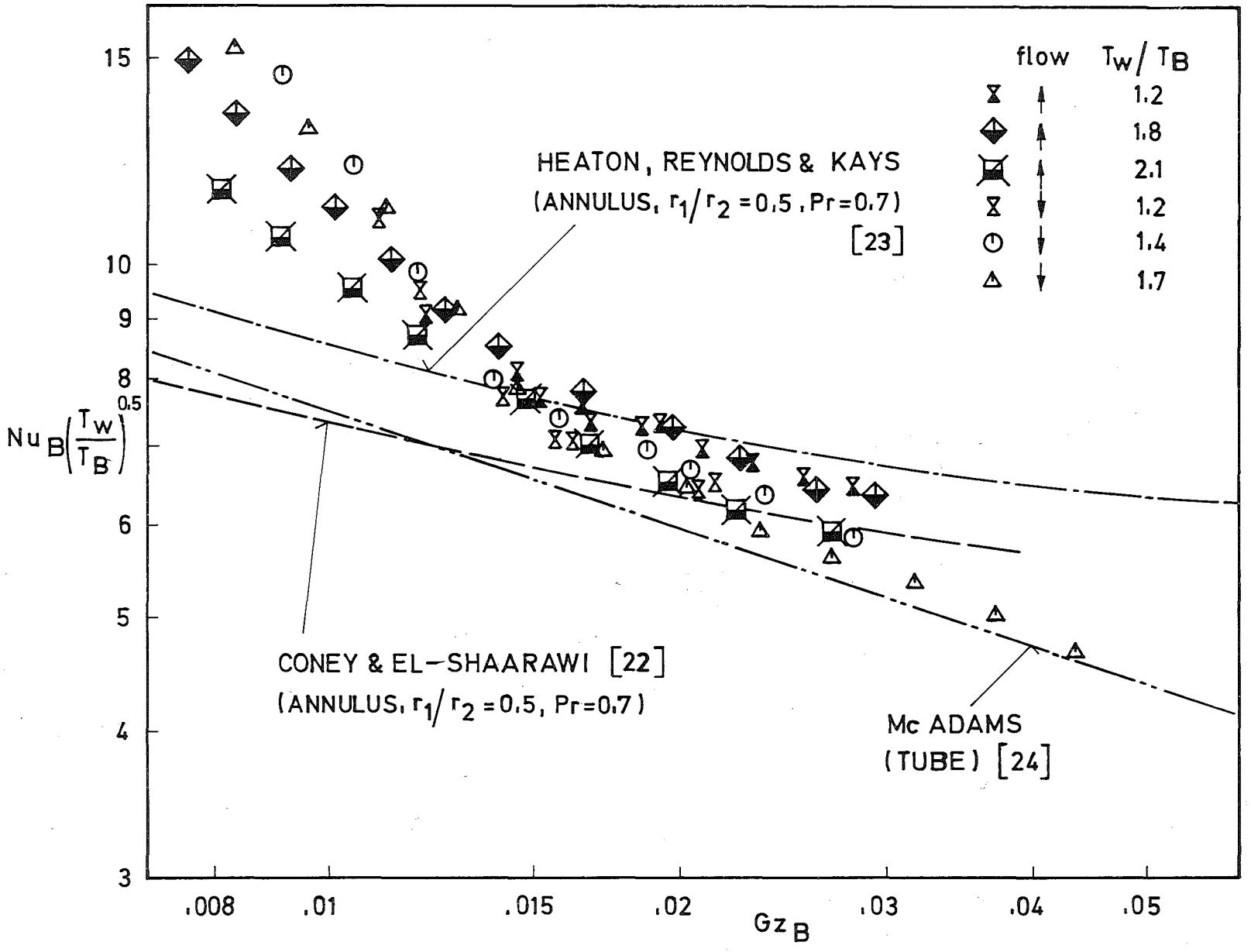

Fig.38: Nusselt number corrected for temperature effect $\left[Nu_B\left(\frac{T_W}{T_B}\right)^{0.5}\right]$

vs. Graetz number Gz_B for test section 18/40.4 and $Re_{\overline{W}} \leq 3000$

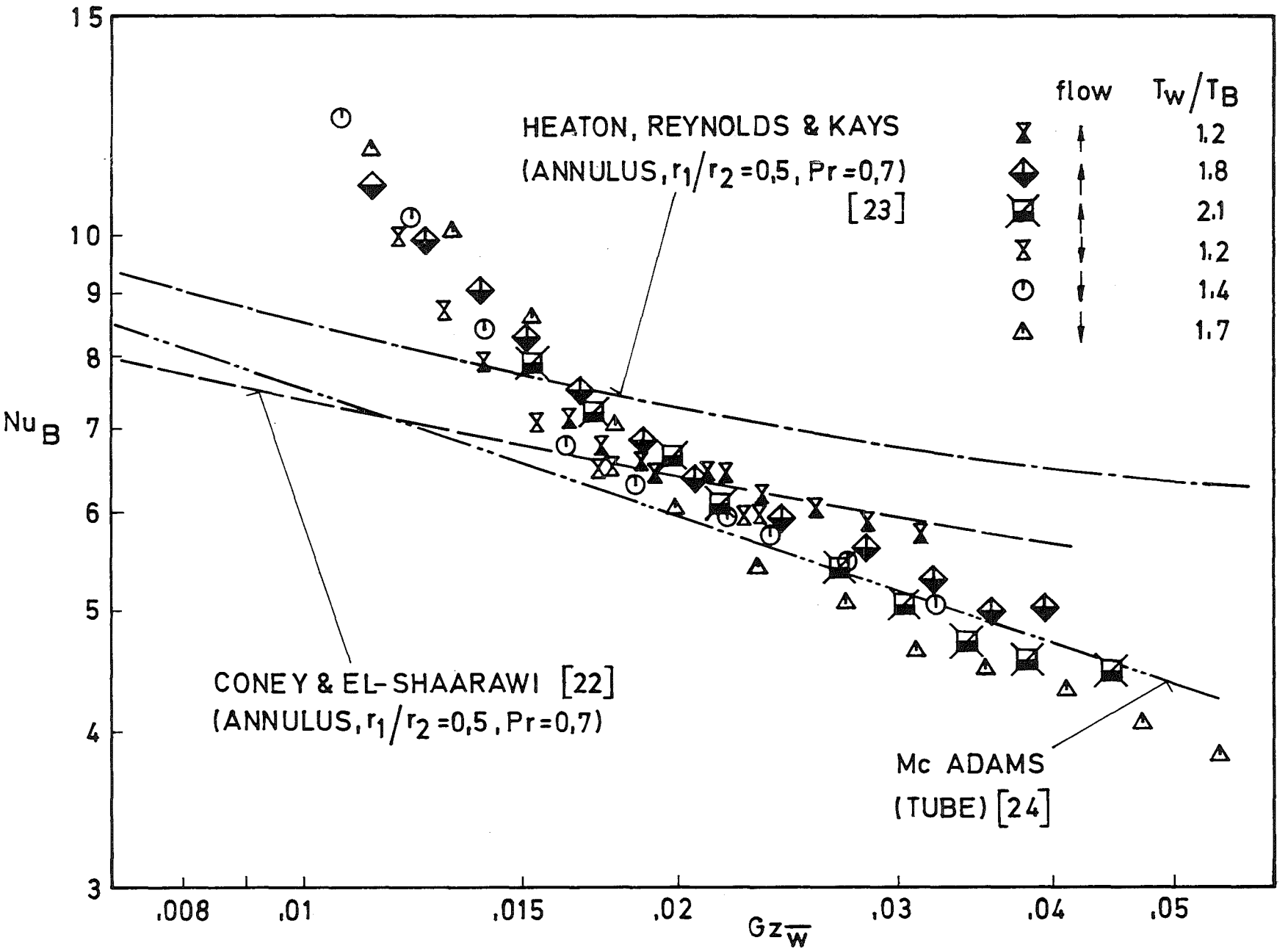

Fig.39: Nusselt number Nu_B versus Graetz number $Gz_{\overline{W}}$ based on temperature $T_{\overline{W}}$ for test section 18/40.4 and $Re_{\overline{W}} \leq 3000$.